

**SUPPORTED CATALYSTS, FROM POLYMERS TO GOLD
NANOPARTICLES SUPPORTS**

A Dissertation
Presented to
The Academic Faculty

by

William J. Sommer

In Partial Fulfillment
of the Requirements for the Degree
Doctor of Philosophy in the
School of Chemistry and Biochemistry

Georgia Institute of Technology
August, 2007

© Copyright 2007 by William J. Sommer

**SUPPORTED CATALYSTS, FROM POLYMERS TO GOLD
NANOPARTICLES SUPPORTS**

Approved by:

Dr. Marcus Weck, Advisor
School of Chemistry and Biochemistry
Georgia Institute of Technology

Dr. E. Kent Barefield
School of Chemistry and Biochemistry
Georgia Institute of Technology

Dr. Mostafa A. El-Sayed
School of Chemistry and Biochemistry
Georgia Institute of Technology

Dr. Christoph J. Fahrni
School of Chemistry and Biochemistry
Georgia Institute of Technology

Dr. Christopher W. Jones
School of Chemical and Biochemical
Engineering
Georgia Institute of Technology

Date Approved: May 21, 2007

To Ofelia, Annie and my parents

ACKNOWLEDGEMENTS

First, I would like to thank my wife, my daughter and my family. They were always here to support me and hear my complaints even though some months they did not see me very often. Secondly, I want to thank several members of the Weck group who helped me “grow”. They not only help me become a better scientist but also a better person. They were only a few of these persons in the lab and they were very valuable to the group. The first person is Warren Gerhardt. He showed me other values in life and was always there to add a note of fun in the lab. He was also there through adversity. I will miss these long nights in the lab where we got to talk about everything and anything. I also want to thank Michael Holbach, an amazing person and talent who taught a lot of things. I also want to mention Paul Stubbs, Joe Carlise and Matija Crne. Finally, I will miss playing badminton with my good friend Alpay Kimyonok with whom I had a lot of discussion about life. I also want to thank my undergraduate research advisor Steve Nolan, for the chance he gave me to work in his lab. He gave me a taste of research in chemistry and trusted me enough to give me my own project! He is a very special adviser and a very special friend that I will never forget. Finally, the one without anything would have been possible, my advisor Marcus Weck. Even though I criticized him a lot I admire his drive to get where he is and his incredible knowledge in chemistry. Thank you for taking me in your group and believing in my abilities to accomplish something in the group. I would also like to thank my committee members, Dr. E. Kent Barefield, Dr. Mostapha A. El-Sayed and Christoph J. Fahrni for their great inputs and for allowing me to look at my research differently. Finally, a special thank to Dr. Christopher W. Jones

for reminding me that I did not know everything about my project. His inputs on a regular basis made me a better scientist.

TABLE OF CONTENTS

	Page
ACKNOWLEDGEMENTS.....	iv
LIST OF TABLES.....	ix
LIST OF FIGURES.....	x
LIST OF SCHEMES.....	xiii
LIST OF SYMBOLS AND ABBREVIATIONS.....	xiv
SUMMARY.....	xvi

CHAPTER

1 Supported Catalysts: an Overview

1.1. Introduction.....	2
1.2. Inorganic Supports.....	4
1.2.1. Pd on Carbon.....	5
1.2.2. Pd on Metal Oxides.....	5
1.2.3. Silica Supports.....	5
1.3. Organic Polymers.....	7
1.3.1. Insoluble Organic Polymers.....	8
1.3.2. Soluble Polymers.....	10
1.4. Nanoparticles.....	18
1.5. Conclusion.....	19
1.6. References.....	20

2 Organometallic Complexes Investigated in this Thesis

2.1. Pincers.....	24
2.1.1. Introduction.....	24

2.1.2. Coupling Chemistry Using Pincer Complexes.....	24
2.1.3. Supported Pincer Complexes.....	28
2.2. <i>N</i> -Heterocyclic Carbenes.....	32
2.2.1. Introduction.....	32
2.2.2. Coupling Chemistry with <i>N</i> -heterocyclic Carbene Complexes.....	32
2.2.3. Supported <i>N</i> -heterocyclic Carbene Complexes.....	33
2.3. Design Elements and Challenges.....	36
2.4. References.....	41
3 Polymer and Silica Supported SCS-Pd Pincer Complexes	
3.1. Introduction.....	48
3.2. Ether Linked SCS-Pd Pincer Complexes.....	49
3.2.1. Poisoning Studies.....	52
3.3. Nitrogen Linked SCS-Pd Pincer Complexes.....	56
3.4. Conclusion.....	60
3.5. Experimental Section	60
3.6. References.....	66
4 Polymer and Silica Supported PCP-Pd Pincer Complexes	
4.1. Introduction.....	69
4.2. Results and Discussion.....	71
4.3. Conclusion.....	90
4.4. Experimental Section.....	91
4.5. References.....	98
5 Polymer Supported <i>N</i>-heterocyclic Carbene Complexes	
5.1. Introduction.....	102
5.2. Results and Discussion.....	103

5.3. Conclusion.....	120
5.4. Experimental Section.....	120
5.5. References.....	137
6 Gold Nanoparticles as a Support	
6.1. Introduction.....	142
6.2. Results and Discussion.....	143
6.3. Conclusion.....	155
6.4. Experimental Section.....	155
6.5. References.....	169
7 Summary and Next Steps.....	156
7.1. Summary.....	173
7.2. Soluble Polystyrene as a Support.....	177
7.3. Cross-linked Polystyrene as a Support.....	178
7.4. Conclusion.....	179
APPENDIX A: XAS Results.....	181

LIST OF TABLES

Table	Page
Table 5.1: Catalytic Results for the Suzuki-Miyaura Coupling reactions.....	106
Table 5.2: Leaching Test Results.....	111
Table 5.3: Catalytic Results for the Sonogashira Coupling Reactions.....	116
Table 6.1: Optimization of 1,3 dipolar cycloaddition conditions for gold nanoparticles functionalization.....	147
Table 6.2: Yields of 1,3 dipolar cycloadditions on gold nanoparticles using the library of alkynes.....	150
Table 6.3: Catalytic Results for the Suzuki-Miyaura Coupling reactions.....	154

LIST OF FIGURES

Figure	Page
Figure 1.1: Schematic of Supported Catalysts.....	3
Figure 1.2: Silica Supported Catalysts.....	6
Figure 1.3: SBA-15 Tethered Pd Complex.....	7
Figure 1.4: Pd(II) Supported Complex Poly(styrene) resin.....	9
Figure 1.5: Crosslinkers with Salen and BINAP ligands.....	10
Figure 1.6: Soluble Polymers used as Supports for Catalysts.....	11
Figure 1.7: Schematic of the Removal of PEG Supported Catalysts.....	12
Figure 1.8: Butadiene Dimerization Reaction.....	12
Figure 1.9: The Different Type of Dendrimer and Dendrons Supported Catalysts.....	14
Figure 1.10: G3 Poly(propylene imine) Dendrimer Functionalized with Diphenyl Phosphines at the Periphery.....	15
Figure 1.13: Poly(styrene) Supported Salen-Co Complex.....	16
Figure 1.12: Hydrolytic Kinetic Resolution of Epichlorohydrin.....	17
Figure 1.13: Palladium Complex Supported on Superparamagnetic Maghemite.....	19
Figure 2.1: Pincer Ligands.....	25
Figure 2.2. Catalytic Cycle of Heck-Mizoroki Reaction.....	26
Figure 2.3. Catalytic Cycle of the Suzuki-Miyaura Reaction.....	26
Figure 2.4: Mechanism Proposed by Jensen and Morales-Morales for Pincer Complexes.....	28
Figure 2.5: Examples of Supported Pincer Complexes.....	30
Figure 2.6: <i>N</i> -Heterocyclic Carbene Ligands.....	32

Figure 2.7: Examples of Highly Active <i>N</i> -Heterocyclic Carbene Complexes.....	33
Figure 2.8: Merrifield Resin Supported Pd-NHC Complex.....	35
Figure 2.9: Polymer Supported Pd-NHC Complex.....	36
Figure 2.10: Silica Supported Pd-NHC Complex.....	37
Figure 2.11: Catalytic Cycle of the Sonogashira Reaction.....	40
Figure 3.1: Supported Pincer Complexes Synthesized.....	49
Figure 3.2: Recycling of Silica Supported O-SCS-Pd Pincer.....	51
Figure 3.3: Three Phases Test.....	52
Figure 3.4: Poisoning Studies.....	54
Figure 3.5: Kinetic Plots of Poly(norbornene) Supported O-SCS-Pd Pincer.....	55
Figure 3.6: Kinetic Plots of Poison Containing Catalysis for Poly(norbornene) Supported O-SCS-Pd Pincer.....	55
Figure 3.7: Supported SCS-Pd Pincer Complexes Synthesized by Bergbreiter <i>et al.</i>	56
Figure 3.8: Kintaic Plots of Poly(norbornene) Supported N-SCS-Pd Pincer.....	58
Figure 3.9: Recycling Experiment Using SBA-15 Supported N-SCS-Pd Pincer (21).....	59
Figure 4.1: Pd-PCP Pincer Studied by Eberhard.....	70
Figure 4.2: The Immobilized Palladated Pincer Complexes Evaluated in this Chapter....	71
Figure 4.3: Heck Reaction Conditions.....	72
Figure 4.4: Conversion vs. Time for Heck Coupling Using 1	73
Figure 4.5: Conversion vs. Time for Heck Coupling Using 2	75
Figure 4.6: Conversion vs. Time for Heck Coupling Using 3	77
Figure 4.7: Conversion vs. Time for Heck Coupling Using 4	78
Figure 4.8: Postulated Mechanism by Louie <i>et al.</i> for the Synthesis of [Pd(0){P(<i>o</i> -Tol) ₃] ₂ . a) Deprotonation, b) β-H Elimination, c) Reductive Elimination d) Disproportionation.....	79

Figure 4.9: Optimized Structures of the Calculated Exchange Pathway of Phosphine by a Trimethyl Amine Base of Palladated Pincer Complexes. A) Chemdraw Representation of Structures Used in Calculation, B) Fully Intact Complex, C) Removal of one Phosphine, D) Addition of the Amine Base, E) Rearrangement to a Distorted Square Planar Confirmation, and F) Exchange of the Second Phosphine by Another Amine Base.....	82
------------------------------------------------------------------------------------------------------------------------------------------------------------------------------------------------------------------------------------------------------------------------------------------------------------------------------------------------------------------------------------------------------------------------------	----

Figure 4.10: Free energy diagram of the relevant minima for the initial steps of the proposed decomposition pathway computed at the BP86/LAV3P/6-31G* level of theory.....	84
----------------------------------------------------------------------------------------------------------------------------------------------------------------------------	----

Figure 5.1: Kinetic Study for a) the Suzuki-Miyaura Reaction with 6a (×), b) the Sonogashira Reaction with 6a (▲), c) the Suzuki-Miyaura Reaction with 6a in the Presence of QuadraPure [®] (■), d) the Sonogashira Reaction with 6a in the Presence of QuadraPure [®] (◆), and e) the Suzuki-Miyaura Reaction with 6a with the Addition of QuadraPure [®] after 20 minutes (*).	110
-----------------------------------------------------------------------------------------------------------------------------------------------------------------------------------------------------------------------------------------------------------------------------------------------------------------------------------------------------------------------------------------------------------------------------------------------------	-----

LIST OF SCHEMES

Scheme	Page
Scheme 3.1: Synthesis of Poly(norbornene) SCS-Pd Pincer.....	50
Scheme 3.2: Synthesis of Amide Linked Supported SCS-Pd Pincer.....	57
Scheme 4.1: Synthesis of Pd-Cl N-{3,5-bis[(diphenylphosphanyl)-methyl]-phenyl}- acetamide.....	72
Scheme 4.2: Synthesis of Polymer 2	74
Scheme 4.3: Synthesis of Polymer 3	76
Scheme 4.4: Proposed initial steps of the decomposition of the palladated complex.....	80
Scheme 4.5: Computational Explored Ligand Exchange Mechanism.....	81
Scheme 4.6: Proposed Decomposition Pathway Generating the Amine.....	87
Scheme 5.1: Synthesis of the Polymer Supported NHC-based Catalysts 6 , 7 and 9 Utilized in this Study.....	104
Scheme 5.2: The Catalytic Reactions that have been Employed to Evaluate Catalysts 6 , 7 and 9	105
Scheme 6.1: Synthesis of the Azide Functionalized Gold Nanoparticles.....	145
Scheme 6.2: Library of Alkynes Used as Substrates in the 1,3 Dipolar Cycloadditions and the Functionalized Nanoparticles before and after the Transformation.....	149
Scheme 6.3: Synthesis of the Palladium Complex Supported Gold Nanoparticles	153

LIST OF SYMBOLS AND ABBREVIATIONS

Ar	aryl
Bn	benzene
Bu	butyl
°C	degrees Celcius
cat.	catalytic
CDCl ₃	deuterated chloroform
CHCl ₃	chloroform
δ	chemical shift
DMF	N,N-dimethylformamide
DMSO	dimethylsulfoxide
EI	electron ionization
ESI	electron spray ionization
EtOAc	ethyl acetate
equiv	equivalent
g	gram
h	hour
HRMS	high-resolution mass spectrometry
Hz	Hertz
IR	infra red
J	coupling constant
λ	wavelength

M	molar
MeOH	methanol
Mes	mesityl benzene
mg	milligram
MHZ	megahertz
min	minute
mL	milliliter
mmol	millimole
mole	mole
mol%	mole percent
NHC	<i>N</i> -heterocyclic carbene
nm	nanometer
NMR	nuclear magnetic resonance
Ph	phenyl
ppm	part per million
s	second
TEM	transmission electron microscopy
THF	tetrahydrofuran

SUMMARY

In today's world, the need to limit the use of nonrenewable resources and the importance of recycling has been recognized. One important contribution of chemists toward the general goal of limiting their use is to find catalysts that can be reused and recycled thereby limiting the need for expensive metal precursors and metal waste. Strategies to recycle catalysts are multifold and range from the employment of soluble polymers as catalyst supports to the use of membrane-encapsulated catalyst. The use of soluble polymers as a support not only offers the advantage of being soluble under the catalytic reaction conditions but also, to be removable by changing the conditions of the surrounding media. Despite the great potential of these soluble supported catalysts, their use is very limited in today's synthesis. In addition, no set of rules have been established to guide the synthesis of efficient supported catalysts. In order to establish a "tool box" for the synthesis of supported catalysts, the study of several parameters such as the choice of the support and the choice and the stability of the catalyst are necessary. To establish this set of rules, a limited number of catalytic transformations, were studied. These catalytic reactions are the Heck-Mizoroki, Suzuki-Miyaura and Sonogashira coupling reactions. These transformations became fundamental for the synthesis of drugs and materials. The first and second chapters provide background information by describing and evaluating the main supports that were previously used for catalysts and the two main catalysts that are used in this thesis, the palladium pincer complex and the palladium *N*-heterocyclic complex. In chapter 3, the synthesis of a soluble polymer supported catalyst is described. The polymer chosen for the study is poly(norbornene), and the catalyst is a

1,3-disubstituted benzene ligand with sulfurs in the side-chains able to chelate to the metal center, better known as pincer ligand. These ligands are abbreviated by the three atoms that coordinate to the metal center, in this study, SCS. The metal used for the investigation of the activity of this supported pincer is palladium. The importance of the nature of the linkage on the stability of the Pd-SCS pincer complex has been reported in the literature, leading to the synthesis of Pd-SCS pincer complex tethered to the polymer via an ether and an amide linkage. The synthesized poly(norbornene) supported Pd-SCS pincer complexes were evaluated using the Heck transformation of iodobenzene with *n*-butyl acrylate. Kinetic studies and leaching tests using poly(vinyl pyridine) and mercury were carried out resulting in the conclusion that the active species during the catalysis is not the palladium pincer complex but a leached palladium (0) species. In chapter 4, Pd-PCP pincer complexes with the ether and amide tether were synthesized. Kinetic and poisoning studies were carried out resulting in a similar conclusion. Furthermore, ³¹P NMR experiments were conducted to investigate the unstability of the complex. Following this study, in-situ XAS as well as computational calculations were carried out. The conclusion from this investigation argues that triethylamine is a key ingredient for the decomposition of the Pd-PCP complex. The overall conclusion from these two different studies is that Pd(II) pincer complexes decomposes during the Heck reaction when triethylamine is used for the coupling of iodobenzene to *n*-butyl acrylate in DMF at 120 °C. Stemming from this investigation, a reported more stable complex, Pd-NHC, was tethered onto poly(norbornene). The system was evaluated using Suzuki-Miyaura, Heck and Sonogashira reactions. Similar poisoning and kinetic studies were utilized to investigate the stability of the supported NHC Pd complexes. The result of this

investigation suggests that supported Pd-NHC complexes are stable under Suzuki-Miyaura and Sonogashira but decompose under Heck conditions. However, when the system was recycled, a decrease in activity for the Suzuki-Miyaura transformation and solubility was observed. In chapter 6, gold monolayer protected clusters (MPC) were investigated as potential candidates as supports. To examine the potential of MPC as a support, a NHC-Pd complex was grafted onto the particles. To functionalize the gold nanoparticles, a new method was developed. Using azide moieties added to the gold nanoparticles, the catalyst was added via microwave assisted 1,3 dipolar cycloaddition. The system was evaluated using Suzuki-Miyaura transformations under microwave conditions. The system exhibited quantitative conversions for a variety of substrates. However, when the system was recycled, aggregation of the particles and decrease in catalytic activity was observed. In summary, this thesis describes the synthesis and evaluation of poly(norbornene) supported Pd-pincer and Pd-NHC complexes and of gold nanoparticles supported Pd-NHC complex. It also detail the combination of kinetic and poisoning studies developed to evaluate a potential supported catalyst.

CHAPTER 1

SUPPORTED CATALYSTS: AN OVERVIEW

Abstract

In this chapter, an overview of supported catalysts is presented. A brief description of diverse inorganic support with a focus on palladium is given. The inorganic supports discussed include Pd/C, Pd on metal oxides and Pd complexes supported on silica. The importance of these supports resides in the easiness to remove them from solution after the completion of the reaction. Organic polymer supports are discussed. Two main families are identified for these supports, the insoluble and soluble polymers. Insoluble polymers are evaluated using poly(styrene) supported Pd complexes and Co-salen complex used as a cross-linker as examples of the versatility of these supports. The soluble polymer section discusses the increase catalytic activity provided by these systems. Soluble polystyrene with Co-salen complex and poly(ethylene glycol) supported palladacycles. This last example became the basis on my research on the poly(norbornene) supported Pd-pincer complexes. Furthermore, the choice and design of the different supports is reviewed. The different catalysts selected to be supported are evaluated with a special attention for catalyst activities. The design principles for the catalytic systems are evaluated. Finally, an overall appraisal of the different systems reviewed is presented. Stemming from these reports, several questions stayed unanswered such as what is the effect of the support on the catalyst, what is the effect of the tethered on the stability of the metal complex, what kind of support should be used and what studies are necessary to evaluate the activity of the new synthesized systems.

1.1. Introduction

The increasing strain put on our natural resources leads scientists to devise different ways to limit the pollution and waste generation. Chemists addressed these issues by designing catalysts that can be recovered and recycled several times as another way to save resources and limit waste.^[1-3] A catalyst is defined often as a substance that increases the rate of a reaction without being consumed in the process.^[4] A more rigorous and precise definition was formulated by the UK Science Research Council in 1975 by: “A system is said to be ‘catalyzed’ when the rate of change from state I to state II is increased by contact with a specific material agent which is not a component of the system in either state, and when the magnitude of the effect is such as to correspond to one or more of the following descriptions:

- (a) Essentially, measurable change from state I to state II occurs only in the presence of the agent.
- (b) A similarly enhanced rate of change is found with the same sample of agent in repeated experiments using fresh reactants.
- (c) The quantity of matter changed is many times greater than that of the agent.”

Scientists have devised general ways to remove and recycle a given catalyst.^[2, 3] In the late 60s, early experiments using solid supports to reuse reagents and catalysts were reported.^[5] The interest in this new field grew considerably in the late 70s and early 80s.^[4, 6-9] The range of catalysts supported increased exponentially from enzymes to Pd complexes.^[2, 10] Furthermore, the range of supports expanded from solid polymers to silica and soluble polymers.^[6, 7, 10-12] In these systems three parts can be tuned, the

support, the linker and the catalyst (Figure 1.1). Any changes of any of these parameters can influence the behavior of the system during the reaction.^[2, 4]

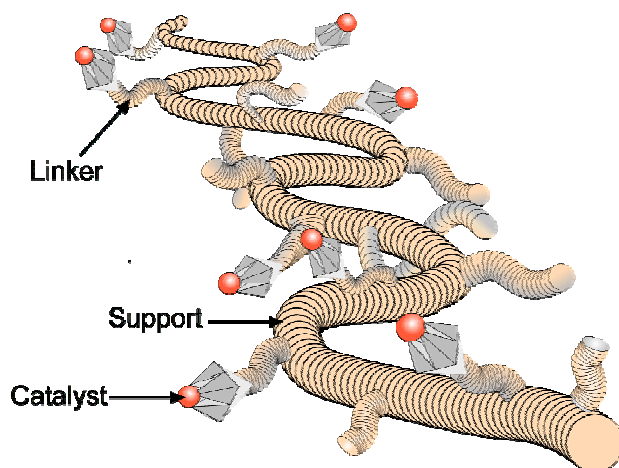


Figure 1.1. Schematic of the tunable variables of a supported catalyst

What are the advantages of supporting catalysts?

One of the main advantages of supported catalysts is the easiness to separate the catalyst from the reaction mixture.^[2, 4] In contrast to molecular catalysts, the separation of the often costly catalyst from the products after complete reaction is very difficult. By using supported catalysts, the separation can be achieved via a variety of methods ranging from coarse filtration to precipitation.

However, some disadvantages of using supported catalysts subsist, such as the low efficiencies of the catalysts and the low reproducibility of the catalysis due to the variation on the structure of the support.^[4] Furthermore, the lack of specificity is a major drawback of supported catalysts. Generally, supported catalysts are not as selective and

efficient as their homogeneous counterparts. Nevertheless, scientists have actively worked to overcome these drawbacks by identifying new supports to be used and by modifying well known catalysts to develop supported catalysts with better selectivity, reproducibility and efficiencies.^[4, 6-9]

Three different types of supports can be identified: organic polymers, inorganic solids and nanoparticles.

In this chapter, inorganic solid supports will be discussed, followed by organic polymer support and nanoparticles used as a support. An emphasis on supported palladium catalyst for coupling reactions will be given. The core of this thesis rests on the use of supported Pd complexes for a variety of coupling reactions. Following the evaluation of the carefully chosen examples, that illustrate the advantages and disadvantages of each type of support, the choice of supports that I investigated for my thesis will be discussed.

1.2. Inorganic Supports

Inorganic supports have been used in science for more than a century. They encompass a wide variety of materials from silica to zeolites. In this section, Pd on carbon (Pd/C) and Pd on metal oxides used for the Heck-Mizoroki reaction will be briefly reviewed. Pd on mesoporous materials for the oxidation of alcohols will be discussed more in details.

1.2.1. Pd on Carbon

Pd/C has been used since the early 70s for a wide variety of coupling reactions such as Suzuki-Miyaura and Heck-Mizoroki.^[13] The reaction of interest for this thesis is the Heck transformation because of its importance and its efficiency. The Heck-Mizoroki reaction consists of the coupling of an α -olefin with a halogenated aryl. Pd/C has been used extensively for the Heck-Mizoroki transformation.^[9] Numerous reports demonstrated the versatility of this heterogeneous catalyst with a variety of substrates such as activated aryl chloride, aryl iodides, iodopyrimidines or diazonium salts reacting with vinyl ethers, acrylates or styrenes.^[9, 14-18] It is important to note that these reactions are performed without the addition of extra ligands.

1.2.2. Pd on Metal Oxides

The use of Pd on metal oxides started in the 90s with MgO for the coupling of chlorobenzene with styrene.^[19] Since this report, numerous oxides have been used such as Al₂O₃, SiO₂, TiO₂, or ZrO₂ for the coupling of aryl halides with acrylates,^[20-22] acrylonitrile,^[23] alkene^[24] or styrene.^[25, 26]

1.2.3. Silica Supports

Mesoporous silica is widely used as a heterogeneous support for catalysts.^[11, 12, 27] This material comes in a variety of forms with different pore sizes and functionalities. The functionalization of these supports is usually accomplished by grafting a silica terminated functionality of a catalyst on the surface (Figure 1.2).^[11] These silica supports such as MCM-41 or SBA-15 have highly ordered channels and monodisperse pore

channels. They also have a high surface area allowing for a higher density of the functionality in the pores of the solid. Silica offers the advantage of having better mechanical and thermal stability than their homogeneous analogues. It also allows for easy removal of the catalyst by simple filtration.

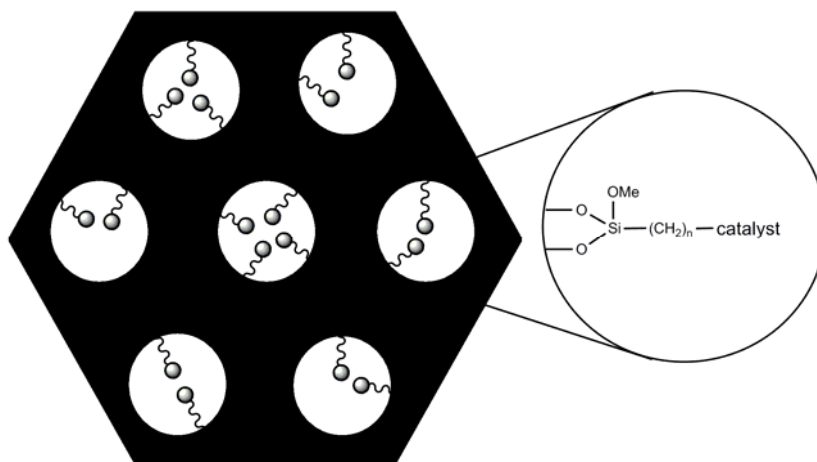


Figure 1.2. Schematic of Silica supported catalysts

A recent example illustrating the use of SBA-15 as a support shows the surface functionalization of the solid support with a bipyridylamide ligand complexed with $\text{Pd}(\text{OAc})_2$ (Figure 1.3).^[28] This example is very relevant to my thesis because the authors grafted a Pd complex on the support and evaluated the nature of the catalyst by conducting careful kinetic studies and leaching tests which are corner stones of my thesis investigations. This catalytic system was used for the aerobic oxidation of a variety of alcohols.

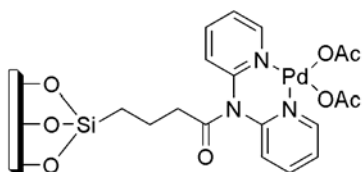


Figure 1.3. SBA-15 tethered Pd complex

The authors reported the use of this support up to twelve times without any losses in catalytic performance or purity of the product. Furthermore, the supported catalyst was tested for any leaching, and it was shown that the catalytically active species was the organometallic complex. The authors noted that because of the properties of SBA-15, catalyst aggregation was impossible in the pores contributing to the high stability of this catalyst.

1.3. Organic Polymers

Organic polymers have seen an increase in interest as support in catalysis in the past 20 years.^[4, 6, 8] The interest sparks from the different advantages that polymers offer over inorganic supports. They can be functionalized easily allowing for the tunability of the supports toward the chemical environment and are often chemically inert, assuring no interference with the catalyst.^[2] Organic polymers can be organized into two distinct categories, insoluble polymers and soluble polymers.

1.3.1. Insoluble organic polymers

The advantages offered by solid supports such as insoluble polymers are multiple, including mechanical stability, chemical inertness under reaction condition and easy removal from the reaction.^[3] The most common polymer used for solid phase synthesis is cross-linked poly(styrene).^[2, 3] It offers the advantage of being easy to synthesize and to functionalize. Furthermore, several type of poly(styrene) are commercially available with a choice of functionalities, different loading values, different diameter sizes and different degrees of cross-linking. The syntheses of poly(styrene) as a support consist of reacting crosslinkers, such as divinylbenzene as a comonomer, with styrene, resulting into a cross linked matrix.^[3] These newly synthesized resins are microporous when a cross-linking ratio of 0.2% to 2% is used and macroporous for a crosslinking ratio of more than 10%. In this section, microporous solid supported catalyst will be discussed.

Poly(styrene) supported phosphine-based transition metal complexes received a lot of attention early on.^[29] Phosphines are known to coordinate to a variety of transition metal such as Pd or Pt.^[3] Direct substitution of halogenated poly(styrene) by the desired phosphines is a straight forward way to obtain the desired moiety on the support.^[3] Following this substitution the metal can be introduced by ligand exchange. One of the most interesting use of these supported phosphine ligands is the introduction of Pd complexes for coupling reactions such as the Heck transformation. In the following example, a Pd(II) complex with a bidentate phosphine ligand was supported onto poly(styrene) (Figure 1.4).^[30] I chose this example because it is a perfect illustration of the use of solid supported catalyst for the Heck transformation and its added advantages over homogeneous Pd complexes. In this report the authors noted the high activity of

their catalyst toward the coupling of methyl acrylate with iodobenzene. Furthermore, the supported catalyst had a higher turnover number than its solution analogue. It was suggested that the solution analogue could aggregate and be deactivated, which is prevented when the catalyst is bound to a solid support. Finally, the catalyst was recycled 5 times without any substantial loss of activity. This article reports the successful support of a Pd(II) complex on a poly(styrene) resin for the Heck catalysis.

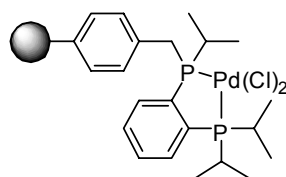


Figure 1.4. Pd(II) complex supported poly(styrene) resin

Another clever way to tether a catalyst on the support was introduced by Seebach *et al.* in 1999.^[31] The authors grafted complex chiral ligands such as BINAP or salen into the matrix of cross-linked poly(styrene). These ligands are introduced through the crosslinker by substituting both sides of the ligand with terminal alkenes (Figure 1.5). The crosslinker is then polymerized with styrene to yield the resin supported catalyst. Seebach *et al.* indicated that these newly supported catalysts performed as well as their small molecules analogues. The authors were able to recycle the catalyst several times with only small loss in activities and stereoselectivity. However, one of the major drawbacks of these different supported catalysts was the poor catalyst loading, of about 0.13-0.2 mmol/g, on the support.

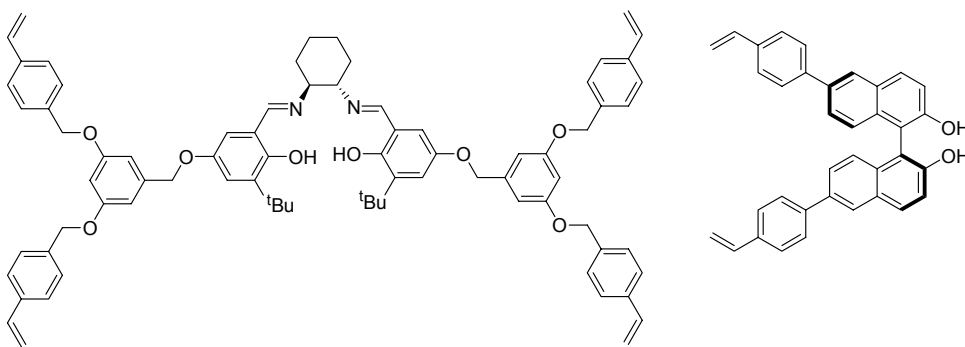


Figure 1.5. Crosslinkers with salen and BINAP ligands

In summary, catalysts supported on resins offer several major advantages such as easy removal and mechanical strength, however, the disadvantages associated with these supports outweigh their advantages. These disadvantages include poor catalyst loadings, slower reaction rates, challenging characterization of the system and in most cases loss in catalytic performance.

1.3.2. Soluble polymers

In contrast to insoluble polymer supports, soluble polymers offer a good handle on the loading of the catalyst with better selectivity and better rates, and the ability to use a multitude of analytical techniques to characterize the systems. Soluble polymers became very popular in the last 20 years starting with the use of poly(ethylene glycol).^[4] The emergence of the use of other soluble supports started a few years later with the functionalization of a variety of polymers and macromolecules such as dendrimers and

linear poly(styrene) (For an extensive list of polymers used as supports see Figure 1.6). In this section, a few examples of the PEG, dendrimers and linear poly(styrene) supported systems with their advantages and their drawbacks will be described. These systems are the most performants and gives a good idea of the different soluble polymers currently used by scientists.

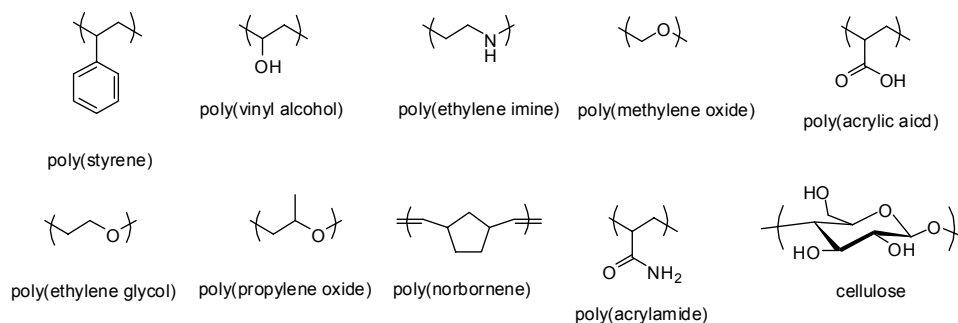


Figure 1.6. Soluble polymers used as a support for catalysts

1.3.2.1. Poly(ethylene glycol)

Poly(ethylene glycol) offers the advantage of being cheap, easy to produce and easy to modify. Furthermore, its intrinsic properties, such as the selective solubility, makes it the polymer of choice as a support for reusable catalyst.^[4] Poly(ethylene glycol) is not soluble at room temperature and needs to be heated to get into solution, as much as 1g of polymer in 10 mL of solvent can be dissolved, offering an easy way to remove the polymer after the reaction. After the catalysis, the reaction is cooled inducing the precipitation of the polymer (Figure 1.7). The polymer is then removed via centrifugation

or filtration. An abundance of publications show the close to quantitative removal of a variety of catalysts supported onto poly(ethylene glycol).^[4]

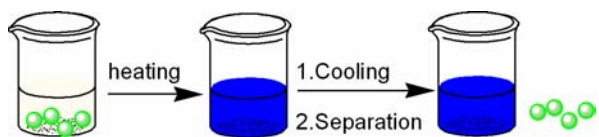


Figure 1.7. Schematic of the removal of PEG supported catalyst

An example of the efficiency of PEG as a support is the synthesis of diphenylphosphines terminated PEG.^[32] The authors determined that about 0.6 mol equivalent of PPh_2 were present per gram of oligomer. The phosphines were complexed with $\text{Pd}(\text{OAc})_2$ to give the active catalyst. This system was used for the dimerization of butadiene (Figure 1.8).

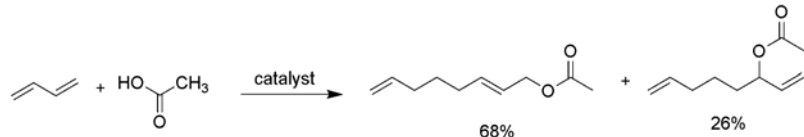


Figure 1.8. Butadiene dimerization reaction

The supported catalyst showed high efficiency and very good recyclability. Using the technique described above to remove the supported catalyst, the catalyst was reused up to five times without any noticeable loss of activity. This report is one of the first

examples of a supported Pd complex that can be reused several times. Stemming from this report, Bergbreiter *et al.* supported on PEG a 1,3-disubstituted benzene ligand with heteroatoms in the side-chains able to chelate to palladium, known as Pd-pincer complexes.^[33]

Poly(ethylene glycol) offers a good alternative to solid support by being soluble during the catalysis and solid at room temperature. However, one of the drawbacks of this system is its low catalyst loading.

1.3.2.2. Dendrimers

Dendrimers are macromolecules with perfectly branched repeat units emanating from a central core.^[8] These well-defined molecules can enable the precise control of the catalyst structure. They offer the advantage of being not only soluble in a variety of solvents but also recoverable by simple filtration or precipitation. These macromolecules can have selectivity and kinetics similar to their small molecules analogues. Furthermore, the highly controlled architecture of these systems allows for fine-tuning of the catalyst.^[8] There are two main ways that a dendrimer can be functionalized with a catalyst. It can be either functionalized on the periphery or in the core (Figure 1.9). Each method offers advantages and drawbacks. The periphery functionalized dendrimers offer the advantage of being highly functionalized, therefore having performance similar to their small molecule counterparts. These periphery functionalized systems have multiple reaction sites, being favorable for catalysis involving bimetallic mechanism. However, for catalysts having bimetallic mechanism deactivation, the periphery functionalized dendrimer can accelerate the deactivation process. The core functionalized dendrimers

can be more selective and more able to stop the bimetallic deactivation process. However, the synthesis of these systems is costly and their performance reduced due to site accessibility.

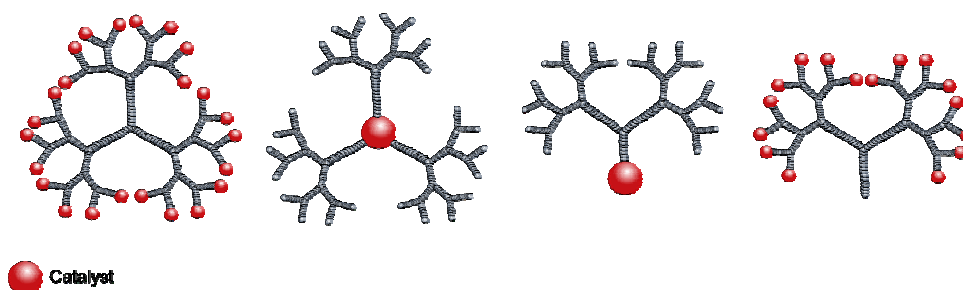


Figure 1.9. The different type of dendrimers and dendrons supported catalysts

One example of periphery functionalized dendrimers is the functionalization of G3 poly(propylene imine) with diphenyl phosphines (Figure 1.10).^[34] With diphenyl phosphines at the periphery of the dendrimer, Brinkmann *et al.* synthesized a variety of metal complexes using Ni, Ir, Pd or Rh precursors. In this example, the complex of interest is bis(diphenyl-phosphine)PdCl₂. The functionalization of this dendrimer with a Pd complex for Heck catalysis provides another example of a soluble supported Pd complex to be compared to the supported system of intent.

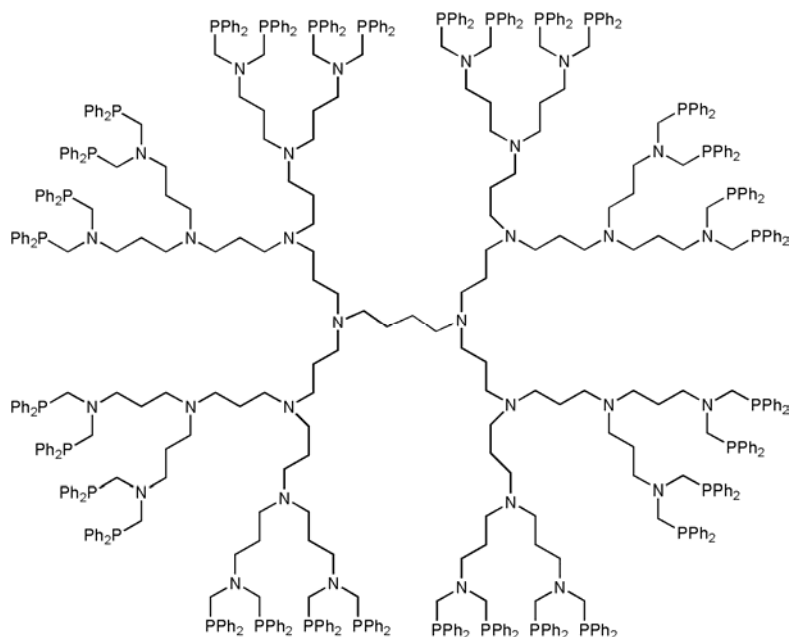


Figure 1.10. G3 poly(propylene imine) dendrimer functionalized with diphenyl phosphines at the periphery

The authors used the dendrimer supported Pd complex to catalyze the Heck reaction of iodobenzene with styrene. Using sodium acetate as the base and dimethylformamide as the solvent, they observed a conversion of 90%. The synthesized dendrimer system allowed them to recover the catalyst by simply adding diethyl ether to the mixture. Using this recovery process, the authors were able to recover the catalyst up to 98% after catalysis. Furthermore, they were able to reuse their catalyst at least three times without any significant loss of conversion for each consecutive catalysis. The authors also noted an increase of thermal stability compared to the low molecular weight analogues.

Dendrimers used as a support offers the advantages of being highly controllable and tunable. However, the prohibitive cost to synthesize or buy these macromolecules is a major drawback.

1.3.2.3. Poly(styrene)

Linear poly(styrene) used as a support benefits from the extensive work that has been carried out with this polymer and its cross-linked analogues. The monomer is easily modified with the desired functionality. Linear poly(styrene) can also be chloromethylated followed by the addition of the desired functionality.^[35]

Despite the widespread applications of poly(styrene) derivatives, only a few examples of catalysts supported on linear poly(styrene) have been reported.^[35] A very interesting example illustrating the stability of the poly(styrene) and the activity of the functionality is the grafting of the Co(II)-salen complex onto the polymer (Figure 1.11).^[36] The unique feature of this supported catalyst was the synthesis of an asymmetrical salen ligand to be attached on poly(styrene). The styrene salen monomer was synthesized and polymerized to 12mers and 24mers.

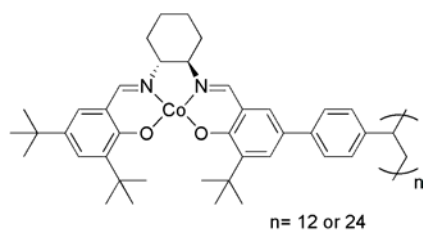


Figure 1.11. Poly(styrene) supported salen-Co complex

This supported Co(II)-salen catalyst was innovative by the way the salen was attached to the support. In earlier examples, the salen was tethered to the support from both sides of the ligand. Having this salen-Co catalyst in a pendant fashion is believed to be the contributing factor to the higher performance of this supported catalyst compared to previously reported systems. Furthermore, it offered the possibility to tune the loading of the catalyst by copolymerizing simple styrene unit with the ligand bound monomer. The supported salen-Co complex exhibited very similar catalytic performance for the hydrolytic kinetic resolution of epichlorohydrin (Figure 1.12) to its small molecule analogue. The reaction was completed in 2 hours with >99% ee. Furthermore, this system was recycled up to four times without any significant decreases in yields or enantioselectivity.

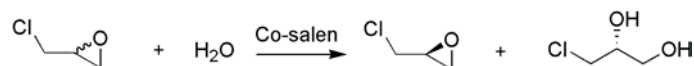


Figure 1.12. Hydrolytic kinetic resolution of epichlorohydrin

This example illustrates the versatility of linear poly(styrene) as a support and the ability to recycle this system without any significant losses in selectivity and conversions. However, one of the drawbacks of this method was the inability to introduce the Co metal to the monomer. It was noticed that the free radical polymerization could not occur with the metallated ligand. This problem adds uncertainties to the system and introduces

questions about the role non-coordinated salen can have during the catalysis, and the role of non-coordinated Co that can be trapped in the polymer matrix on catalyst performance.

1.4. Nanoparticles

Over the past few years, nanoparticles have emerged in the literature as a good alternative to the more common solid and polymer supports.^[37] The ability to easily functionalize these particles made these new systems attractive.^[38] Furthermore, their intrinsic properties depended on the type of particles synthesized and their capacity to be monodisperse, ranging from nanometer to micrometer scale, offering to scientists the ability to explore a new area that showed promising results.^[37]

One of the most interesting examples is the first silica coated nanoparticle supported Pd-NHC. In this study, the authors synthesized superparamagnetic maghemite ($\gamma\text{-Fe}_2\text{O}_3$) to support the palladium complex (Figure 1.13).^[39] The small size of these nanoparticles (~ 11 nm) allowed them to be partially soluble in organic solvents, making them homogeneous under reaction conditions. The authors carried out Suzuki, Heck and Sonogashira reactions with common reagents. The different coupling reactions yielded close to quantitative conversions with iodo and bromo-aryls. Furthermore, the nanoparticles could be removed from the reaction vessel using a small permanent magnet. When performing recycling experiments, the conversions for each coupling reactions slightly declined after each cycle yielding 93%, 92% and 89% for the Suzuki, Heck and Sonogashira coupling respectively for the fifth cycle.

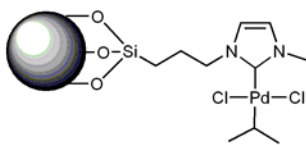


Figure 1.13. Palladium complex supported on superparamagnetic maghemite

1.5. Conclusion

The different supports described herein offer advantages and drawbacks. In our quest to find a good support, I chose a soluble polymer that we were very familiar with, poly(norbornene). Poly(norbornene) supports have the unique advantage that a) the support is often soluble during the catalytic reaction but can be removed from the reaction media and reused by simple precipitation methods, b) poly(norbornene)s can be synthesized *via* ring-opening metathesis polymerization (ROMP), a highly controlled, functional group tolerant and often living polymerization method that allows for the formation of controlled architectures such as random and block copolymers thereby allowing to control catalyst density,^[40-45] and c) as a result of its functional group tolerance, ROMP can be carried out on fully functional and characterized monomers thereby eliminating low yielding post-polymerization reactions. Another support that sparked our curiosity was gold nanoparticles. They offer unique properties such as being monodisperse and tunable. Furthermore, they are easy to synthesize and to functionalize. However, one of the most attractive features of these particles is the nearly infinite ability to solubilize them and precipitate them without any alteration or aggregation.

Stemming from these reviews, three supports were chosen, silica support for our heterogeneous catalysis, poly(norbornene) and gold nanoparticles for homogeneous catalysis. The next step for this project was to choose relevant catalyst to be supported

and studied. The next section will discuss the different catalysts that we chose and the antecedent in the literature supporting them.

1.6. References

- [1] W. A. Herrmann, K. Ofele, D. von Preysing, S. K. Schneider, *J. Organomet. Chem.* **2003**, 687, 229.
- [2] N. E. Leadbeater, M. Marco, *Chem. Rev.* **2002**, 102, 3217.
- [3] C. A. McNamara, M. J. Dixon, M. Bradley, *Chem. Rev.* **2002**, 102, 3275.
- [4] D. E. Bergbreiter, *Chem. Rev.* **2002**, 102, 3345.
- [5] C. C. Lezznoff, *Chem. Soc. Rev.* **1974**, 3, 65.
- [6] T. J. Dickerson, N. N. Reed, K. D. Janda, *Chem. Rev.* **2002**, 102, 3325.
- [7] Q.-H. Fan, Y.-M. Li, A. S. C. Chan, *Chem. Rev.* **2002**, 102, 3385.
- [8] R. van Heerbeek, P. C. J. Kamer, P. W. N. M. van Leeuwen, J. N. H. Reek, *Chem. Rev.* **2002**, 102, 3717.
- [9] L. X. Yin, J. Liebscher, *Chem. Rev.* **2007**, 107, 133.
- [10] A. G. M. Barrett, B. T. Hopkins, J. Kobberling, *Chem. Rev.* **2002**, 102, 3301.
- [11] G. Fink, B. Steinmetz, J. Zechlin, C. Przybyla, B. Tesche, *Chem. Rev.* **2000**, 100, 1377.
- [12] R. Duchateau, *Chem. Rev.* **2002**, 102, 3525.
- [13] M. Julia, M. Duteil, C. Grard, E. Kuntz, *Bull. Soc. Chim. Fr.* **1973**, 2791.
- [14] A. Eisenstadt, *Chem. Ind. (Dekker)* **1998**, 75, 415.
- [15] R. G. Heidenreich, J. G. E. Krauter, J. Pietsch, K. Köhler, *J. Mol. Catal. A* **2002**, 182-183, 499.

- [16] X. Xie, J. Lu, J. H. Bo Chen, X. She, X. Pan, *Tetrahedron Lett.* **2004**, 45, 809.
- [17] C. M. Andersson, A. Hallberg, J. G. Doyle Daves, *J. Org. Chem.* **1987**, 52, 3529.
- [18] S. S. Pröckl, W. Kleist, M. A. Gruber, K. Köhler, *Angew. Chem., Int. Ed.* **2004**, 43, 1881.
- [19] K. Kaneda, M. Higuchi, T. Imanaka, *J. Mol. Catal.* **1990**, 63, L33.
- [20] H. Hagiwara, Y. Shimizu, T. Hoshi, T. Suzuki, M. Ando, K. Ohkubo, C. Yokoyama, *Tetrahedron Lett.* **2001**, 42, 4349.
- [21] A. Biffis, M. Zecca, M. Basato, *Eur. J. Inorg. Chem.* **2001**, 1131.
- [22] F. Zhao, K. Murakami, M. Shirai, M. Arai, *J. Catal.* **2000**, 194, 479.
- [23] A. Wali, S. M. Pillai, S. Satish, *React. Kinet. Catal. Lett.* **1997**, 60, 189.
- [24] A. Cwik, Z. Hell, F. Figueras, *Adv. Synth. Catal.* **2006**, 348, 523.
- [25] M. Wagner, K. Köhler, L. Djakovitch, S. Weinkauf, V. Hagen, M. Muhler, *Top. Catal.* **2000**, 13, 319.
- [26] K. Köhler, M. Wagner, L. Djakovitch, *Catal. Today* **2001**, 66, 101.
- [27] F.-S. Xiao, *Top. Catal.* **2005**, 35, 9.
- [28] B. Karimi, S. Abedi, J. H. Clark, V. Budarin, *Angew. Chem., Int. Ed.* **2006**, 45, 4776.
- [29] S. Jang, *Tetrahedron Lett.* **1997**, 38, 1793.
- [30] P.-W. Wang, M. A. Fox, *J. Org. Chem.* **1994**, 59, 5358.
- [31] H. Sellner, C. Faber, P. B. Rheiner, D. Seebach, *Chem. Eur. J.* **2000**, 6, 3692.
- [32] D. E. Bergbreiter, D. A. Weatherford, *J. Org. Chem.* **1989**, 54, 2726.
- [33] D. E. Bergbreiter, P. L. Osburn, Y. S. Liu, *J. Am. Chem. Soc.* **1999**, 121, 9531.

- [34] M. T. Reetz, G. Lohmer, R. Schwickardi, *Angew. Chem., Int. Ed. Engl.* **1997**, *36*, 1526.
- [35] J. Chen, G. Yang, H. Zhang, Z. Chen, *React. Funct. Pol.* **2006**, *66*, 1434.
- [36] X. Zheng, C. W. Jones, M. Weck, *Chem. Eur. J.* **2006**, *12*, 576.
- [37] M.-C. Daniel, D. Astruc, *Chem. Rev.* **2004**, *104*, 293.
- [38] N. L. Rosi, C. A. Mirkin, *Chem. Rev.* **2005**, *105*, 1547.
- [39] P. D. Stevens, G. Li, J. Fan, M. Yen, Y. Gao, *J. Chem. Soc., Chem. Commun.* **2005**, 4435.
- [40] B. Chen, H. F. Sleiman, *Macromolecules* **2004**, *37*, 5866.
- [41] T.-L. Choi, R. H. Grubbs, *Angew. Chem., Int. Ed.* **2003**, *42*, 1743.
- [42] J. A. Love, J. P. Morgan, T. M. Trnka, R. H. Grubbs, *Angew. Chem., Int. Ed. Engl.* **2002**, *41*, 4035.
- [43] J. M. Pollino, L. P. Stubbs, M. Weck, *Macromolecules* **2003**, *36*, 2230.
- [44] C. Slugovc, S. Demel, S. Riegler, J. Hobisch, F. Stelzer, *J. Mol. Catal. A* **2004**, *213*, 107.
- [45] C. Slugovc, S. Riegler, G. Hayn, R. Saf, F. Stelzer, *Macromol. Rapid Commun.* **2003**, *24*, 435.

CHAPTER 2

ORGANOMETALLIC COMPLEXES INVESTIGATED IN THIS THESIS

Abstract

This chapter describes the different organometallic complexes that are studied in this thesis. A particular emphasis is given to palladium complexes catalyzing C-C coupling reactions, in particular, the Heck-Mizoroki, the Suzuki-Miyaura and the Sonogashira reactions. Pd-pincer complexes are described in depth giving background information about its performance as catalysts and its efficiencies when tethered on a support. A description of the work done by Morales-Morales and Jensen is given with their controversial mechanism of their catalytic Pd(II)/Pd(IV) cycle for Pd-pincer complexes. The depiction of the high stability and catalytic versatility of these palladacycle is given. It is followed by a description of the work Bergbreiter *et al.* have published describing poly(ethylene glycol) supported Pd-SCS pincer complexes. A review of N-heterocyclic carbene (NHC) complexes with the reaction it can catalyze is also given. Several examples of supported Pd-NHC complexes is described illustrating the stability of these organometallic complexes and their catalytic versatility. Following the presentation of both complexes, the key catalytic reactions investigated in this thesis is presented. A more in depth review is given about Heck catalysis using pincer complexes and Suzuki-Miyaura and Sonogashira coupling using NHC based metal complexes.

2.1. Pincer Complexes

2.1.1. Introduction

Metallated pincer complexes are defined as complexes containing a monoanionic tridentate ligands with an anionic core flanked by two neutral two electron donors on each side of the metal.^[1] These ligands are usually named after the three atoms that coordinate to the metal center, e.g. SCS, PCP, NCN, CNC, and CCC (Figure 2.1). These ligands can be complexed with a vast library of metals ranging from common metals such as palladium^[2] to exotic ones such as uranium.^[3] The resulting complexes can be employed in a variety of catalytic transformations.^[4] Palladated pincer complexes have been used widely not only for reactions such as the Heck, Suzuki or Sonogashira couplings,^[2, 5-11] but also for Michael additions,^[12, 13] boronations of allyl alcohols^[14] and asymmetric allylations.^[15] Iridium pincer complexes have been studied extensively as dehydrogenation catalysts.^[4, 16] Rhodium and ruthenium pincer complexes have also been reported but only few studies have been carried out to investigate their catalytic activities.^[17, 18] The second area of intense research activity using metallated pincer complexes is the employment of these pincer complexes as tunable metal coordination recognition units in self-assembly.^[19-21]

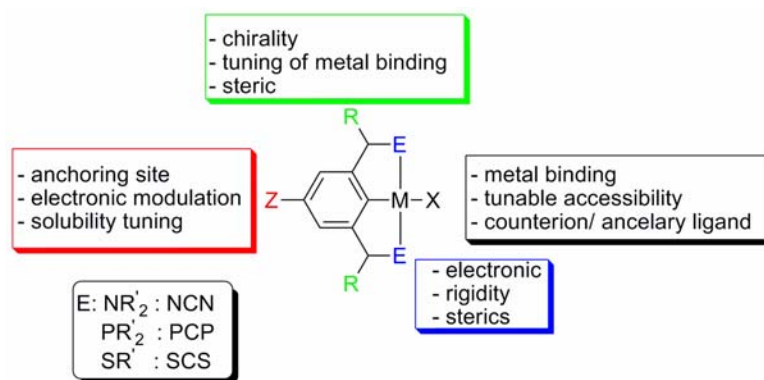


Figure 2.1. Metallated Pincer Complex

2.1.2. Coupling chemistry using pincers complexes

The perceived stability of pincer complexes, made them perfect suitors for reactions such as Heck or Suzuki couplings. The Heck-Mizoroki reaction consists of the coupling of an α -olefin with a halogenated aryl. The mechanism of this reaction involves an oxidative addition of an aryl halide to the Pd complex, followed by a 1,2-insertion of the alkene cosubstrate to yield the desired product after a β -elimination (Figure 2.2).

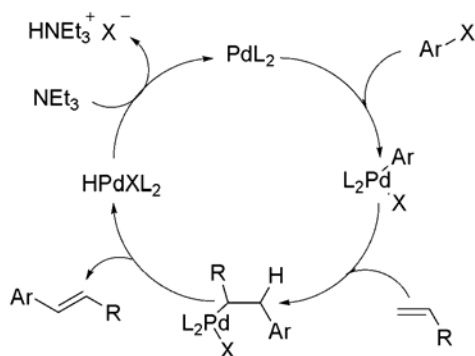


Figure 2.2. Catalytic cycle of Heck-Mizoroki reaction

The Suzuki-Miyaura coupling involves the coupling of an aryl boronic acid with an aryl halide. The mechanism of this reaction involves the oxidative addition of the aryl boronic acid, followed by the transmetalation of the boronate substrate to finally generate the desired product via reductive elimination (Figure 2.3).

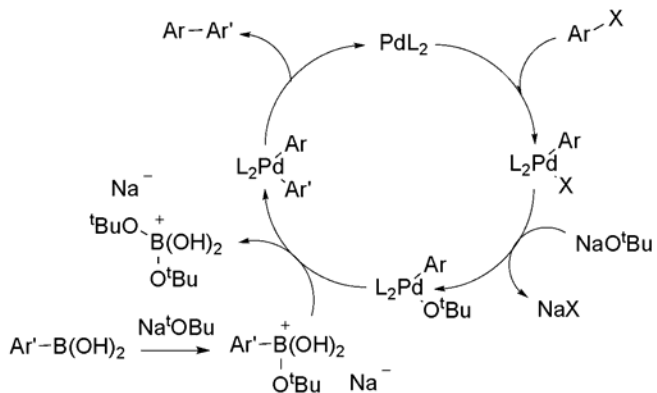


Figure 2.3. Catalytic cycle of the Suzuki-Miyaura reaction

These reactions became corner stones of organic chemistry for their contribution in the synthesis of drugs and materials.^[4]

Taking PCP pincers, Milstein *et al.* reported a high turnover of up to 500,000, for the coupling of iodobenzene with methylacrylate at 140 °C with no sign of decomposition.^[2] Stemming from these reports, several groups developed better performing PCP pincers for the Heck-Mizoroki reaction.^[22-24] While these complexes showed great promise, speculations were raised about the mechanism of the catalysis.^{[23,}
^{24]} The typical mechanism for Heck catalysis involves a Pd(0)/Pd(II) cycle,^[25] however, the PCP pincer complex has a Pd(II) center. Jensen and Morales-Morales proposed a new catalytic cycle involving Pd(II)/Pd(IV) species (Figure 2.4).^[23, 24] This mechanism is still under debate and has not been proven so far. At the same time, several groups investigated the activity of these pincer complexes for the Suzuki-Miyaura coupling.^[26, 27] The results confirmed the high activity of these complexes, with a turnover of up to 92,000 for the coupling of phenyl boronic acids with bromobenzene, and their stability under reaction conditions.^[26]

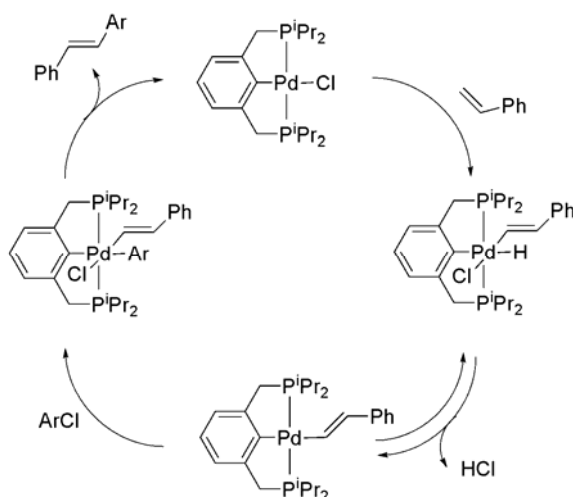


Figure 2.4. Heck reaction mechanism using Pd(II) pincer complexes proposed by Jensen and Morales-Morales

2.1.3. Supported pincer complexes

With the wide variety of transformations that metallated pincer complexes are able to catalyze and the stability of metallated pincer complexes under wide reaction conditions, several groups started to investigate the activity of such complexes on supports (some examples of supported pincer complexes are presented in Figure 2.5).^[2, 8] The goal of these studies was to synthesize highly stable, recoverable and recyclable catalysts. To accomplish this goal, metallated pincer complexes, in particular palladated complexes were immobilized on different supports ranging from polymers to clays.^[9, 28, 29] Bergbreiter and coworkers immobilized Pd-SCS pincer complexes onto poly(ethylene glycol) and investigated their catalytic activities in the Heck coupling of iodobenzene with methyl acrylate and styrene.^[5, 6, 30-32] In general, the authors found that the activities

of these supported complexes are comparable to their small molecule analogous. Furthermore, they were able to show that the supported complexes could be recycled by simple precipitation of the polymer and reused.^[5, 6, 30-32] It was noted that some decomposition was occurring for some supported Pd-SCS pincer complexes.^[5] However, Bergbreiter *et al.* seemed to circumvent this problem by modifying the tether of the ligand to the polymer.^[5, 6, 30-32] A similar system was reported by Pollino and Weck using poly(norbornene) to support Pd-SCS type pincer complexes.^[9] They demonstrated that a reaction mixture containing poly(norbornene)-supported Pd-SCS type pincer complexes was highly active in the Heck coupling of iodobenzene with a variety of acrylates, affording near quantitative conversions for each reaction.^[33]

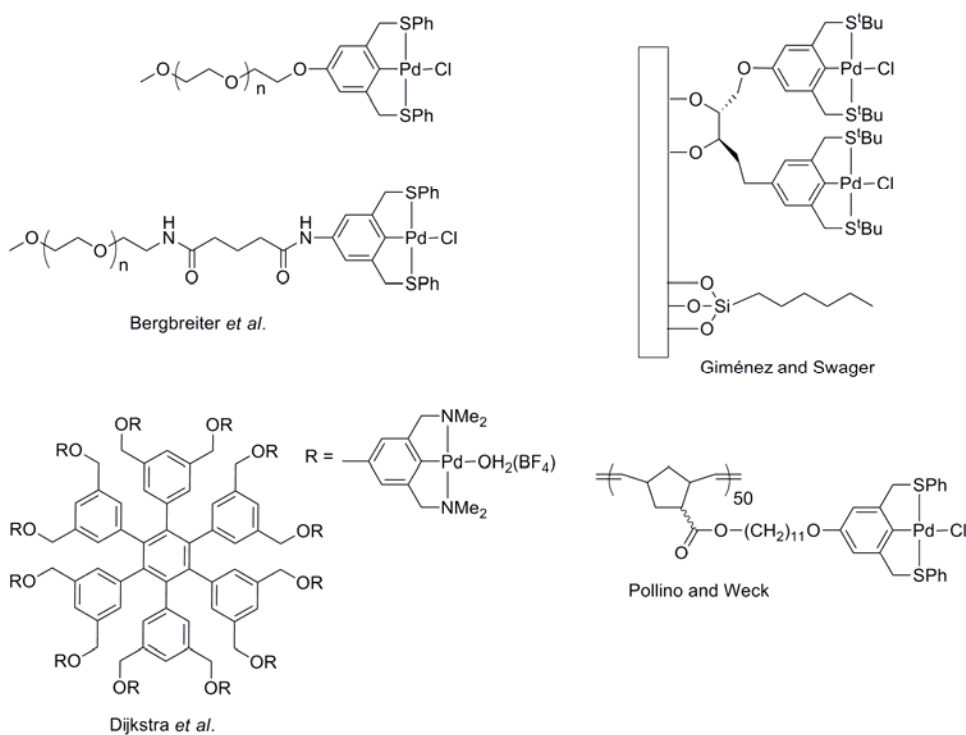


Figure 2.5. Examples of supported pincer complexes

Using a modified approach toward supported pincer complexes, Dijkstra *et al.* synthesized different generations of metallo dendrimers with Pd-NCN pincer complexes as peripheral groups.^[34, 35] The authors studied the activity of their second generation dendrimers containing twelve palladated pincer complexes in a running continuous nanofiltration membrane in the Michael addition of methyl vinyl ketone with α -cyanoacetate. Only slight decreases in conversions after five cycles were observed.^[34, 35] Silica immobilized second generation PAMAM dendrimers with Pd-PCP pincer complexes at the periphery were also employed as supported catalyst. Chanthateyanonth

et al. investigated the cyclocarbonylation of 2-allylphenol using these supported complexes.^[36] Conversions ranging from 87% to 99% after three catalytic cycles were obtained.^[36] A similar support was used by Giménez *et al.* to support dinuclear Pd-SCS pincer complexes.^[28] In this work, the authors studied the activity of their catalysts in the aldol reaction of methylisocyanoacetate. They found similar activities for their system in comparison to the small molecule analogous.^[28] A less common support was used by Poyatos *et al.* who supported Pd-CNC pincer complexes onto montmorillonite K-10 clay and investigated the activity of these complexes in the Heck coupling reaction of bromobenzene with styrene.^[29] They were able to recycle their catalyst up to ten times without noticing any significant decrease in conversions.^[29, 37] Another example in this field came from Atlava *et al.* who supported Pd-CCC pincer complexes onto Merrifield resins as potential catalysts for the Heck reaction between aryl halides and various alkenes.^[38] Quantitative conversions for several supported complexes within 24 hours were obtained.

These different reports evaluated the activities and stabilities of supported pincer complexes and concluded that these organometallic complexes were highly stable under reaction conditions and very active for a wide range of catalytic reactions. Furthermore, our group had good expertise on the SCS pincer synthesis having worked extensively with this complex. Therefore, metallated pincer complexes were chosen as catalysts of choice to be supported on poly(norbornene) and on silica.

2.2. *N*-Heterocyclic carbenes

2.2.1. Introduction

N-Heterocyclic carbenes, first synthesized by Arduengo, have been studied extensively over the past decade (Figure 2.6).^[39-44] This class of ligands has several advantages over the closely related phosphine ligands including their increased stability to high temperatures and air.^[43-49] Over the past decade, metal complexes containing NHC ligands have been utilized as catalysts for a variety of transformations.^[44, 50-52] The vast majority of all reports employ NHC-containing ruthenium complexes as catalysts in olefin metathesis, with RCM getting the most attention.^[52-58] Olefin metathesis catalysts based on NHC ligands have the highest activities reported to date.^[52, 56] Furthermore, they are able to catalyze RCM reactions of sterically demanding compounds and are tolerant to a wide variety of functional groups resulting in the transformation of adducts that were unreactive to earlier olefin metathesis catalysts.^[52, 59]

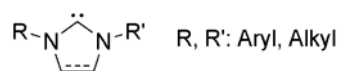


Figure 2.6. *N*-Heterocyclic carbene ligand

2.2.2. Coupling chemistry with *N*-heterocyclic carbenes

N-Heterocyclic carbenes were metallated with Pd and used as catalysts in Heck catalysis.^[49] The coupling of aryl bromides and aryl chlorides with α -olefin was reported with yields >99% and low catalyst loading of 0.1-1 mol%.^[44] Following this report, several research groups used this new ligand for the Suzuki coupling of aryl chlorides

with aryl boronic acids. It was reported as being the most active agent for aryl chlorides coupling with aryl boronic acids.^[44] The advantages of these systems were the user-friendly procedure that was developed and the ease of synthesizing *N*-heterocyclic carbenes. A new type of unsymmetrical NHC ligands was developed a few years later showing great activity for Suzuki, Heck and Sonogashira couplings (Figure 2.7).^[60, 61] The authors reported turnover numbers of 1.7×10^6 for the Heck coupling of bromoacetophenone with butyl acrylate and 1.1×10^5 for the Suzuki coupling of bromoacetophenone with phenylboronic acid.^[60, 61]

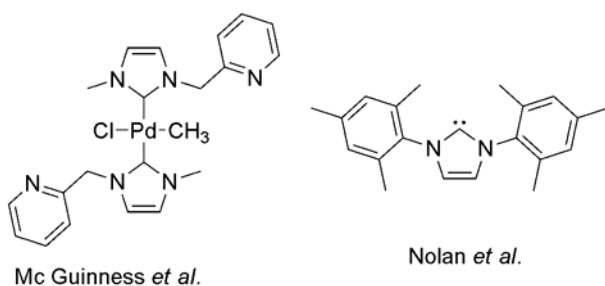


Figure 2.7. Examples of highly active Pd-*N*-heterocyclic complex and ligand

2.2.3. Supported *N*-heterocyclic carbenes

Since organometallic NHC complexes have shown great performances in a wide variety of reactions, demonstrating their utility in the synthesis of complex molecules that have applications ranging from drug precursors to polymers, they are perfect candidates to be supported. Several research groups have made significant contributions towards the synthesis of supported NHC complexes and shown that the catalytic activity is indeed

maintained.^[62-65] Over the past five years, NHCs have been grafted onto different supports ranging from monolithic supports to soluble poly(styrene)s.^[62, 66, 67] The following examples illustrate important advantages and disadvantages of supporting NHC complexes.

The first report of a polymer supported NHC-Pd complex was provided by Herrmann and coworkers in 2000.^[68] They used a di-NHC chelate ligand coordinated to a palladium halide complex (Figure 2.8). The authors anchored this complex through the NHC ligand onto an insoluble poly(styrene)-based Wang resin. They studied the catalytic activity of their system for the Heck reaction. By carrying out several coupling reactions with activated and non-activated arylbromides, they were able to get quantitative conversions for most of the substrates tested. Furthermore, the authors also conducted recycling experiments for the coupling reaction of 1-(4-bromo-phenyl)-ethanone with styrene yielding near quantitative conversions for up to fifteen cycles. However, Herrmann *et al.* noticed small amounts of palladium leaching after each cycle suggesting, at least, partial decomposition.

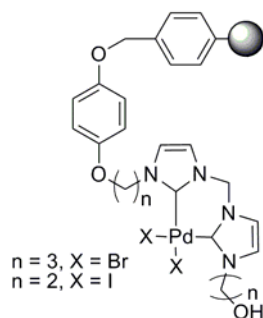


Figure 2.8. Merrifield resin supported Pd-NHC complex

In close analogy to their report of a supported olefin metathesis catalyst onto poly(2-oxazoline), Weberskirch and coworkers presented a supported Pd-NHC complex onto the same support (Figure 2.9).^[69] Again, this water soluble amphiphilic polymer with hydrophobic pendant chains, containing the Pd-NHC complexes, forms micelles. Weberskirch *et al.* investigated the activity of their catalyst for the Suzuki and Heck coupling reactions in water. For the Heck transformation, they optimized their system for each polymer by screening different bases and different reaction temperatures for the coupling of styrene with iodobenzene. The authors reported the highest TOF (2700 h^{-1}) with quantitative conversions for the Heck catalysis of iodobenzene with styrene using K_2CO_3 at 110°C in water. A similar process has been implemented for the Suzuki transformation of activated and non-activated aryl iodides and bromides with phenyl boronic acid. TOF up to 5200 h^{-1} were obtained with quantitative conversions for the Suzuki reaction in water at 110°C . Following this report, Weberskirch *et al.* fully characterized the system using gel-permeation chromatography, TEM and dynamic light

scattering.^[69] They determined the size of the micelle aggregates to be 10-30 nm. Finally, they conducted recycling experiments for the Heck catalysis of iodobenzene with styrene at 90 °C with K₂CO₃ as the base. Decreased conversions from 89% for the first cycle to 76% for the third one were obtained. The authors argued that the separation of the micelles from the product might play a role in the lower conversions for the later cycles.

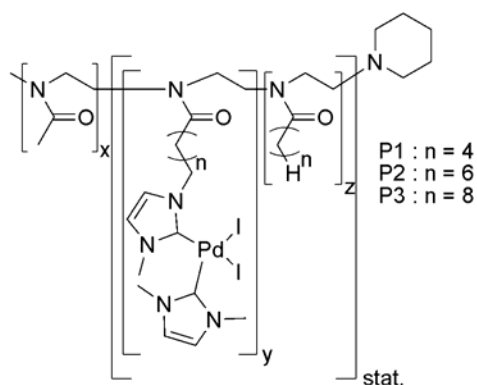


Figure 2.9. Polymer supported Pd-NHC complex

A more recent report on Pd-NHC complexes supported on insoluble supports comes from Karim and Enders who described the immobilization of an NHC-Pd complex/ionic liquid matrix onto silica (Figure 2.10).^[70] They studied the activity of the catalytic system towards the Heck catalysis of aryl iodide with alkyl acrylates and showed that their catalytic system was highly active with nearly quantitative conversions

for most of the Heck transformations studied. They finally recycled their catalyst three times yielding up to 89% conversions after 26 hours for the third cycle.

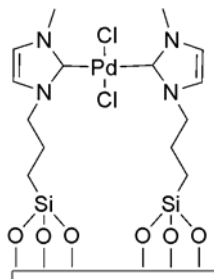


Figure 2.10. Silica supported Pd-NHC complex

These specific reports illustrate the stability and versatility of the NHC ligand. Its stability to reaction condition as well as its easy to be synthesis made this ligand an ideal candidate to be supported on poly(norbornene). Furthermore, the highly controlled ring-opening metathesis polymerization (ROMP) of palladium functionalized norbornenes will allow us to tune the catalyst loading and the solubility of our system.

2.3. Design Elements and challenges

The major goal of this thesis is to develop a set of tools to guide the synthesis of supported catalysts. To achieve this goal, we need to understand the impact of each component of our supported catalyst on our catalysis. These factors are the support, the

tether of the catalyst to the support and the catalyst. Several objectives are essential to the achievement of our goal.

These objectives include,

- The evaluation of the catalyst to be supported. We need to choose a stable system that is efficient and that catalyzes important transformation. The palladated pincer and *N*-Heterocyclic carbene are prime candidates to the different key criteria that were identified. At the start of my thesis research, palladated pincer complexes had been widely studied and showed high activity toward a wide variety of catalytic transformations. Palladated pincer complexes had been reported to be stable under reaction conditions and they catalyze one of the most prominent transformations, the carbon coupling transformation.
- The evaluation of the support to be used. The supports of interest have to meet several characteristics: i) they need to be removable from the reaction, ii) they need to be easily modifiable; and iii) they need to be tunable. The supports chosen are the poly(norbornene) and gold nanoparticles. Poly(norbornene) was chosen for its highly controlled polymerization using the Grubbs catalyst. The norbornene monomer also allows for easy functionalization and the polymerization catalyst tolerates a wide array of functionalities. The functionalities that will be added are Pd-SCS complex, Pd-PCP complex, Pd-NHC and Ru-NHC complexes. Gold nanoparticles are easily synthesized and can be functionalized with different functionalities.

- The design, synthesis and evaluation of the newly synthesized system. The chosen catalysts, Pd-SCS, Pd-PCP, Pd-NHC and Ru-NHC, need to be modified to be tethered on the different support. Pd-SCS pincer complexes have been studied by the Weck group for their self assembly abilities. The studies were conducted using poly(norbornene) as a support. The synthesis for the supported Pd-SCS complex has been previously reported. The modification of Pd-PCP complexes for its tethering on the polymers, has not been reported. The synthesis of this complex will have to be determined. Pd-NHC complex has a limited history on supports. However, the synthesis and modifications of the NHC ligand is straightforward. The Pd-pincer complexes and Pd-NHC complexes were carefully chosen for their tolerability to modifications causing minimal impacts on their activities.
- The catalysis tethered on the different supports will have to be evaluated using a set of well-known catalytic reaction, the Heck-Mizoroki, the Suzuki-Miyaura, and the Sonogashira transformations. The Heck-Mizoroki has been described in chapter 1, this is the coupling of usually an halogenated aryl with a terminal olefin. The Suzuki-Miyaura reaction is the cross- coupling between a halogenated aryl and an organoboronic acid aryl. The Sonogashira coupling, consist on the coupling of aryl or vinyl halides with terminal alkynes. The mechanism of this reaction starts with the oxidative addition of the halogenated substrate onto the Pd complex,

followed by the transmetallation of the copper acetylide and finally, the generation of the desired product by reductive elimination (Figure 2.11).

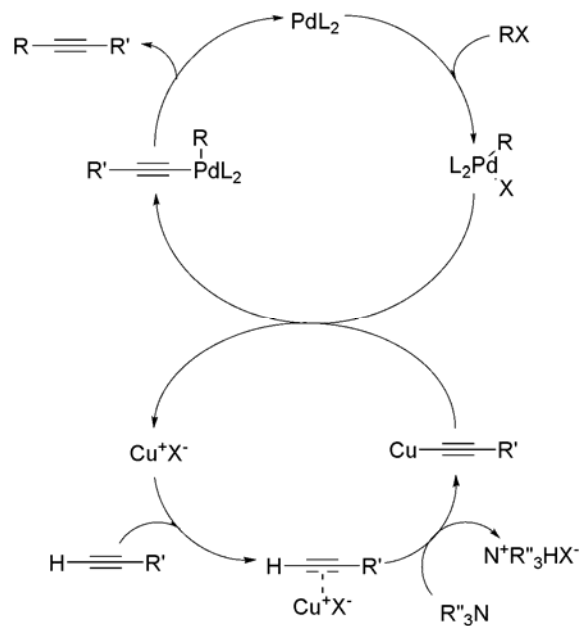


Figure 2.11. Catalytic cycle of the Sonogashira reaction

- The stability of the Pd complexes for each system. Each supported catalyst will go through different tests to evaluate if the catalytic species is actually the organometallic complex tethered on the support. The test will consist on adding molecules that can trap any leached Pd, such as mercury, poly(vinyl pyridine) or quadrapure. These tests will help to determine if

the supported catalyst act as well as palladium reservoirs or if the supported complex is the actual catalyst. These studies are crucial to determine if the catalytic complexes that were chosen are actually stable.

This thesis will address the different objectives aforementioned. The progress toward achieving our goal follows four major achievements. The design and the synthesis of palladated SCS pincers with different tethers on a variety of supports conducted us to design different test to evaluate the active catalytic species under reaction conditions (Chapter 3), the design and synthesis of a believed to be more stable pincer complex, the PCP-Pd pincer, with a thorough study of the catalysis and the decomposition of the complex (Chapter 4), the synthesis and evaluation of a new candidate, the *N*-Heterocyclic carbene palladium complex supported on poly(norbornene) (Chapter 5), the synthesis of salen-Co and *N*-Heterocyclic carbene palladium complexes on gold nanoparticles (Chapter 6), and will conclude with Chapter 7 describing new perspectives that this work brought and the new support and catalyst that can be studied to add new data in our “tool box”.

2.4. References

- [1] C. J. Moulton, B. L. Shaw, *J. Chem. Soc., Dalton Trans.* **1976**, 1020.
- [2] M. Ohff, A. Ohff, M. E. van der Boom, D. Milstein, *J. Am. Chem. Soc.* **1997**, *119*, 11687.
- [3] D. Pugh, J. A. Wright, S. Freeman, A. Danopoulos, *J. Chem. Soc., Chem. Comm.* **2006**, 775.

- [4] D. Morales-Morales, R. Redon, C. Yung, C. M. Jensen, *Inorg. Chim. Acta* **2004**, 357, 2953.
- [5] D. E. Bergbreiter, P. L. Osburn, Y. S. Liu, *J. Am. Chem. Soc.* **1999**, 121, 9531.
- [6] D. E. Bergbreiter, P. L. Osburn, A. Wilson, E. M. Sink, *J. Am. Chem. Soc.* **2000**, 122, 9058.
- [7] F. E. Hahn, M. C. Jahnke, V. Gomez-Benitez, D. Morales-Morales, T. Pape, *Organometallics* **2005**, 24, 6458.
- [8] M. Ohff, A. Ohff, D. Milstein, *J. Chem. Soc., Chem. Commun.* **1999**, 4, 357.
- [9] J. M. Pollino, M. Weck, *Org. Lett.* **2002**, 4, 753.
- [10] J. Vicente, J.-A. Abad, J. López-Serrano, P. G. Jones, C. Nájera, L. Botella-Segura, *Organometallics* **2005**, 24, 5044.
- [11] M. E. Van der Boom, D. Milstein, *Chem. Rev.* **2003**, 103, 1759.
- [12] I. P. Beletskaya, A. V. Chuchuryukin, G. van Koten, H. P. Dijkstra, G. P. M. van Klink, A. N. Kashin, S. E. Nefedov, I. L. Eremenko, *Russ. J. Org. Chem. (Engl. Transl.)* **2003**, 39, 1342.
- [13] K. Takenaka, M. Minakawa, Y. Uozumi, *J. Am. Chem. Soc.* **2005**, 127, 12273.
- [14] V. J. Olsson, S. Sebelius, N. Selander, K. J. Szabó, *J. Am. Chem. Soc.* **2006**, 128, 4588.
- [15] O. A. Wallner, V. J. Olsson, L. Eriksson, K. J. Szabó, *Inorg. Chim. Acta* **2005**, 359, 1767.
- [16] X. Zhang, T. J. Emge, A. S. Goldman, *Inorg. Chim. Acta* **2004**, 357, 3014.
- [17] T. Karlen, P. Dani, D. M. Grove, P. Steenwinkel, G. van Koten, *Organometallics* **1996**, 15, 5687.

- [18] M. Bassetti, A. Capone, M. Salamone, *Organometallics* **2004**, 23, 247.
- [19] J. M. Pollino, L. P. Stubbs, M. Weck, *Macromolecules* **2003**, 36, 2230.
- [20] J. M. Pollino, M. Weck, *Synthesis* **2002**, 9, 1277.
- [21] J. M. Pollino, M. Weck, *J. Am. Chem. Soc.* **2004**, 126, 563.
- [22] M. Beller, T. H. Riermeier, *Eur. J. Inorg. Chem.* **1998**, 29.
- [23] D. Morales-Morales, R. Redon, C. Yung, C. M. Jensen, *J. Chem. Soc., Chem. Commun.* **2000**, 17, 1619.
- [24] D. Morales-Morales, C. Grause, K. Kasaoka, R. Redon, R. E. Cramer, C. M. Jensen, *Inorg. Chim. Acta* **2000**, 300, 958.
- [25] I. P. Beletskaya, A. V. Cheprakov, *Chem. Rev.* **2000**, 100, 3009.
- [26] R. B. Bedford, S. M. Draper, P. N. Scully, W. S. L., *New J. Chem.* **2000**, 24.
- [27] D. Zim, A. S. Gruber, G. Ebeling, J. Dupont, A. L. Monteiro, *Org. Lett.* **2000**, 2, 2881.
- [28] R. Gimenez, T. M. Swager, *J. Mol. Catal. A.* **2001**, 166, 265.
- [29] M. Poyatos, F. Márquez, E. Peris, C. Claver, E. Fernandez, *New J. Chem.* **2003**, 27, 425.
- [30] D. E. Bergbreiter, *Chem. Rev.* **2002**, 102, 3345.
- [31] D. E. Bergbreiter, J. Li, *J. Chem. Soc., Chem. Comm.* **2004**, 42.
- [32] D. E. Bergbreiter, P. L. Osburn, J. D. Frels, *J. Am. Chem. Soc.* **2001**, 123, 11105.
- [33] J. M. Pollino, M. Weck, *Synthesis* **2002**, 9, 1277.
- [34] H. P. Dijkstra, N. Ronde, G. P. M. van Klink, D. Vogt, G. Van Koten, *Adv. Synth. Catal.* **2003**, 345, 364.

- [35] H. P. Dijkstra, M. Q. Slagt, A. McDonald, C. A. Kruithof, R. Kreiter, A. M. Mills, M. Lutz, A. L. Spek, W. Klopper, G. P. M. v. Klink, G. v. Koten, *Eur. J. Inorg. Chem.* **2003**, 830.
- [36] R. Chanthateyanonth, H. Alper, *Adv. Synth. Catal.* **2004**, 346, 1375.
- [37] E. Peris, R. H. Crabtree, *Coord. Chem. Rev.* **2004**, 248, 2239.
- [38] B. Altava, M. I. Burguete, E. García-Verdugo, N. Karbass, S. V. Luis, A. Puzary, V. Sans, *Tetrahedron Lett.* **2006**, 47, 2311.
- [39] A. J. Arduengo, III, F. Davidson, H. V. R. Dias, J. R. Goerlich, D. Khasnis, W. J. Marshall, T. K. Prakasha, *J. Am. Chem. Soc.* **1997**, 119, 12742.
- [40] A. J. Arduengo, III, R. L. Harlow, M. Kline, *J. Am. Chem. Soc.* **1991**, 113, 361.
- [41] A. J. Arduengo, III, R. Krafczyk, R. Schmutzler, *Tetrahedron* **1999**, 55, 14523.
- [42] N. M. Scott, S. P. Nolan, *Eur. J. Inorg. Chem.* **2005**, 1815.
- [43] F. K. Zinn, M. S. Viciu, S. P. Nolan, *Ann. Rep. Prog. Chem., Sect. B: Org. Chem.* **2004**, 100, 231.
- [44] W. A. Herrmann, *Angew. Chem., Int. Ed.* **2002**, 41, 1290.
- [45] M. Regitz, *Angew. Chem., Int. Ed. Engl.* **1996**, 35, 725.
- [46] J. Huang, L. Jafarpour, A. C. Hillier, E. D. Stevens, S. P. Nolan, *Organometallics* **2001**, 20, 2878.
- [47] D. Bourissou, O. Guerret, F. P. Gabbaï, G. Bertrand, *Chem. Rev.* **2000**, 100, 39.
- [48] H. M. Lee, C. Y. Lu, C. Y. Chen, W. L. Chen, H. C. Lin, P. L. Chiu, P. Y. Cheng, *Tetrahedron* **2004**, 60, 5807.
- [49] W. A. Herrmann, C. Köcher, *Angew. Chem., Int. Ed. Engl.* **1997**, 109, 2256.

- [50] W. A. Herrmann, M. Elison, J. Fisher, C. Köcher, G. R. J. Artus, *Angew. Chem., Int. Ed. Engl.* **1995**, *34*, 2371.
- [51] A. C. Hillier, G. A. Grasa, M. S. Viciu, H. M. Lee, C. Yang, S. P. Nolan, *J. Organomet. Chem.* **2002**, *653*, 69.
- [52] T. M. Trnka, R. H. Grubbs, *Acc. Chem. Res.* **2001**, *34*, 18.
- [53] E. L. Dias, S. T. Nguyen, R. H. Grubbs, *J. Am. Chem. Soc.* **1997**, *119*, 3887.
- [54] A. Fürstner, L. Ackermann, B. Gabor, R. Goddard, C. W. Lehmann, R. Mynott, F. Stelzer, O. R. Thiel, *Chem. Eur. J.* **2001**, *7*, 3236.
- [55] A. Fürstner, O. R. Thiel, L. Ackermann, H.-J. Schanz, S. P. Nolan, *J. Org. Chem.* **2000**, *65*, 2204.
- [56] J. Huang, E. D. Stevens, S. P. Nolan, J. L. Petersen, *J. Am. Chem. Soc.* **1999**, *121*, 2674.
- [57] K. Weigl, K. Köhler, S. Dechert, F. Meyer, *Organometallics* **2005**, *24*, 4049.
- [58] E. Despagne-Ayoub, R. H. Grubbs, *Organometallics* **2005**, *24*, 338.
- [59] R. H. Grubbs, *Tetrahedron* **2004**, *60*, 7117.
- [60] D. S. McGuinness, K. J. Cavell, *Organometallics* **2000**, *19*, 741.
- [61] C. Zhang, J. Huang, M. L. Trudell, S. P. Nolan, *J. Org. Chem.* **1999**, *64*, 3804.
- [62] M. R. Buchmeiser, *New J. Chem.* **2004**, *28*, 549.
- [63] M. R. Buchmeiser, *Catal. Today* **2005**, *105*, 612.
- [64] A. H. Hoveyda, D. G. Gillingham, J. J. V. Veldhuizen, O. Kataoka, S. B. Garber, J. S. Kingsbury, J. P. A. Harrity, *Org. Biomol. Chem.* **2004**, *2*, 8.
- [65] S. C. Schürer, S. Gessler, N. Buschmann, S. Blechert, *Angew. Chem., Int. Ed. Engl.* **2000**, *39*, 3898.

- [66] K. Grela, M. Tryznowski, M. Bienek, *Tetrahedron Lett.* **2002**, 43, 9055.
- [67] L. Jafarpour, M.-P. Heck, C. Baylon, H. M. Lee, C. Mioskowski, S. P. Nolan, *Organometallics* **2002**, 21, 671.
- [68] J. Schwarz, V. P. W. Bohm, M. G. Gardiner, M. Grosche, W. A. Herrmann, W. Hieringer, G. Raudaschl-Sieber, *Chem. Eur. J.* **2000**, 6, 1773.
- [69] D. Schönfelder, K. Fischer, M. Schmidt, O. Nuyken, R. Weberskirch, *Macromolecules* **2005**, 38, 254.
- [70] B. Karimi, D. Enders, *Org. Lett.* **2006**, 8, 1237.

CHAPTER 3

POLYMER AND SILICA SUPPORTED SCS-Pd PINCER

Abstract

This chapter compiles the results obtained with different supported SCS-Pd pincer complexes. SCS-Pd(II) pincer complexes were covalently bound to silica (SBA-15), poly(norbornene) and merrifield resin via either ether, amide or urea linkages. Stemming from previous results reported in the literature on the role of the functional group linking the complex to the support on the stability of the Pd-SCS pincer complex, the different systems synthesized were evaluated in the Heck coupling of iodobenzene with *n*-butyl acrylate. Kinetic experiments for each system were conducted to determine the kinetic order of the catalytic reaction. From these studies, induction time was observed, hinting that the Pd complex had to go through some transformation before being catalytically active. To sustain this hypothesis, poisoning studies using poly(vinyl pyridine) and mercury as trap to any leached out palladium were conducted for each system. The results showed total quenching of the catalytic activity when either poison was used. These results confirmed our hypothesis of a chemical transformation of the complex before the catalysis. The overall results of the kinetic and poisoning studies indicates that the SCS-Pd(II) pincer complexes decompose when triethylamine is used as a base in DMF at 120 °C for the Heck coupling of *n*-butyl acrylate with iodobenzene, independently of the nature of the linkage between the catalyst and the support. The supported complexes acts solely as reservoir of catalytically active palladium(0),

responsible for the catalysis. Contrary to literature reports, no evidence of catalysis by the SCS-Pd(II) pincer complex was found.

The research described in this chapter was highly collaborative. All research on silica was performed by the research group of Professor Christopher Jones.

3.1. Introduction

As described in chapter 2, pincer complexes with palladium have been touted as one of the most promising, well defined catalyst for Heck and Suzuki coupling reactions.^[1-5] The reported stability and activity of the pincer complexes made it a perfect catalyst to be immobilized. The pincer complexes were immobilized onto poly(norbornene) and silica (Figure 3.1).^[6, 7] Two basic classes of supports were investigated: supports that are soluble under reaction conditions and insoluble supports. Poly(norbornene) was chosen as the soluble support. The ring-opening metathesis polymerization (ROMP) of functionalized norbornenes is a demonstrated living polymerization that permits good control of catalyst loading and the incorporation of other functionalized co-monomers.^[8-15] Finally, because of its solubility under reaction conditions, the catalysis can be carried out under homogeneous conditions while having the ability to recover the polymer supported catalysts through simple precipitation methods.^[6, 7, 13, 16-18] Additionally, the use of nanoporous silica SBA-15 as a solid support was also investigated. The advantage of heterogeneous silica supported catalysts is their easy recovery.^[6, 7, 18]

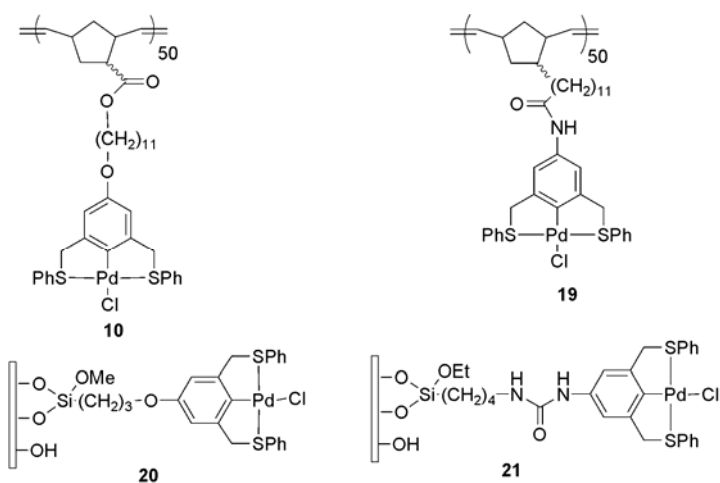
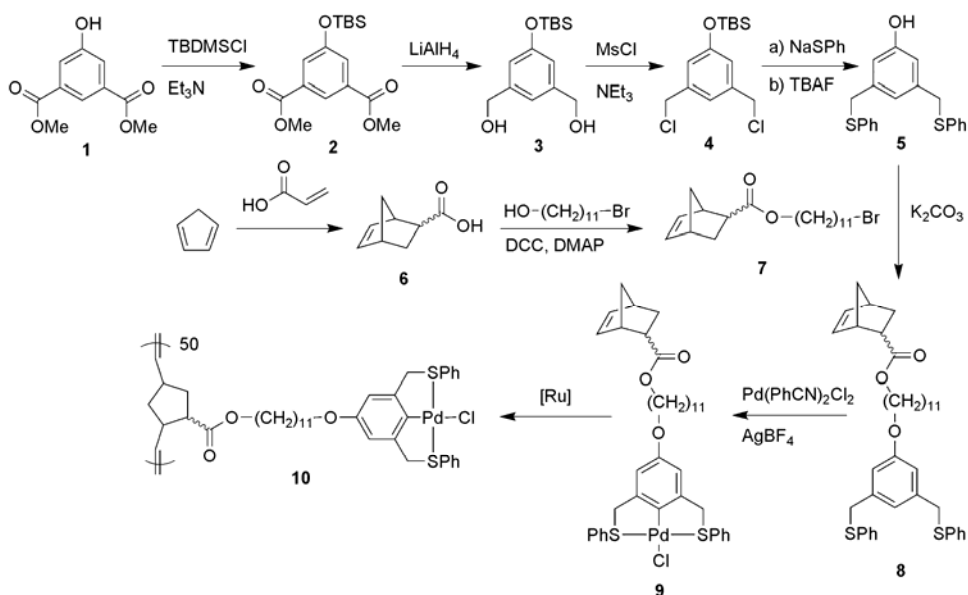


Figure 3.1. Supported pincer complexes synthesized.

3.2. Ether linked SCS-Pd Pincers

The first metallated pincer complexes that we, in collaboration with the Jones group, investigated for their stability under reaction conditions were Pd(II)-SCS pincer complexes supported on SBA-15 (100 Å pore size) and poly(norbornene) (Figure 3.1).



Scheme 3.1. Synthesis of poly(norbornene) supported SCS-Pd pincer.

The poly(norbornene) supported SCS-Pd pincer complex was synthesized following previously reported procedures (Scheme 3.1).²⁰

The stability of all catalysts was investigated through a series of kinetic studies as well as poisoning experiments. In the leaching studies, activation times of up to 20 minutes were observed for the poly(norbornene) and silica supported catalyst. Furthermore, when the silica supported catalysts were recycled, a decline in conversions after each run was detected. (Figure 3.2)

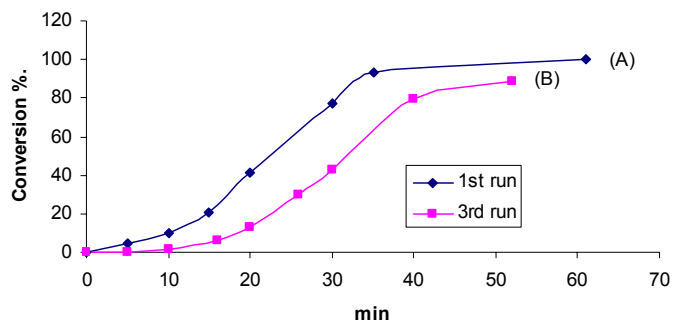


Figure 3.2. Recycling of silica supported O-SCS-Pd pincer.

To strengthen our findings further, a three-phase test was conducted. This test, proposed by Lipshutz *et al.* consists of anchoring one of the reagents onto a solid support while using a solid supported catalyst.^[19] Catalysis can not occur unless the catalyst leaches from the support to interact with the anchored substrate. Dr. Yu, from the Jones group, immobilized iodobenzene onto nanoporous silica and added, SCS-Pd pincer complexes tethered via an ether linkage to nanoporous silica (**20**), as the catalyst (Figure 3.3).

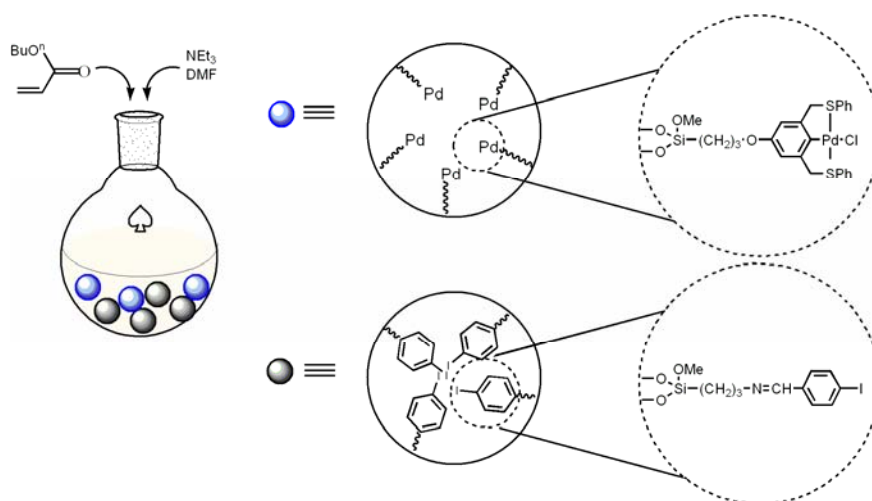


Figure 3.3. Three phase test.

Under the Heck reaction conditions conversions of the anchored iodobenzene were observed. These results suggested that some Pd was leaching out of the Pd-pincer complexes. To verify this hypothesis, a filtration test was carried out by removing the silica supported catalyst from the reaction mixture, followed by the addition of new reagents to the filtrate. Conversions of the newly added reagents were observed, confirming our hypothesis that leached Pd species were at least partially responsible for the catalysis.

3.2.1. Poisoning Studies

To further investigate if catalysis occurred on the supported Pd-pincer complexes, a variety of poisoning studies were carried out. These poisons were selected to bind selectively to ‘unprotected’ Pd(0) sources, *i.e.* Pd(0) species that are not protected by a

well-defined ligand. These poisons were designed to remove any unprotected Pd(0) species from the reaction solution, thereby shutting down any catalytic activity arising from them. If the supported Pd(II) pincer complexes were responsible for the catalysis, conversions should be observed even in the presence of the poisons. The first poison that was employed was poly(vinyl pyridine) (PVPy). PVPy is heterogeneous under reaction conditions and is known to coordinate to Pd(0).^[6, 7, 20, 21] The second poison was mercury which is able to form an amalgam with Pd(0) thereby removing the palladium from the reaction solution (Figure 3.4). It has been demonstrated that mercury (0) only binds to heterogeneous metal particles and not to homogeneous ligand protected molecular metal. To probe this, a reaction was setup where the Pd-SCS pincer complex is known to remain bound to the ligand during the transformation. The Weck group has done extensive studies with SCS-Pd pincer complexes as recognition unit for self-assembly of pyridines. The reaction consisted of reacting **10** with an equimolar amount of pyridine in the presence of a three hundred fold excess of mercury. The self assembly event can easily be monitored via ¹H NMR. The reaction showed quantitative self-assembly of the pyridine with the Pd-SCS complex in the presence of mercury, confirming that mercury could not interact with the molecular homogeneous SCS-Pd pincer complex.

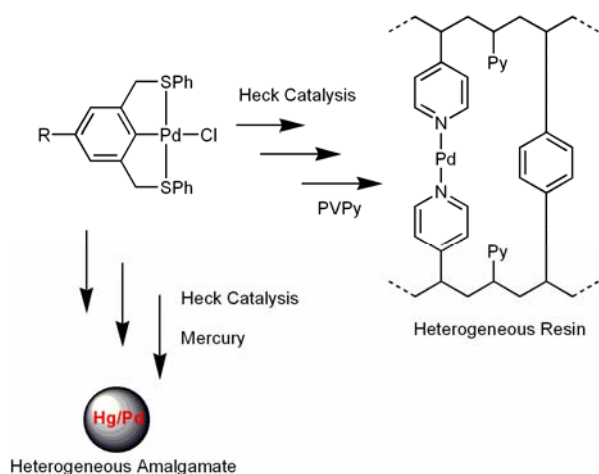


Figure 3.4. Poisoning Studies.

Both poisoning methods terminate any catalytic activity of unprotected Pd(0) species by sequestration and removal from the reaction medium.^[20, 22, 23] Again, it is important to note that both of these poisons have no effect on molecular organometallic catalysts. The PVPy tests were carried out with all supported Pd(II)-SCS-O-pincer complexes by adding the poison at the beginning of the reaction and, in a different reaction, after 40% conversion was achieved. If PVPy was added at the beginning of the Heck reaction containing either **10** or **20**, no conversions were observed. When adding the PVPy poison after 40% conversions, catalysis was completely quenched (Figure 3.5).

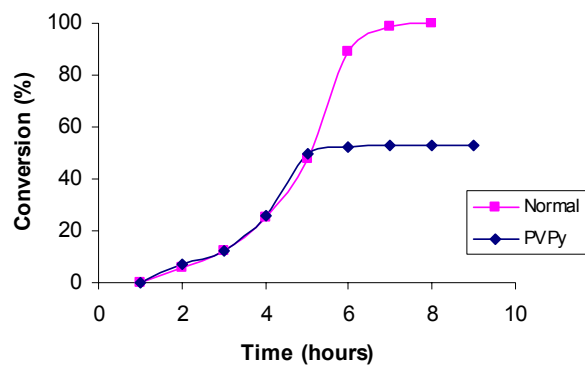


Figure 3.5. Kinetic plots of poly(norbornene) supported O-SCS-Pd pincer.

Addition of Hg(0) to a reaction mixture containing either **10** or **20** resulted in negligible conversions in all case (Figure 3.6).

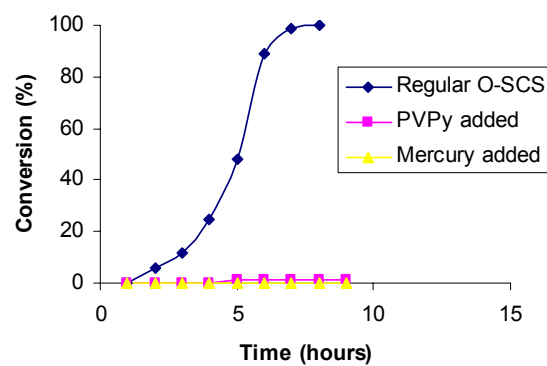


Figure 3.6. Kinetic plot of poison containing catalysis for poly(norbornene) supported O-SCS-Pd pincer.

The combination of these kinetic investigations, three-phase test and poisoning studies proved that Pd(II)-SCS pincer complexes tethered with an ether linkage onto supports such as mesoporous silica or onto poly(norbornene) are not catalytically active in the Heck reaction but act solely as a Pd reservoir. This conclusion was not fully unexpected since Bergbreiter *et al.* evoked a decrease in activity when they examined Pd(II)-SCS pincer complexes tethered to poly(ethylene glycol) (**22**) via an ether linkage in the Heck reaction (Figure 3.7).^[7] In the same contribution, supported Pd(II)-SCS pincer complexes attached to the poly(ethylene glycol) support via an amide linkage (**23**) instead of the ether linkage were suggested as fully stable catalysts since no decrease in activity was observed when carrying out recycling experiments.^[6, 7]

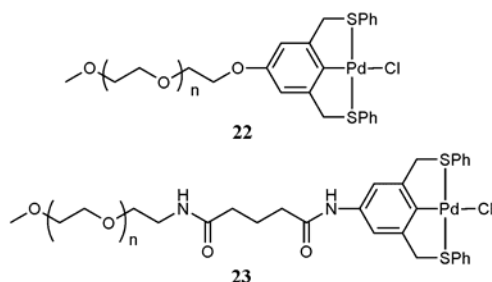
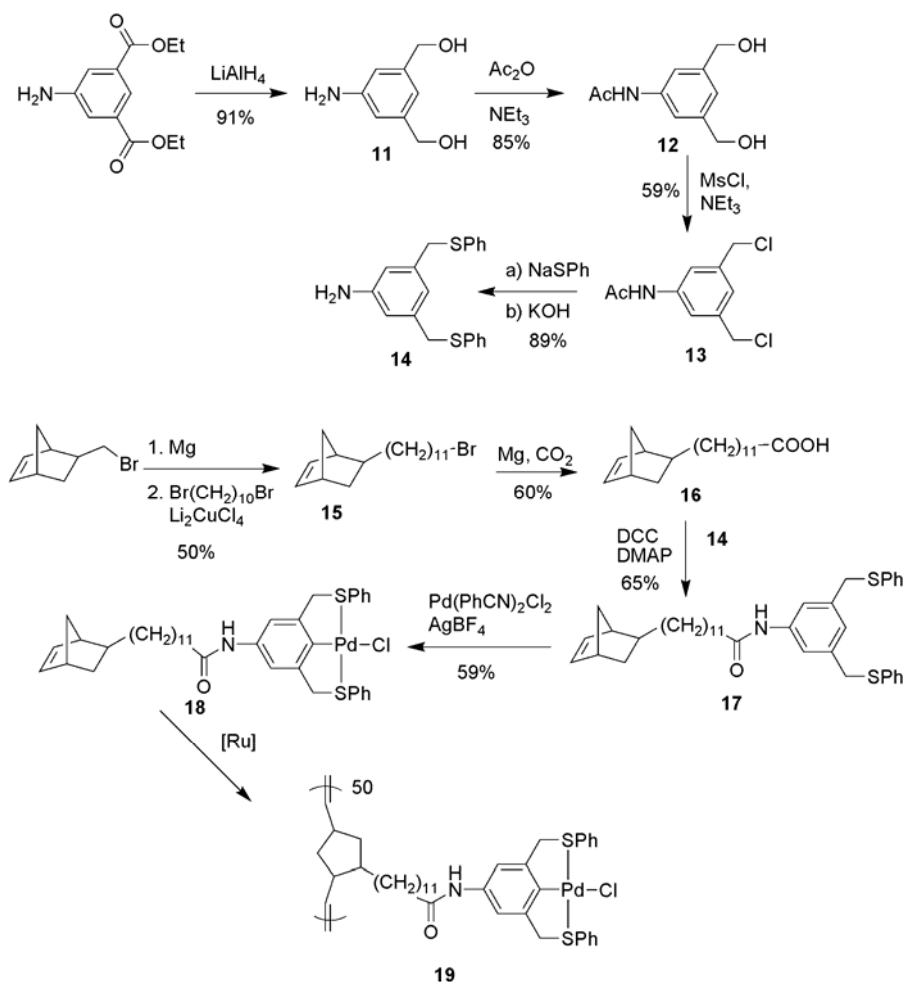


Figure 3.7. Supported SCS-Pd pincer complexes synthesized by Bergbreiter *et al.*.

3.3. Nitrogen linked SCS-Pd Pincer complexes

To investigate these potentially stable complexes, supported Pd(II)-SCS pincer complexes tethered to their respective support via an amide linkage were synthesized (Scheme 3.2).



Scheme 3.2. Synthesis of amide linked supported SCS-Pd pincer.

Three supports were investigated: poly(norbornene) (**19**), nanoporous silica (**21**) and Merrifield resin. The activities of all amide linked Pd-pincer complexes in the Heck

catalysis of iodobenzene and *n*-butyl acrylate were faster with no induction times observed (Figure 3.8).

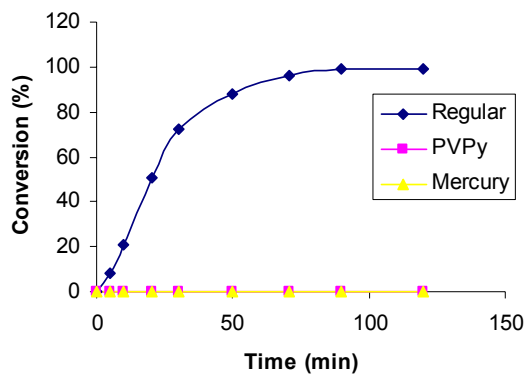


Figure 3.8. Kinetic plots of poly(norbornene) supported N-SCS-Pd pincer.

However, when **21** was recycled and reused, an induction time of up to ten minutes was observed after the first run and the activity decreased for each additional run (Figure 3.9).

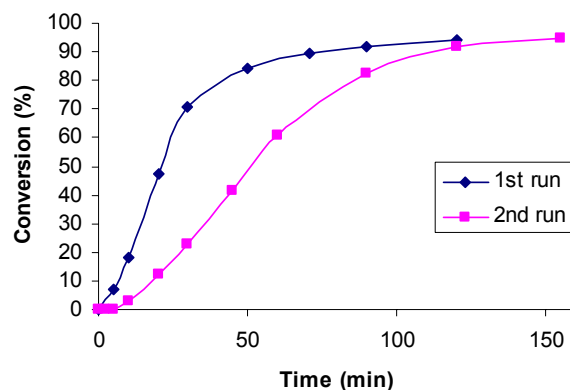


Figure 3.9. Recycling experiment using SBA-15 supported N-SCS-Pd pincer (**21**).

Kinetic and poisoning tests as outlined for the Pd(II)-SCS-O-pincer complexes were carried out to test the true active species of these catalysts. The use of PVPy or Hg(0) yielded negligible reactivities with any of the amide linked supported catalysts (Figure 3.8).

When the solid supported Pd(II) pincer complexes were removed by filtration, the filtrate was still able to convert freshly added reagents. Clearly, the amide tethered Pd(II)-SCS complexes are not stable under Heck reaction conditions. At the same time, Bergbreiter *et al.* conducted leaching studies on their supported Pd(II) SCS pincer complexes **22** and **23**.^[24] They conducted kinetic experiments where significant induction times were observed, which were dependent on the amount of reactants, water and other additives present. Additionally, a series of “competition” reactions by adding phosphines to the Heck reaction was carried out. Bergbreiter *et al.* observed a reduction in activity when phosphines were added suggesting that Pd(0) was trapped by the

phosphine ligands. They also carried out a filtration test by removing their polymer from the reaction mixture and adding fresh reagents to the filtrate. They noticed significant conversions from the “catalyst free” solution. The overall conclusions from their studies were similar to ours, confirming that supported SCS-Pd pincer complexes are not the actual catalysts during the Heck reaction.^[6, 7, 24]

3.4. Conclusion

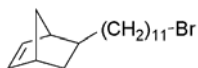
The presented results suggest that all investigated supported Pd(II)-SCS pincer complexes are not stable under Heck reaction conditions and the actual catalytic species is a leached Pd(0) species following the well-known basic Pd(0)-Pd(II) catalytic cycle. Following these conclusive results that SCS-Pd pincers are not stable, I decided to carry out similar studies with PCP-Pd pincers.

3.5. Experimental section

All reactions with air- and moisture sensitive compounds were carried out under dry nitrogen/argon atmosphere using an MBraun UniLab 2000 dry box and/or standard Schlenk line techniques. DMF, *n*-butyl acrylate, and NEt₃ were distilled over calcium hydride. 5-amino-isophthalic acid dimethyl ester, poly(4-vinylpyridine), 3-isocyanatopropyltriethoxysilane and all bases were obtained from commercial sources and generally used without further purification. Gas chromatographic analyses were performed on a Shimadzu GC 14-A gas chromatograph equipped with a flame-ionization detector and with a HP-5 column (length = 30 m, inner diameter = 0.25 mm, and film thickness = 0.25 μm). The temperature program for GC analysis was the following:

heating from 50 °C to 140 °C at 30K/min and heating from 140 °C to 300 °C at 40 K/min under constant pressure with inlet and detector temperatures kept constant at 330 °C. ¹H (300 MHz) and ¹³C NMR (75 MHz) spectra were recorded on a Varian Mercury VX instrument. All spectra were referenced to residual proton solvent. Mass spectral analyses were provided by the Georgia Tech MassSpectrometry Facility using a VG-70se spectrometer. Gel-permeation Chromatography (GPC) analyses were carried out using a Waters 1525 binary pump coupled to a Waters 2414 refractive index detector. The GPC was calibrated using poly(styrene) standards on a Styragel[®] HR 4 and HR 5E column set with CH₂Cl₂ as an eluent. FT-Raman spectra were obtained on a Bruker FRA-106. At least 128 scans were collected for each spectrum, with a resolution of 2-4 cm⁻¹. Elemental analyses were carried out by either Atlantic Microlabs, Norcross GA (CHN analyses) or Galbraith Laboratories, Inc., TN (determination of the palladium loadings of the silica precatalysts). The poly(norbornene)-SCS-Pd pincer was synthesized following previously reported procedures.^[16] Compound **14** was synthesized in three steps following a previously reported procedure.^[25]

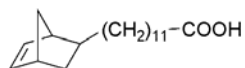
Synthesis of 5-(11-bromoundecyl)bicyclo[2.2.1]hept-2-ene (**15**)



To a stirred solution of THF (50 mL) an Mg (1.652 g, 67 mmol) was added norbornene methyl bromide (9.35 g, 50 mmol). The solution was refluxed for 10 h before being slowly added to a mixture of 1,10-dibromodecane (10 g, 100 mmol) and Li₂CuCl₄

(9 mL, 0.1 M in THF) in THF (100 mL) at -10 °C. The solution was allowed to stir for 24 h at room temperature, at which point it was then washed with ammonium chloride, extracted with diethyl ether (3 × 100 mL), dried over MgSO₄ and the solvent was removed under vacuum. The product was further purified by column chromatography (hexanes); yield: 7.48 g (50%). ¹H NMR (CDCl₃, 300 MHz): δ = 6.08-6.05 (m, 2H, CH=CH), 3.37 (t, *J* = 6.9 Hz, 2H, CH₂Br), 2.72 (t, *J* = 3.2 Hz, 2H), 1.93 (m, 1H), 1.83 (m, 2H), 1.82 (m, 19H), 1.03 (m, 1H), 0.46 (m, 1H); ¹³C NMR (CDCl₃, 300 MHz): δ = 136.6, 135.9, 132.3, 49.5, 46.3, 45.4, 42.5, 41.8, 38.7, 36.6, 34.8, 33.9, 32.8, 32.4, 29.9, 29.6, 29.5, 28.8, 28.7, 28.2. HRMS (EI): *m/z* = 327.1; anal. calcd. for C₁₈H₃₁Br: C, 66.04; H, 9.54; found: C, 66.33; H, 9.59.

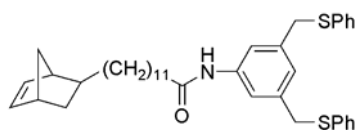
Synthesis of 12-bicyclo[2.2.1]hept-5-en-2-yl-dodecanoic acid (16)



Magnesium (474 mg, 19.5 mmol) and THF (8 mL) were added to a flame-dried flask. Species **15** (5.8 g, 17.7 mmol) was then added in portions of 1 g each. A catalytic amount of 1,2-dibromoethane (1 mL) was added to activate the reaction. The reaction mixture was then refluxed for 12 h under argon. Then CO₂ gas was bubbled into the solution for 15 minutes and the color of the solution turned off-white. At this point, the solution was cooled to room temperature, the unreacted magnesium was filtered off and the solvent was removed under vacuum. The product was further purified using column chromatography (CH₂Cl₂) to yield a orange oil; yield: 3.1 g (60%). ¹H NMR (CDCl₃, 300

MHz): δ = 9.05 (br, 1H, OH), 6.06-5.88 (m, 2H, CH=CH), 2.71 (m, 2H), 2.30 (m, 2H), 1.93 (m, 1H), 1.89 (m, 1H), 1.79 (m, 1H), 1.59 (m, 2H), 1.22 (br, 19H), 0.47 (m, 1H); ^{13}C NMR (CDCl_3 , 300 MHz): δ = 179.7, 136.6, 135.9, 132.3, 49.5, 46.3, 45.4, 45.2, 42.5, 41.8, 38.7, 36.6, 34.8, 34.4, 33.1, 32.4, 29.9, 29.7, 29.5, 29.3, 29.1, 28.9, 28.7, 24.8; HRMS (ESI): m/z = 291.0. anal. calcd. for $\text{C}_{19}\text{H}_{32}\text{O}_2$: C, 78.03; H, 11.03; found: C, 77.94; H, 11.12.

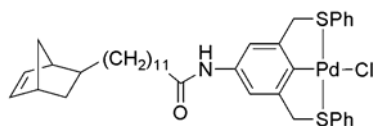
Synthesis of 12-(bicyclo[2.2.1]hept-5-en-2-yl)-N-(3,5-bis(phenylthiomethyl)phenyl)dodecanamide (17)



Compound **16** (242 mg, 0.83 mmol) and 1-hydroxybenzotriazole (112 mg, 0.83 mmol) were stirred in a mixture of methylene chloride (10 mL) and dimethyl formamide (0.5 mL) until complete dissolution of the benzotriazole was observed. *N,N'*-Dicyclohexylcarbodiimide (171 mg, 0.83 mmol) was then added to the solution followed by the addition of **14**. The reaction mixture was stirred for 9 h at room temperature. A precipitate was observed and filtered through a pad of celite. The solvent of the filtrate was removed under vacuum. The product was further purified by column chromatography (1:10 ethyl acetate:hexanes) to yield a yellow oil; yield: 330 mg (65%). ^1H NMR (CDCl_3 , 300 MHz): δ = 7.39 (s, 2H, ArH), 7.31-7.13 (m, 10H, SPh), 6.97 (s, 1H, ArH), 6.11-5.89 (m, 2H, CH=CH), 4.01 (s, 4H), 2.7 (m, 2H), 2.32-2.27 (t, J = 7.4 Hz,

2H), 1.97-1.93 (m, 1H), 1.86-1.78 (m, 1H), 1.73-1.66 (m, 2H), 1.39-1.15 (br m, 19H), 1.08-1.00 (m, 1H), 0.92-0.83 (m, 1H), 0.51-0.45 (m, 1H); ^{13}C NMR (CDCl_3 , 300 MHz): δ = 171.2, 138.4, 138.1, 136.7, 136.6, 136.0, 132.2, 129.4, 128.7, 126.1, 124.7, 118.7, 49.5, 46.3, 45.4, 45.2, 42.5, 41.8, 38.7, 37.7, 36.6, 34.8, 33.1, 32.8, 32.4, 32.0, 29.9, 29.7, 29.5, 29.4, 29.3, 28.7, 25.6; HRMS (ESI): m/z = 612.3. anal. calcd. for $\text{C}_{39}\text{H}_{49}\text{NOS}_2$: C, 76.55; H, 8.07; found C, 76.62; H, 8.15.

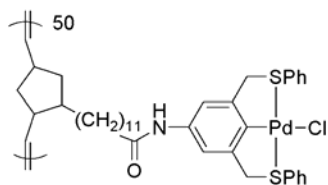
Synthesis of Pd-Cl, 12-(bicyclo[2.2.1]hept-5-en-2-yl)-N-(3,5-bis(phenylthiomethyl)phenyl)dodecanamide (18)



$\text{Pd}(\text{PhCN})_2\text{Cl}_2$ (92 mg, 0.24 mmol) was added to a stirred solution of **17** (150 mg, 0.24 mmol) in 15 mL $\text{CH}_2\text{Cl}_2/\text{CH}_3\text{CN}$ (1:2). The solution was stirred for 30 minutes before the addition of AgBF_4 (119 mg, 0.61 mmol) in one portion. After being stirred for another 30 minutes, the mixture was added to a brine solution (200 mL) and stirred for another 6h. The organic layer was separated, dried over MgSO_4 and the solvent removed under vacuum and was further purified by column chromatography (9:1 methylene chloride:methanol) to yield a yellow powder; yield: 138 mg (59%). ^1H NMR (CDCl_3 , 300 MHz): δ = 8.17 (s, 1H, ArH), 7.72 (d, J = 9.2 Hz, 4H, SPh), 7.29 (m, 8H), 6.08-5.88 (m, 2H, CH=CH), 4.37 (br s, 4H), 2.71 (s, 2H), 2.29-2.24 (t, J = 7.3 Hz, 2H), 1.95-1.75 (m, 1H), 1.32 (t, J = 6.1 Hz, 2H), 1.31-1.15 (br m, 19H), 1.08-1.00 (m, 1H), 0.92-0.83 (m,

1H), 0.51-0.45 (m, 1H); ^{13}C NMR (CDCl_3 , 300 MHz): δ = 171.9, 149.3, 136.6, 136.0, 132.2, 131.8, 130.9, 129.4, 113.8, 51.3, 49.5, 45.3, 42.4, 38.7, 37.5, 34.7, 32.4, 29.9, 29.6, 29.5, 29.3, 28.6, 25.7; HRMS (ESI): m/z = 782.9; anal. calcd. for $\text{C}_{40}\text{H}_{50}\text{ClINO}_2\text{PdS}_2$: C, 61.37; H, 6.44; N, 1.79; found: C, 61.09; H, 6.48; N, 1.84.

Polymerization of Pd-Cl 12-(bicyclo[2.2.1]hept-5-en-2-yl)-N-(3,5-bis(phenylthiomethyl)phenyl)dodecanamide (19)



Monomer **18** (85 mg, 0.11 mmol) was dissolved in CDCl_3 and stirred before the addition of the third generation Grubbs catalyst (2 mg, 0.002 mmol). The polymerization was monitored via ^1H NMR. After completion of the polymerization, ethyl vinyl ether was added (2 drops). The polymer was precipitated at least three times and washed with methanol to yield an orange solid; yield: 70 mg (82%). ^1H NMR (DMSO-d_6 , 300 MHz): δ = 9.63 (br s, 1H, NH), 7.73 (br s, 5H), 7.32 (br m, 8H), 5.41-5.10 (br m, 2H), 4.51 (br m, 4H), 3.31 (s, 4H), 2.13 (br m, 2H), 1.45-0.88 (br m, 23H); ^{13}C NMR (DMSO-d_6 , 300 MHz): δ = 170.3, 149.4, 136.2, 131.9, 130.4, 129.3, 113.0, 50.0, 36.4, 30.8, 29.7, 29.4, 25.2.

3.5. References

- [1] M. Albrecht, G. v. Koten, *Angew. Chem., Int. Ed. Engl.* **2001**, *40*, 3750.
- [2] W. A. Hermann, V. P. W. Bohm, C. P. Reisinger, *J. Organomet. Chem.* **1999**, *576*, 23.
- [3] D. Morales-Morales, C. Grause, K. Kasaoka, R. Redon, R. E. Cramer, C. M. Jensen, *Inorg. Chim. Acta* **2000**, *300*, 958.
- [4] M. E. Van der Boom, D. Milstein, *Chem. Rev.* **2003**, *103*, 1759.
- [5] A. S. Gruber, D. E. Zim, G., A. L. Monteiro, J. Dupont, *Org. Lett.* **2000**, *2*, 1287.
- [6] K. Yu, W. Sommer, C. W. Jones, M. Weck, *Adv. Synth. Catal.* **2004**, *347*, 161.
- [7] K. Yu, W. Sommer, M. Weck, C. W. Jones, *J. Catal.* **2004**, *226*, 101.
- [8] T. M. Trnka, R. H. Grubbs, *Acc. Chem. Res.* **2001**, *34*, 18.
- [9] A. Fürstner, *Angew. Chem., Int. Ed. Engl.* **2000**, *39*, 3012.
- [10] T.-L. Choi, R. H. Grubbs, *Angew. Chem., Int. Ed.* **2003**, *42*, 1743.
- [11] J. A. Love, J. P. Morgan, T. M. Trnka, R. H. Grubbs, *Angew. Chem., Int. Ed. Engl.* **2001**, *41*, 4035.
- [12] B. Chen, H. F. Sleiman, *Macromolecules* **2004**, *37*, 5866.
- [13] J. M. Pollino, L. P. Stubbs, M. Weck, *Macromolecules* **2003**, *36*, 2230.
- [14] C. Slugovc, S. Demel, S. Riegler, J. Hobisch, F. Stelzer, *J. Mol. Catal. A* **2004**, *213*, 107.
- [15] C. Slugovc, S. Riegler, G. Hayn, R. Saf, F. Stelzer, *Macromol. Rapid Commun.* **2003**, *24*, 435.
- [16] J. M. Pollino, M. Weck, *Synthesis* **2002**, *9*, 1277.

- [17] J. M. Pollino, M. Weck, *Org. Lett.* **2002**, *4*, 753.
- [18] W. J. Sommer, K. Yu, J. Sears, Y. Ji, X. Zheng, R. Davis, C. D. Sherrill, C. W. Jones, M. Weck, *Organometallics* **2005**, *24*, 4351.
- [19] B. H. Lipshutz, S. Tasler, W. Chrisman, B. Spliethoff, B. Tesche, *J. Org. Chem.* **2003**, *68*, 1177.
- [20] S. Klingelhöfer, W. Heitz, A. Greiner, S. Osetreich, S. Förster, M. Antonietti, *J. Am. Chem. Soc.* **1997**, *119*, 10116.
- [21] Y. Uozumi, T. Kimura, *Synlett* **2002**, *12*, 2045.
- [22] C. Paal, W. Hartmann, *Chem. Ber.* **1918**, *51*, 711.
- [23] G. M. Whitesides, M. Hackett, R. L. Brainard, J. P. P. M. Lavalleye, A. F. Sowinski, A. N. Izumi, S. S. Moore, D. W. Brown, E. M. Staudt, *Organometallics* **1985**, *4*, 1819.
- [24] D. E. Bergbreiter, P. L. Osburn, J. Frels, *Adv. Synth. Catal.* **2004**, *347*, 172.
- [25] D. E. Bergbreiter, P. L. Osburn, A. Wilson, E. M. Sink, *J. Am. Chem. Soc.* **2000**, *122*, 9058.

CHAPTER 4

POLYMER AND SILICA SUPPORTED PCP-Pd Pincer COMPLEXES

Abstract

Following the results reported in chapter 2, a variety of palladated PCP pincer complexes, reported as more stable than their Pd-SCS analogues, were synthesized. The different palladacycles were covalently tethered onto polymeric and silica supports via either amide or ether linkages. The role of the nature of the linkages with the Pd-SCS pincer proved to be minimal for the stability of the complexes. To investigate if these findings can be attributed to Pd-PCP complexes, the catalysts were tethered to their respective support using ether and amide linkages. The different catalysts were evaluated in the Heck reaction of iodobenzene and *n*-butyl acrylate in DMF at 120 °C using triethylamine as a base. The stability of the different Pd-PCP complexes was evaluated using kinetic and poisoning studies. The kinetic studies yielded very similar results as the one described in chapter 2, which are the presence of induction time and the decrease in conversion after being recycled. Furthermore, poisoning studies using poly(vinyl pyridine) and mercury added at the beginning of the catalysis resulted in no conversion. To understand the results of the kinetic and poisoning studies, the decomposition under reaction conditions of all complexes studied was investigated using ³¹P NMR, mass spectrometry, XAS and computational methods. The NMR studies indicated the predominant role of the triethylamine in the decomposition of the complex. Furthermore, XAS showed the presence of palladium iodide species, indicating the decomposition of

the Pd-PCP complex into a different species known to distill Pd. In addition, the initial steps of the decomposition pathway of PCP as well as SCS pincer Pd(II) complexes were studied using mass spectroscopy and computational calculations. The first step of this decomposition pathway involves the binding of triethylamine to the Pd while an arm of the pincer is off. These findings together with our previous reports strongly suggest that all Pd(II) pincer complexes are simply precatalysts during the Heck reaction that decompose to form catalytically active Pd(0) species.

This was a highly collaborative study between four research groups: the Jones, Sherill and Davis groups as well as ours. All the work carried out using silica supported Pd-pincer complexes was performed by Dr. Kunquan Yu from Professor Christopher W. Jones' group, the XAS experiments was performed in collaboration with Yaying Ji from Professor Robert J. Davis' lab and the computational simulations were performed in collaboration with John S. Sears of the Sherrill group.

4.1. Introduction

With the work described in chapter 2 on supported SCS-Pd pincer complexes, the demonstration that these complexes leach unidentified Pd(0) species into solution that are catalytically active was done. Furthermore, no catalytic activity could be attributed to any intact pincer species. In view of these results, the investigation of palladated PCP complexes that are reported in the literature to be significantly more stable was carried out.^[1-3] The literature concerning these species in the Heck reaction is somewhat muddled. Eberhard^[4] has demonstrated that palladated PCP pincer complexes with oxygen atoms in place of carbons in the arms are not stable during Heck catalysis (Figure

4.1), Frech ^[5] has shown recently that the palladated pincer ligand could be reduced by sodium to form a binuclear metal complex, whereas there are other reports where immobilized PCP pincers are reported as “recyclable catalysts”.^[6]

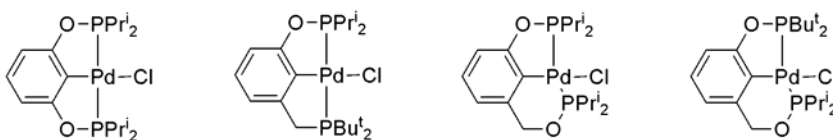


Figure 4.1. Pd-PCP pincer studied by Eberhard.

This chapter describes the results, obtained by myself and my collaborators, on a variety of supported PCP-Pd-pincer complexes. I prepared the small molecule Pd(II) PCP pincer (**1**), that was used as a baseline measurement of catalytic activity, and compared its performance in the Heck reaction with Pd(II)-PCP complexes tethered to a variety of supports ranging from soluble polymers (**2** and **3**) to nanoporous silica, SBA-15 (**4**) (Figure 4.2). Using a variety of techniques such as *in situ* NMR, *in-situ* X-ray Absorption Spectroscopy (XAS) and the poisoning studies described in chapter 3, I investigated the stability of the supported Pd-pincer complexes. Furthermore, other techniques such as mass spectroscopy and computational experiments were used to explore the first steps of the decomposition pathway.

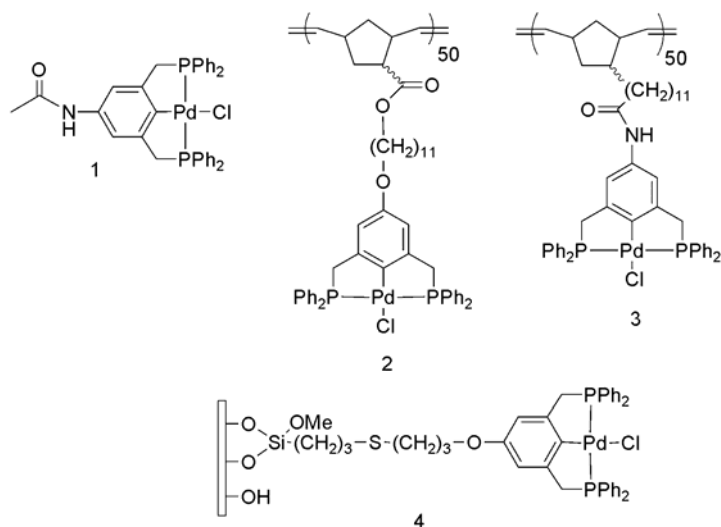


Figure 4.2. The immobilized palladated pincer complexes evaluated in this chapter.

4.2. Results and Discussion.

The investigation was conducted using four different catalysts with similar structures. Complex **1** was used as the standard for all catalytic reactions for comparison with the supported systems. The polymer-supported catalysts **2** and **3** were synthesized to study the effect of the linker attachment on the catalytic activity. It has been suggested in the literature that ether derivatives of pincer complexes are less stable than their amide counterparts.^[7] Therefore, two polymeric catalysts that are identical except for the heteroatom functionality that attaches the pincer complex to the support were prepared. For **2**, the catalyst was attached to the polymer backbone via an ether linkage while in the case of **3**, an amide linkage was employed. Both polymers are highly soluble under reaction conditions allowing a close comparison with **1**. The silica-supported catalyst **4**

was synthesized to study the influence of a heterogeneous reaction mixture on the catalysis and to compare the catalytic activity of a solid supported system to the soluble polymer catalysts and the small molecule analog.

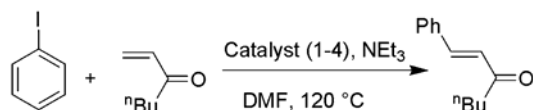
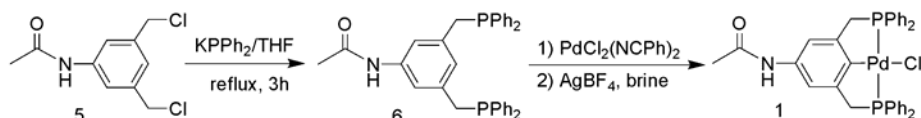


Figure 4.3. Heck reaction conditions.

The standard Heck reaction conditions are outlined in Figure 4.3. The catalysis was carried out using 1.5 equivalents of distilled triethylamine, one equivalent of iodobenzene and 1.25 equivalents of *n*-butyl acrylate in DMF at 120 °C. The catalyst loading was 10 mol% for the polymer supported pincer and 0.3 mol% for the SBA-15 supported pincer.



Scheme 4.1. Synthesis of Pd-Cl N-{3,5-bis-[(diphenylphosphanyl)-methyl]-phenyl}-acetamide **1**.

The synthesis of **1** was carried out by reacting **5** (synthesized according to literature procedures⁹) with potassium diphenylphosphide in THF under reflux for three

hours to yield **6**, which was used without further purification. Compound **6** was then dissolved in a mixture of CH₂Cl₂/ MeCN (1:2) followed by the addition of PdCl₂(NPh)₂ and AgBF₄ to yield **1**, after purification, as a yellow solid (Scheme 4.1).

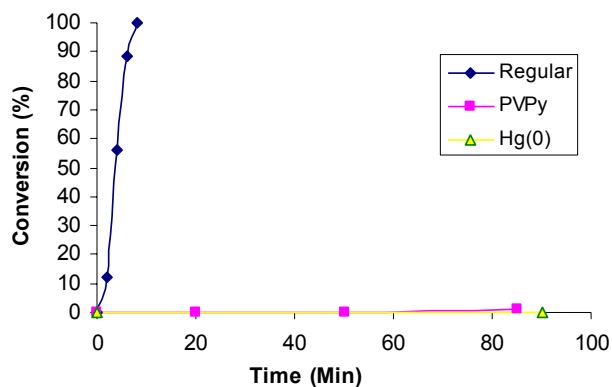
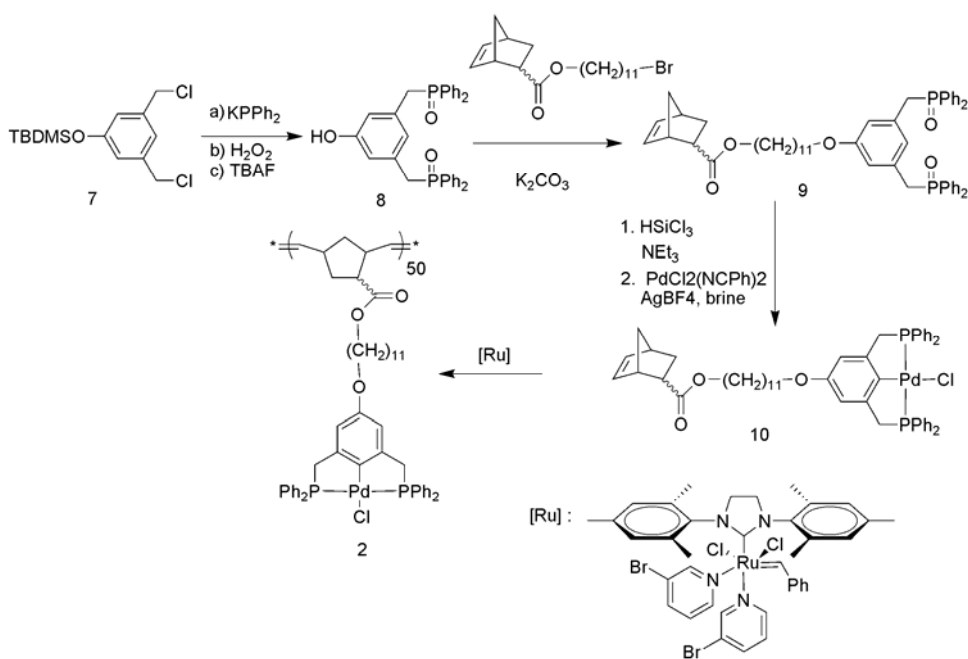


Figure 4.4. Conversion vs. time for Heck coupling using **1**.

The use of **1** in Heck catalysis was investigated by monitoring the disappearance of iodobenzene *via* gas chromatography (GC). I observed quantitative conversion using **1** as catalyst within 20 minutes (Figure 4.4). To examine the catalytic behavior in more detail, poisoning studies were carried out. As demonstrated in chapter 3, highly cross-linked poly(vinylpyridine) (PVPy) traps soluble Pd species by coordinating to the metal center and removing it from solution⁷⁷ while leaving support-tethered Pd-species untouched.^{56-57,77} For the poisoning test, 300 equivalents of PVPy were added to the catalytic reaction, resulting in less than 2% conversion of iodobenzene after three hours. A second poisoning test was carried out by adding mercury. Hg(0) is known to react with

Pd(0), forming an amalgamate, thereby quenching the activity of the leached palladium.^[8-10] When adding 100 equivalents of mercury to the catalytic reaction, again, less than 2% conversion of iodobenzene was observed after three hours. These results clearly suggest that **1** decomposes under reaction conditions.^[7, 11, 12]



Scheme 4.2. Synthesis of polymer **2**.

The synthesis of polymer **2** was accomplished by adding potassium diphenylphosphide to **7**, which was synthesized using a literature procedure,^[13] followed by the oxidation of the phosphorus using an aqueous solution of 10% H₂O₂. The *tert*-butyl dimethyl silyl group was then removed using TBAF to yield **8** as a white solid,

which was reacted with the cyclo[2.2.1]hept-5-ene-2-carboxylic acid 11-bromo-undecyl ester using potassium carbonate in DMF to yield a brown oil. The oil was immediately reacted with trichlorosilane and triethylamine in xylenes to deprotect the phosphines. The deprotected pincer was then reacted with $\text{PdCl}_2(\text{NCPh})_2$ and AgBF_4 to yield monomer **10** as an orange solid. The monomer was polymerized using the third generation Grubbs catalyst at room temperature under air (Scheme 4.2).^[14] Quantitative conversion was obtained in 20 minutes.

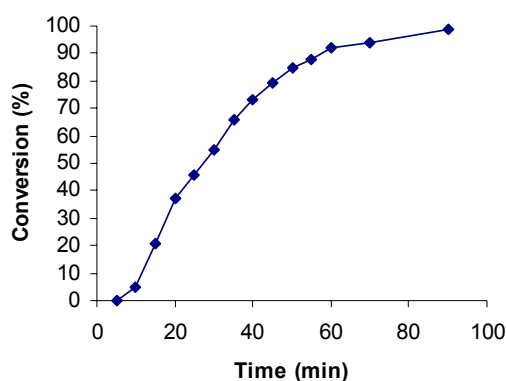
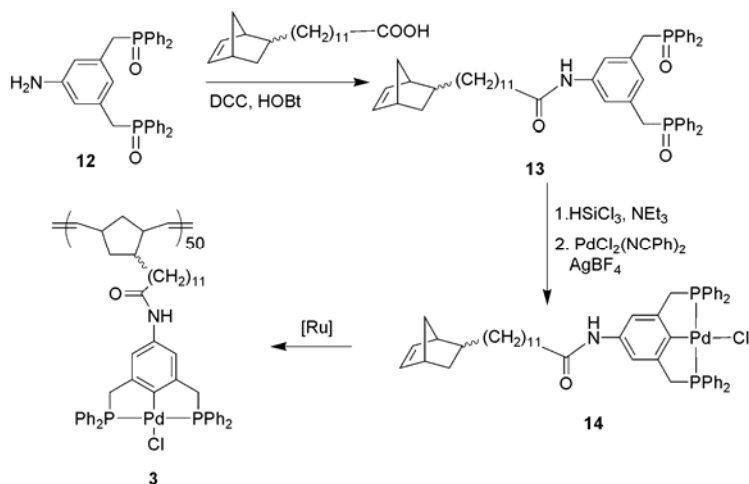


Figure 4.5. Conversion vs. time for Heck coupling using **2**.

Again, the use of polymer **2** under Heck conditions was measured using GC by following the disappearance of iodobenzene (Figure 4.5). I observed quantitative conversion within 90 minutes. In analogy to the experiments outlined above for **1**, poisoning studies were carried out. The addition of 300 equivalents of PVPy resulted in the retardation of the reaction with only 1% conversion observed after 24 hours. Furthermore, the addition of 100 equivalents of mercury to the Heck reaction mixture

yielded similar results. Again, these experiments suggest that the active species for the Heck reaction is not a well-defined palladium species but a leached Pd moiety that contains Pd(0) in the catalytic cycle.



Scheme 4.3. Synthesis of polymer **3**.

Polymer **3** was synthesized starting with the coupling of complex **12** and 12-bicyclo[2.2.1]hept-5-en-2-yl-dodecanoic acid using dicyclohexylcarbodiimide and 1-hydroxybenzotriazole to yield **13**. Reduction of the phosphorus using trichlorosilane and triethylamine in xylenes, followed by the addition of the PdCl₂(NCPh)₂ and AgBF₄, yielded monomer **14** (Scheme 4.3). The monomer was polymerized using the third generation Grubbs catalyst **11** in a 50:1 monomer to catalyst ratio.

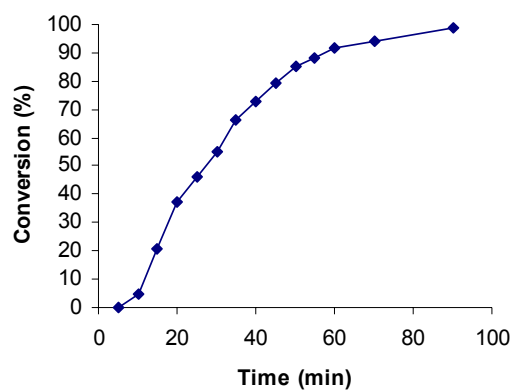


Figure 4.6. Conversion vs. time for Heck coupling using **3**.

The same reactivity experiments as outlined above for **1** and **2** were carried out. While quantitative conversion without the addition of poison was observed within 60 minutes (Figure 4.6), the two poisoning tests using 300 equivalents of PVPy and 100 equivalents of mercury resulted into the near total quenching of the catalytic reaction. Both reactions yielded less than 1% conversion after 24 hours. These results showed that the leaching of the palladium is independent of the tether group of the immobilized pincer complex, and correlates well with the other experiments discussed above.

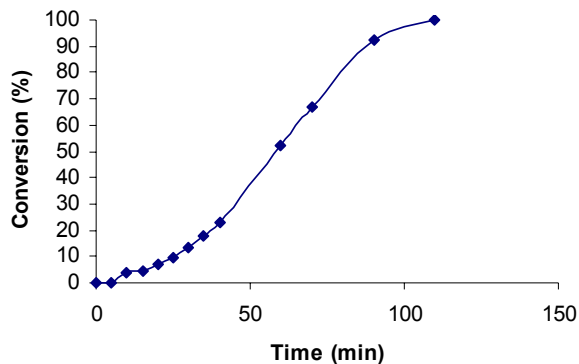


Figure 4.7. Conversion vs. time for Heck coupling using **4**.

Using **4** as Heck catalyst resulted in the quantitative conversion of iodobenzene within two hours (Figure 4.7). The PVPy and mercury leaching tests were carried out and no conversions were observed in the presence of either poison.

These reactivity experiments clearly demonstrate that palladated PCP complexes decompose under the reaction conditions studied. Furthermore, the decomposition is independent of the support or the linker attachment. While small differences in the kinetics of the reactions were observed for the different supports, poisoning studies for all systems studied demonstrate that no catalytic activity stems from a support-tethered Pd(II) species; rather, leached Pd species are the active moieties. These results are analogous to our recent reported study on supported SCS pincer complexes, clearly demonstrating that the added stability of the PCP ligand system is not enough to prevent decomposition.^[11, 12]

Investigations into the decomposition pathway.

A variety of decomposition pathways of these complexes during reaction conditions are imaginable. The most likely decomposition pathway of palladacycles starts with the exchange of one ligand of the pincer ligand (arm off) by the nitrogen-containing base. As outlined in the literature, the high strain of palladated pincer complexes as a result of their distorted square planar configuration makes them likely to de-chelate under appropriate reaction conditions thereby relieving the strain.^[15] After base or solvent coordination, the resulting complex resembles a half-pincer complex. Hartwig and Louie have shown that half pincer complexes containing an amine base as ligand are able to undergo β -hydride elimination, a common reaction pathway of palladium amides with β -hydrogens, resulting in a palladium hydride species (Figure 4.8).^[15]

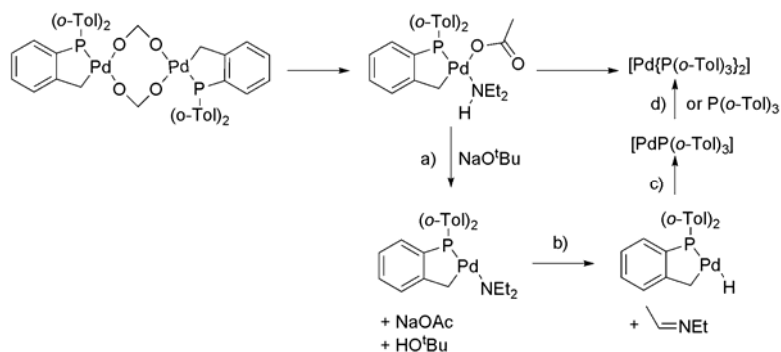
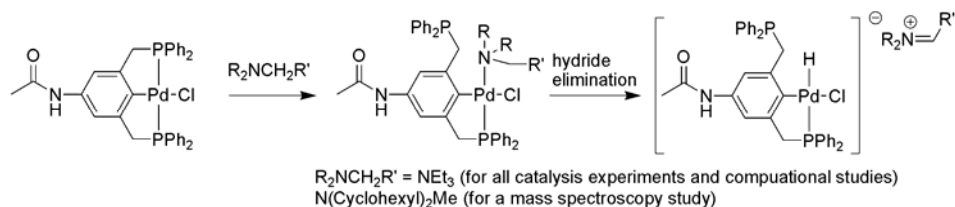


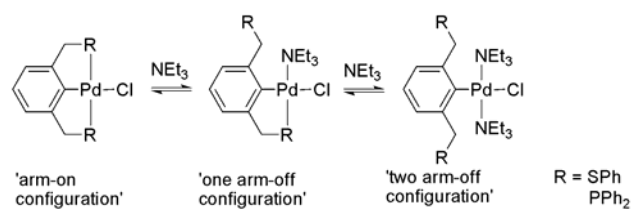
Figure 4.8. Postulated mechanism by Louie *et al.* for the synthesis of $[\text{Pd}(0)\{\text{P}(o\text{-Tol})_3\}_2]$. a) deprotonation, b) β -H elimination, c) reductive elimination, d) disproportionation.

My collaborators and I proposed that the second step of the catalyst decomposition may follow the same pathway of β -hydrogen elimination as outlined in Scheme 4.4, creating a charged palladium hydride species with the imminium ion as a counterion.



Scheme 4.4. Proposed initial steps of the decomposition of the palladated pincer complex.

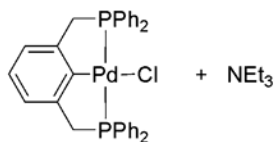
To investigate this proposed decomposition pathway, I carried out a variety of *in situ* low and high temperature NMR experiments and mass spectroscopy experiments, supported by electronic structure computations and XAS studies. The hypothesis that the palladated PCP pincer is in an equilibrium between an arm-on configuration, *i.e.* a phosphine, bound to the palladium via a dative bond, and an open coordination site as a result of the breakage of this dative bond (arm-off configuration) is essential to most potential decomposition mechanisms.^[16-18] Therefore, initially I concentrated my research efforts to evaluate this hypothesis.



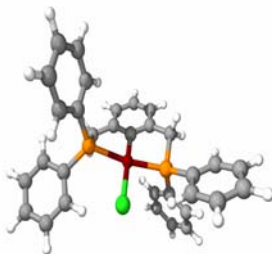
Scheme 4.5. Computational explored ligand exchange mechanism.

Electronic structure computations were carried out to establish the energetics of the replacement of the phosphine ligands by the amine base (Scheme 4.5).

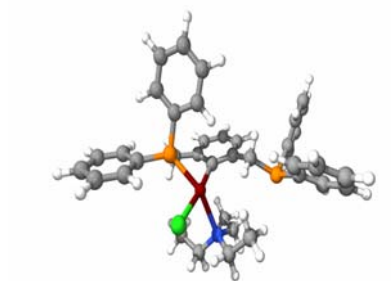
A



B



C



D

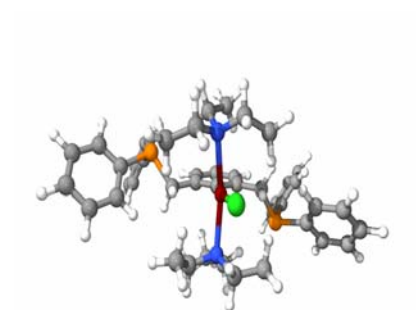


Figure 4.9. Optimized structures of the calculated exchange pathway of phosphine by a trimethyl amine base of palladated pincer complexes. A) Chemdraw representation of structures used in calculation, B) fully intact complex, C) removal of one phosphine, D) addition of the amine base, E) rearrangement to a distorted square planar confirmation, and F) exchange of the second phosphine by another amine base.

Optimized geometries (computed using the BP86 density functional method with a LAV3P/6-31G* basis, see below) are presented in Figure 4.9 and relative energies for the PCP system are depicted in Figure 4.10.

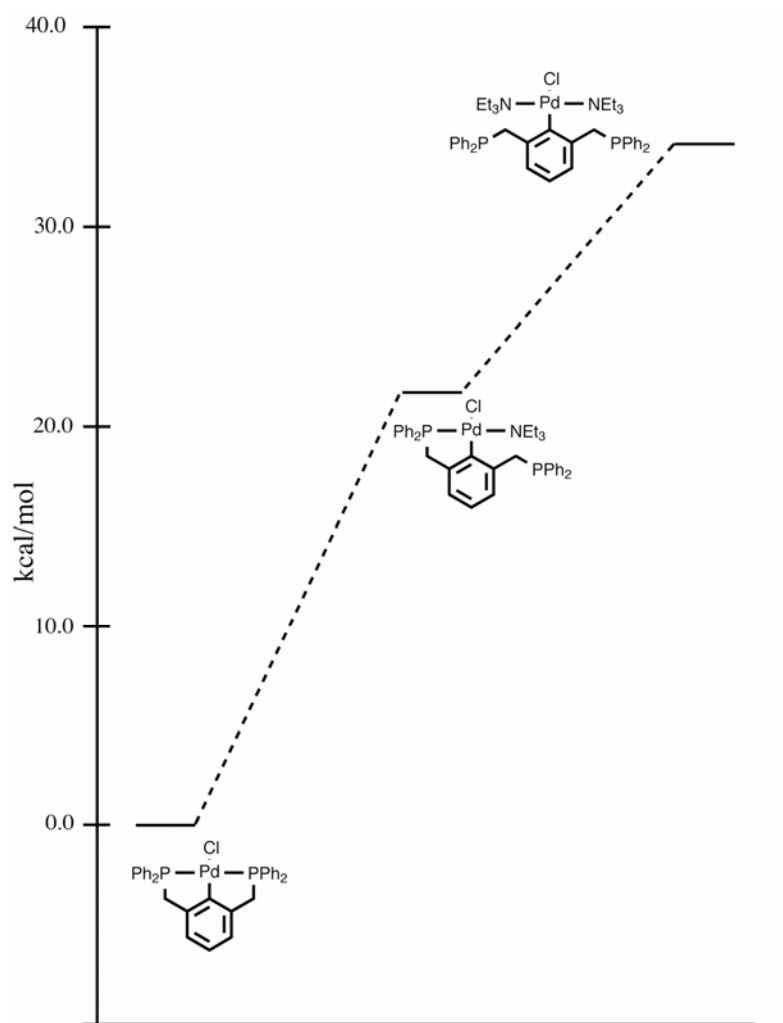


Figure 4.10. Free energy diagram of the relevant minima for the initial steps of the proposed decomposition pathway computed at the BP86/LAV3P/6-31G* level of theory.

These calculations suggested that the 'one arm off configuration' of palladated PCP complexes requires about 21 kcal/mol in the presence of a coordinating ligand such

as the amine, an uphill reaction energy that could be overcome at high temperatures such as the reaction conditions (preliminary computations for the simpler SCS system indicate that the transition state for this associative displacement is only an additional 2-3 kcal/mol beyond the reaction energy). Removal of the second arm and replacing it with another ligand such as the solvent and/or the amine base is estimated to cost an additional 13 kcal/mol relative to the 'one arm-off' configuration'. After the initial removal of the first arm, the coordination sphere around the palladium is a highly distorted square planar one (Figure 8C), which is highly unfavorable. However, this can be overcome during the second phosphine removal that converts the metal complex back into a square planar configuration (Figure 8D), which explains why the second ligand exchange is less unfavorable than the first one. Based on these calculations, we hypothesize that the high temperatures during the reaction conditions allow the phosphorus ligands to come off of the metal center and to be replaced by other ligands such as the amine base. To support this hypothesis a series of ^{31}P NMR experiment using **1** was carried out.

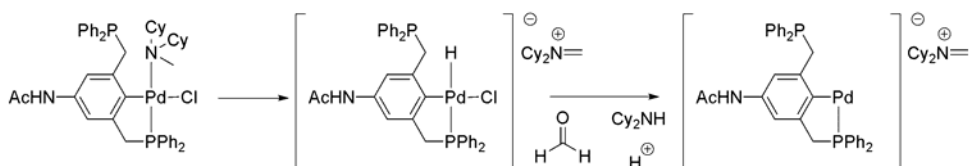
If an arm on/off equilibrium would take place in the absence of additional ligands, one might expect to freeze out these states leading to two distinct ^{31}P NMR signals at low temperatures that should coalesce at higher temperatures. However, only a single phosphorus signal at 15.7 ppm at -70 °C was detected in a variety of solvents clearly demonstrating the stability of the Pd-P bonds at low temperatures. To investigate the role of the reactants towards the decomposition of the catalyst, we carried out a series of NMR experiments with triethylamine and/or iodobenzene present in the catalyst solution. Initially, equimolar ratios of **1**, triethylamine and iodobenzene were observed *in-situ* at 120 °C in DMF. Over a period of several hours, only one phosphorus signal was detected.

However, addition of three more equivalents of triethylamine resulted in the formation of two new signals in the phosphorus NMR at 7.7 and -4.2 ppm. Furthermore, palladium black formation was visible confirming the decomposition of the metal complex. While I was not able to assign these two new signals in the NMR unequivocally, they are clearly indicative of a new phosphorus species.

To further investigate if both iodobenzene and triethyl amine are needed for decomposition, or if the decomposition pathway might follow the one outlined in Scheme 5, *i.e.* only the amine base is needed, additional experiments were carried out to verify the role of each reactant. Addition of iodobenzene to the metal complex at 120 °C in DMF resulted in no changes in the NMR over a period of 24 hours and no palladium black formation was observed, even when 20 equivalents of iodobenzene were added. In contrast, the addition of seven equivalents of triethylamine without the presence of an aryl iodide species resulted in the formation of a new signal, 19 ppm upfield from the original signal. These results suggest that triethylamine plays an essential role in the decomposition of the palladium/pincer complex.

Theoretical investigations of the second step of the proposed decomposition pathway, the β -hydride elimination, would be very challenging and beyond the scope of the present study. Nevertheless, initial computations of subsequent steps for the simpler SCS system indicated that hydride transfer to the aromatic carbon and concomitant cleavage of the carbon-palladium bond was energetically downhill by at least 20 kcal/mol relative to the intact palladacycle. To probe the proposed β -hydride elimination step of the decomposition pathway, I carried out a series of mass spectroscopy experiments. Based on the work of Hartwig and Louie,^[15] the amine base will exist, after β -hydride

elimination, as an imminium ion that can be hydrolyzed to yield a secondary amine, and aldehyde. The presence of this secondary amine can be easily characterized using mass spectroscopy. Therefore, characterization of a reaction mixture using mass spectroscopy-ESI gives a facile method to evaluate the proposed β -hydride elimination decomposition step. For ease of characterization, N,N-dicyclohexyl-N-methyl amine was employed in the mass spectroscopy studies instead of the otherwise used triethyl amine (Scheme 4.6).



Scheme 4.6. Proposed decomposition pathway generating the amine

The experiments were carried out by dissolving a mixture of catalyst **1** and N,N-dicyclohexyl N-methyl amine in DMF and heating it at 120 °C for several hours. Every hour, an aliquot was taken from the reaction mixture and analyzed by mass spectroscopy. All aliquots analyzed via mass spec (ESI) spectra showed molecular ion signals at 182.3. This molecular ion signal is indicative of the presence of N,N-dicyclohexyl amine. This result strongly supports the hypothesis that the decomposition pathway goes through a β -hydrogen elimination step before the palladium (0) leaches out.

In chapter 3, the decomposition of palladated SCS pincer complexes during Heck catalysis was described.^[11, 12] To investigate whether these palladated SCS pincer catalysts also follow the decomposition pathway identified for their PCP analogous,

Yaying Ji, from Professor Davis group, carried out XAS experiments and John Sears from Professor Sherrill group, the computational studies. The electronic structure computations of the palladated SCS pincer complex suggested that the one arm off configuration is only 7.0 kcal/mol higher in energy than the palladated SCS pincer complex in the presence of an amine base. Furthermore, removal of the second arm is calculated to be downhill relative to the 'one arm off configuration' by 0.6 kcal/mol. These calculations were supported by the observation of palladium black formation in the reaction vessel when adding only a single equivalent of triethyl amine to a poly(norbornene) supported SCS Pd(II) pincer complex. This is in stark contrast to the required seven equivalents of triethylamine required for the visible decomposition of the PCP analogue, **1**, and can be explained by the known lesser stability of SCS complexes.^[7, 19]

The *in-situ* XAS data on both the polymeric and silica immobilized palladated SCS pincer complexes during Heck reaction conditions, show the formation of palladium iodide species while no metallic palladium was found under reaction conditions (for a detailed description of the XAS data, see Appendix A). It has been reported in the literature that soluble palladium species are stored as palladium halides such as the bridged $[\text{Pd}_2\text{I}_6]^{2-}$ anion.^[20] Our XAS study clearly validates these reports. It is important to note that the majority of the computational and NMR studies, in contrast to all XAS experiments, were carried out in the absence of an aryl iodide. When no aryl iodide was present during the NMR experiments, palladium black formation was observed suggesting the formation of metallic palladium. However, when NMR experiments were carried out in the presence of aryl iodide, palladium black formation was significantly

less pronounced, suggesting the storage of the majority of palladium in a form other than Pd(0). Based on the XAS results, palladium iodide species are therefore the likely storage species. Overall, the XAS results clearly demonstrated that the SCS pincer complexes are altered under reaction conditions, thereby substantiating the NMR and computational studies while suggesting that the most abundant soluble palladium species under reaction conditions are palladium iodides.

By combining the experimental and computational data on the decomposition of palladated PCP and SCS pincer complexes, it is obvious that the amine base plays the key role in the decomposition pathway. Based on the above outlined data, it was suggested that catalyst decomposition could occur through exchange of a phosphorus or sulfur ligand (one arm of the pincer ligand) with triethyl amine followed by a β -hydrogen elimination of the base and a rapid second ligand exchange thereby changing the pincer ligands from tridentate ligands to monodentate ones. Furthermore, the calculations follow the reported trend of PCP-based complexes being significantly more stable than their SCS counterpart.^[19] However, at the commonly employed reaction temperatures, both complexes decompose, thereby releasing soluble palladium species. Although the XAS studies clearly indicated that the primary Pd species in solution was a Pd(II) moiety, the Hg(0) poisoning studies unequivocally showed that the catalytic cycle contains a Pd(0) intermediate, as Hg(0) addition quenches essentially all activity. As noted in chapter 3, however, the nature of the true zero valent catalyst can not be conclusively determined with the data here (Pd(0) colloid^[21] or molecular Pd(0) species^[20, 22, 23]), as it is expected that Hg(0) would poison either type of species. Nonetheless, a number of observations imply that molecular species could be important in the Heck reaction, including the

observed reactivity and the high concentration of $[\text{Pd}_2\text{I}_6]^{2-}$ species in ligand-free Pd catalysts,^{[19], [24]} the XAS observations here, kinetic and other data presented in the literature,^[22, 23] and the fact that enantioselective Heck reactions are possible with chiral ligands.^[25] None of these observations would be expected if Pd(0) colloids were the primary active species.

4.3. Conclusion

It has been demonstrated using a variety of leaching experiments and kinetic studies that palladated PCP pincer complexes (homogeneous species as well as complexes immobilized on soluble and insoluble supports), which have been identified in the literature as stable entities,^[6, 26] decompose under Heck reaction conditions. Through the employment of computational methods, X-ray absorption spectroscopy, mass spectroscopy, and *in situ* NMR spectroscopy, the initial steps of the decomposition pathway of these PCP as well as SCS pincer complexes were proposed. It is important to note that these conclusions are limited to the organic bases used in this paper. Heck catalysis using palladated-pincer ligands have also been carried out using inorganic bases such as K_2CO_3 . The combined data outlined in this contribution with recent reports from the literature^[4, 11, 12, 27] calls into question whether any palladated pincer complexes that have a palladium (II) metal center are truly stable under the reaction conditions for carbon-carbon bond formations such as Heck or Suzuki couplings. Rather, these species should be referred to as precatalysts, and supported analogues as recyclable precatalyst sources. Stemming from these findings, a ligand, identified as more stable in the literature, was investigated. This research led me to the *N*-heterocyclic carbene ligand.

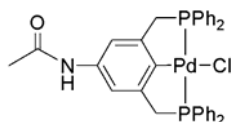
This ligand has been reported to be versatile for a wide variety of catalytical transformation and to be very stable. In chapter 4, my investigations using this ligand is described.

4.5. Experimental Section

All reactions with air- and moisture sensitive compounds were carried out under dry nitrogen/argon atmosphere using an MBraun UniLab 2000 dry box and/or standard Schlenk line techniques. DMF, *n*-butyl acrylate, and NEt_3 were distilled over calcium hydride. 5-amino-isophthalic acid dimethyl ester, poly(4-vinylpyridine) and all bases were obtained from commercial sources and generally used without further purification. Gas chromatographic analyses were performed on a Shimadzu GC 14-A gas chromatograph equipped with a flame-ionization detector with a HP-5 column (length = 30 m, inner diameter = 0.25 mm, and film thickness = 0.25 μm). The temperature program for GC analysis was the following: heating from 50 $^{\circ}\text{C}$ to 140 $^{\circ}\text{C}$ at 30K/min and heating from 140 $^{\circ}\text{C}$ to 300 $^{\circ}\text{C}$ at 40 K/min under constant pressure with inlet and detector temperatures kept constant at 330 $^{\circ}\text{C}$. ^1H (300 MHz) and ^{13}C NMR (75 MHz) spectra were recorded on a Varian Mercury VX instrument. ^{31}P NMR (162 MHz) spectra were recorded on a Bruker AMX 400 MHz instrument using H_3PO_4 as a calibration standard. All spectra were referenced to residual proton solvent. Mass spectral analyses were provided by the Georgia Tech MassSpectrometry Facility using a VG-70se spectrometer. Gel permeation Chromatography analyses were carried out using a Waters 1525 binary pump coupled to a Waters 2414 refractive index detector. The GPC was calibrated using polystyrene standards on a Styragel[®] HR 4 and HR 5E column set with

CH₂Cl₂ as an eluent. FT-Raman spectra were obtained on a Bruker FRA-106. At least 128 scans were collected for each spectrum, with a resolution of 2-4 cm⁻¹. Elemental analyses were carried out by either Atlantic Microlabs, Norcross GA (CHN analyses) or Galbraith Laboratories, Inc., TN.

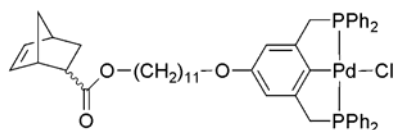
Synthesis of Pd-Cl N-{3,5-Bis-[(diphenylphosphanyl)-methyl]-phenyl}-acetamide (1).



Inside a nitrogen filled dry box, KPPH₂ (4.1 mL, 0.5 M in THF) was slowly added to a THF solution (20 mL) of **5** (220 mg, 0.94 mmol). The reaction mixture was removed from the dry box, refluxed for three hours, and cooled to room temperature. The solvent was removed under vacuum and dry CH₂Cl₂ (50 mL) was added. The solution was washed with degassed H₂O (2 x 20 mL), dried over anhydrous Na₂SO₄ and the solvent removed. The crude product was re-dissolved in 15 mL CH₂Cl₂/CH₃CN (v/v: 1:2) and Pd(PhCN)₂Cl₂ (320 mg, 0.83 mmol) was added. The reaction mixture was stirred at room temperature for 30 min followed by the addition of AgBF₄ (485 mg, 2.49 mmol). After stirring for an additional 30 min, the mixture was diluted with CH₂Cl₂ (250 mL) and stirred with a saturated brine solution (200 mL) for five hours. The organic layer was then separated, dried over Na₂SO₄ and passed through a short silica gel column. Solvent removal and recrystallization from CH₂Cl₂/Et₂O yielded **1** as a yellow powder. Yield:

340 mg (61%). ^1H NMR (d^6 -DMSO, 300MHz): δ = 9.86 (s, 1H), 8.21-7.77 (m, 10H), 7.48-7.37 (m, 10H, Ph), 7.28 (s, 2H), 4.09 (bs, 4H), 1.96 (s, 3H). Anal. Calcd for $\text{C}_{34}\text{H}_{30}\text{ClNOP}_2\text{Pd}$: C, 60.73; H, 4.50; N, 2.08. Found: C, 60.34; H, 4.32; N, 1.94.

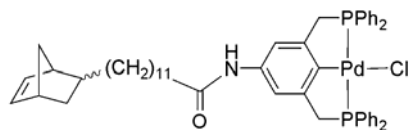
Synthesis of Pd-Cl bicyclo[2.2.1]hept-5-ene-2-carboxylic acid 11-{3,5-bis-[(diphenyl phosphanyl)-methyl]-phenoxy}-undecyl ester (10).



Bicyclo[2.2.1]hept-5-ene-2-carboxylic acid 11-bromo-undecyl ester (767 mg, 2.06 mmol) was slowly added over a period of 15 minutes to a stirred solution of **8** (1.08 g, 2.06 mmol), and potassium carbonate (571 mg, 4.1 mmol) in DMF. The mixture was heated to 90 °C and allowed to stir for 12 hours. The DMF was removed *in vacuo* and the crude product dissolved in methylene chloride (100 mL) and washed with 1N HCl (50 mL), sodium bicarbonate (50 mL) and brine (50 mL). The organic layers were dried over magnesium sulfate and the solvent removed under vacuum to yield **9** as a viscous brown oil which was partially purified via column chromatography (eluent: Ethyl Acetate followed by Methanol), and then used without further purification. Compound **9** (1.37 g, 1.7 mmol) was dissolved in degassed m-xylenes (50 mL) and triethylamine (5.7 mL, 40.5 mmol) was slowly added followed by the dropwise addition of trichlorosilane (4.1 mL, 40.5 mmol). The reaction was heated to 120 °C for ten hours. After the mixture was cooled to room temperature, it was poured into a degassed solution of sodium hydroxide

(500 mL). The product was then extracted from the aqueous reaction mixture with toluene (2 x 100 mL), dried over magnesium sulfate and the solvent removed under vacuum to yield a yellow oil. The oil was dissolved in CH₂Cl₂/CH₃CN (5 mL/ 10 mL) and PdCl₂(NCPh)₂ (652 mg, 1.7 mmol) was added. The solution was stirred for 30 minutes before the addition of the AgBF₄ (823 mg, 4.2 mmol). The mixture turned yellow and was stirred for another 30 minutes, diluted with CH₂Cl₂ (200 mL), poured into a concentrated brine solution (500 mL) and stirred vigorously for five hours. The organic layer was separated, dried over MgSO₄ and the solvent removed under vacuum to yield an orange oil that was purified via column chromatography (1:1 Ethyl Acetate/Hexanes) to yield **2** as an orange solid. Yield 62%. ¹H NMR (CDCl₃, 300 MHz): δ = 7.91 - 7.83 (m, 10H), 7.52 – 7.34 (m, 12H), 6.7 (s, 4H), 6.08 - 5.88 (m, 2H), 4.23 (br s, 4H), 3.83 (t, 2H, *J* = 6.2 Hz), 3.20 – 3.13 (m, 1H), 3.00 – 2.99 (m, 1H), 2.94 – 2.82 (m, 4H), 2.22 – 2.13 (m, 1H), 1.92 – 1.82 (m, 2H), 1.78 – 1.64 (m, 4H), 1.63 – 1.50 (m, 4H), 1.42 – 1.31 (m, 5H), 1.32 – 1.20 (m, 28H). HRMS (ESI): *m/z* = 885.2534. Anal. Calcd for C₅₁H₅₇ClO₃P₂Pd: C, 66.45; H, 6.23; found C, 66.82; H, 6.11.

Synthesis of Pd-Cl 12-Bicyclo[2.2.1]hept-5-en-2-yl-dodecanoic acid {3,5-bis-[(diphenylphosphanyl)-methyl]-phenyl}-amide (14).



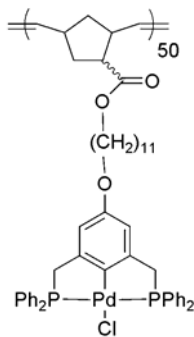
To a solution of 12-bicyclo[2.2.1]hept-5-en-2-yl-dodecanoic acid (120 mg, 0.4 mmol) in CH_2Cl_2 1-hydroxybenzotriazole (55 mg, 0.4 mmol) and dicyclohexylcarbodiimide (85 mg, 0.4 mmol) were added with a few drops of DMF. To the reaction mixture, complex **12** (214 mg, 0.4 mmol) was added and stirred for 12 hours. The reaction mixture was then filtered through a small patch of silica and the solvent removed under vacuum. Without further purification, compound **13** was dissolved in degassed xylenes (50 mL) followed by the addition of triethylamine (0.56 mL, 4 mmol) and drop wise addition of trichlorosilanes (0.56 mL, 4 mmol). The reaction mixture was heated to 120 °C for 12 hours, cooled down to room temperature and transferred into a glove box where the reaction was poured into a degassed solution of sodium hydroxide (2M, 50 mL). The product was then extracted from the aqueous reaction mixture with toluene (2 x 50 mL), dried over MgSO_4 and the solvent removed to yield an off-white oil which was dissolved into $\text{CH}_2\text{Cl}_2/\text{CH}_3\text{CN}$ (5 mL/ 10 mL) followed by the addition of $\text{PdCl}_2(\text{NPh})_2$ (154 mg, 0.4 mmol). The reaction mixture was stirred for 30 minutes before the addition of AgBF_4 (195 mg, 1 mmol). The mixture was stirred for another 30 minutes, diluted with CH_2Cl_2 (200 mL), poured into a saturated brine solution and stirred for 12 hours. The organic phase was then separated, dried over MgSO_4 and the solvent removed to yield an orange oil that was purified via chromatography column (1:1 Ethyl Acetate/Hexanes). Yield 34%. ^1H NMR (CDCl_3 , 300 MHz): δ = 7.92 - 7.84 (m, 10H, PPh_2), 7.51 – 7.34 (m, 12H), 6.4 (s, 4H), 6.06 - 5.89 (m, 2H), 4.37 (br s, 4H), 2.71 (s, 2H), 2.29- 2.24 (t, J = 7.3 Hz, 2H), 1.95- 1.75 (m, 1H), 1.324 (t, J = 6.1 Hz, 2H), 1.324- 1.15 (br m, 19H), 1.08- 1.00 (m, 1H), 0.92- 0.83 (m, 1H), 0.51- 0.45 (m, 1H). ^{13}C NMR (CDCl_3 , 300 MHz): δ = 171.9, 158.0, 149.8, 148.8, 133.9, 133.9, 131.9, 133.8, 132.4,

132.3, 132.2, 131.5, 131.4, 129.9, 129.7, 129.6, 128.1, 127.9, 113.8, 51.3, 49.5, 45.3, 42.4, 38.7, 37.5, 34.7, 32.4, 29.9, 29.6, 29.5, 29.3, 28.6, 25.7. HRMS (ESI): m/z = 905.3275. Anal. Calcd for $C_{51}H_{58}ClNOP_2Pd$: C, 67.70; H, 6.46; N, 1.55; found C, 67.52; H, 6.42; N, 1.67.

General procedure for the synthesis of polymer 2 and 3.

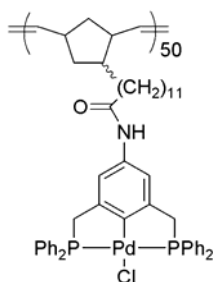
The respective monomers were dissolved in $CDCl_3$ followed by the addition of the desired amount of catalyst. The polymerization was monitored via NMR. After completion of the polymerization a few drops of ethyl vinyl ether were added. The polymer was then purified by reprecipitation from chloroform into cold methanol. The purification procedure was repeated until the resulting methanol solution became colorless. The methanol was decanted and the resulting polymer dried *in vacuo*.

Polymer 2.



^1H NMR (CDCl_3 , 300 MHz): δ = 7.8 (m, 10H), 7.34 (m, 12H), 6.49 (br s, 4H), 5.50 - 5.17 (br m, 2H), 4.23 (br s, 4H), 4.00 – 3.85 (m, 2H), 3.19 – 2.28 (br m, 3H), 2.01 – 1.55 (br m, 8H), 1.53 – 1.02 (m, 14H). ^{13}C NMR (CDCl_3 , 300 MHz): δ 158.0, 149.8, 148.8, 133.9, 133.9, 131.9, 133.8, 132.4, 132.3, 132.2, 131.5, 131.4, 129.9, 129.7, 129.6, 128.1, 127.9.

Polymer 3.



^1H NMR (DMSO , 300 MHz): δ = 7.7 (m, 10H), 7.4 (m, 12H), 6.6 (br s, 4H), 5.53 - 5.14 (br m, 2H), 4.5 (br m, 4H), 3.31 (s, 4H), 2.13 (br m, 2H), 1.45 - 0.88 (br m, 23H). ^{13}C NMR (DMSO , 300 MHz): δ = 170.3, 158.0, 149.8, 148.8, 133.9, 133.9, 131.9, 133.8, 132.4, 132.3, 132.2, 131.5, 131.4, 129.9, 129.7, 129.6, 128.1, 127.9, 118.9, 113.7, 50.0, 36.4, 30.8, 29.7, 29.4, 25.2.

General procedure for the catalysis.

The reaction was carried under an inert atmosphere using freshly distilled NEt_3 and DMF. A vial was loaded with the catalyst, n-butyl acrylate, iodobenzene and DMF.

The solution was heated to 120 °C. When reaching 120 °C, triethylamine was added in one portion to the solution at which point time 0 was taken for the kinetic data analysis.

Mass spectroscopy.

In a reaction flask, catalyst **1** (23.5 mg, 0.035 mmol) and N,N-dicyclohexyl-N-methyl amine (13.6 mg, 0.07 mmol) were dissolved in DMF. The reaction mixture was heated to 120 °C and stirred for one hour before an aliquot (0.007 mL) of the reaction mixture was removed from the vessel and analyzed via ESI mass spectroscopy (MS-ESI). Another two equivalents (based on **1**) of N,N-dicyclohexyl-N-methyl amine were added to the reaction and stirred for an additional hour before another aliquot was taken and analyzed by MS-ESI. The same operation was repeated for 24 hours. ESI mass spectroscopy spectra of all aliquots showed molecular ion signals at 182.3.

References.

- [1] F. Miyazaki, K. Yamaguchi, M. Shibasaki, *Tetrahedron Lett.* **1999**, 40, 7379.
- [2] M. Ohff, A. Ohff, M. E. van der Boom, D. Milstein, *J. Am. Chem. Soc.* **1997**, 119, 11687.
- [3] D. Morales-Morales, C. Grause, K. Kasaoka, R. Redon, R. E. Cramer, C. M. Jensen, *Inorg. Chim. Acta* **2000**, 300, 958.
- [4] M. R. Eberhard, *Org. Lett.* **2004**, 6, 2125.
- [5] C. M. Frech, L. J. W. Shimon, D. Milstein, *Angew. Chem., Int. Ed.* **2005**, 44, 2.
- [6] R. Chanthateyanonth, H. Alper, *Adv. Synth. Catal.* **2004**, 346, 1375.
- [7] D. E. Bergbreiter, P. L. Osburn, Y. S. Liu, *J. Am. Chem. Soc.* **1999**, 121, 9531.
- [8] C. Paal, W. Hartmann, *Chem. Ber.* **1918**, 51, 711.

- [9] G. M. Whitesides, M. Hackett, R. L. Brainard, J. P. P. M. Lavalleye, A. F. Sowinski, A. N. Izumi, S. S. Moore, D. W. Brown, E. M. Staudt, *Organometallics* **1985**, *4*, 1819.
- [10] J. A. Widegren, R. G. Finke, *J. Mol. Catal. A.* **2003**, *198*, 317.
- [11] K. Yu, W. Sommer, C. W. Jones, M. Weck, *Adv. Synth. Catal.* **2004**, *347*, 161.
- [12] K. Yu, W. Sommer, M. Weck, C. W. Jones, *J. Catal.* **2004**, *226*, 101.
- [13] J. T. Link, L. E. Overman, *In Metal-Catalyzed Cross-Coupling Reactions*, Wiley-VCH:, New York, **1998**.
- [14] J. A. Love, J. P. Morgan, T. M. Trnka, R. H. Grubbs, *Angew. Chem., Int. Ed. Engl.* **2002**, *41*, 4035.
- [15] J. Louie, J. F. Hartwig, *Angew. Chem., Int. Ed. Engl.* **1996**, *35*, 2359.
- [16] E. Poverenov, M. Gandelman, L. J. W. Shimon, H. Rozenberg, Y. Ben-David, D. Milstein, *Chem. Eur. J.* **2004**, *10*, 4673.
- [17] M. Bassetti, A. Capone, M. Salamone, *Organometallics* **2004**, *23*, 247.
- [18] V. Calo, A. Nacci, A. Monopoli, A. Detomaso, P. Iliade, *Organometallics* **2003**, *22*, 4193.
- [19] M. E. Van der Boom, D. Milstein, *Chem. Rev.* **2003**, *103*, 1759.
- [20] M. T. Reetz, J. G. De Vries, *J. Chem. Soc., Chem. Commun.* **2004**, 1559.
- [21] J. Le Bars, U. Specht, J. S. Bradley, D. G. Blackmond, *Langmuir* **1999**, *15*, 7621.
- [22] C. C. Cassol, A. P. Umpierre, G. Machado, S. I. Wolke, J. Dupont, *J. Am. Chem. Soc.* **2005**, 3298.
- [23] A. H. M. de Vries, J. M. C. A. Mulders, J. H. M. Mommers, H. J. W. Henderickx, J. G. de Vries, *Org. Lett.* **2003**, 3285.

- [24] It has been argued that precursor complexes such as palladacycles decompose to give active Pd(0) nanoparticles. This is because previous Hg test results where Hg(0) poisons catalysis have been interpreted as proof for catalysis by heterogeneous catalysts (colloids in this case). We hypothesize here that Hg(0) will also extinguish catalysis by molecular Pd(0) “naked” species⁸⁶⁻⁸⁸ that are not protected by strongly-bound ligands. Unfortunately, at times, the historic literature is interpreted as saying that the Hg test distinguishes between homogeneous and heterogeneous catalysis. This is often the case in the context of the original studies. Indeed, the historic literature^{104,105} with the Hg(0) test focuses on hydrogenation reactions with metal complexes in elevated formal oxidation states bound by protective ligands. Certainly, these catalysts are not affected by Hg(0), as they are not M(0) species and they are protected by strong ligands. We have also shown that Pd(II) pincers are also unaffected by Hg(0) when carrying out stoichiometric reactions where the ligand remains intact and the complex is in a Pd(II) state⁵⁷. However, we hypothesize that “naked” molecular Pd(0) species⁸⁶⁻⁸⁸ that have been postulated to be the true active catalytic species in some cases are an example of homogeneous catalysts that should be affected by Hg(0), as a consequence of their lack of protecting strong ligands and their M(0) state.
- [25] M. Shibasaki, E. M. Vogl, T. Ohshima, *Adv. Synth. Catal.* **2004**, 346, 1533.
- [26] T. Karlen, P. Dani, D. M. Grove, P. Steenwinkel, G. van Koten, *Organometallics* **1996**, 15, 5687.
- [27] D. E. Bergbreiter, J. Li, *J. Chem. Soc., Chem. Commun.* **2004**, 42.

CHAPTER 5

POLYMER SUPPORTED N-HETEROCYCLIC CARBENE

Abstract

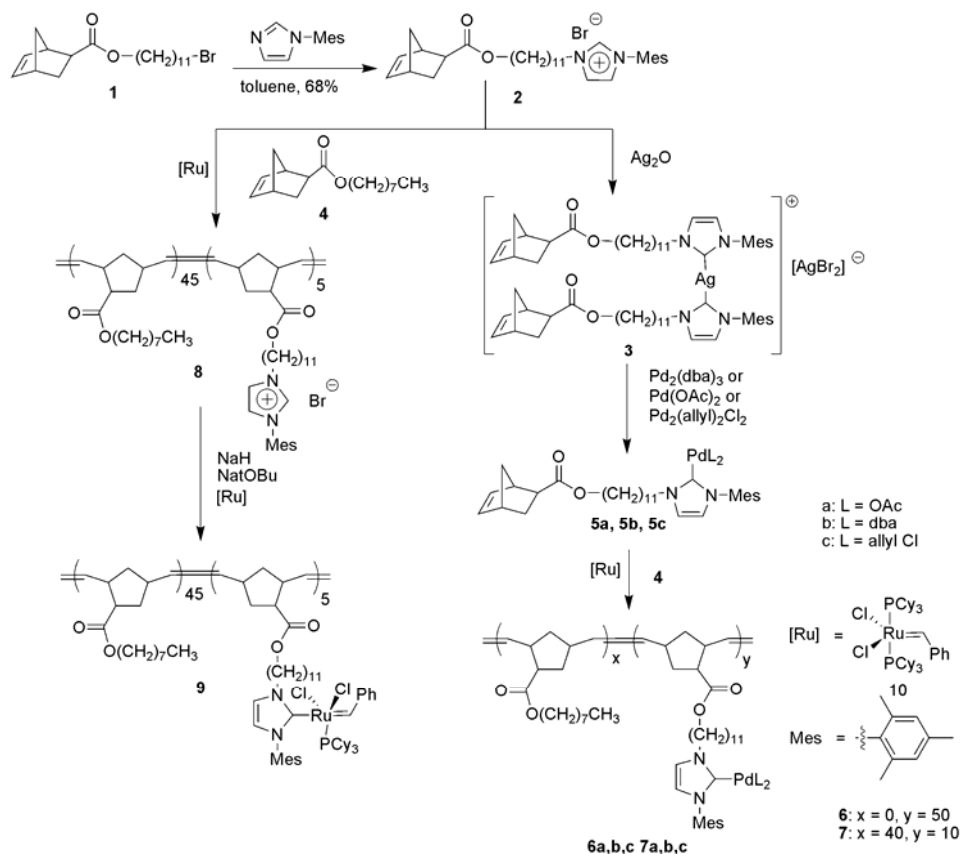
A variety of Pd-*N*-heterocyclic carbenes (NHC) tethered to poly(norbornene) were synthesized. These functionalized norbornenes were then polymerized *via* ring-opening metathesis polymerization in a controlled fashion either before or after metalation with a variety of palladium and ruthenium precursors resulting in the formation of polymer-supported NHC-based metal catalysts. The activities of the palladium-based catalysts in the Suzuki-Miyaura, Sonogashira and Heck coupling reactions were studied in detail. In all cases, the polymeric catalysts demonstrated the same activity as their small molecule analogues. Furthermore, preliminary investigations into the stability of these catalysts using poisoning studies were carried out. A clear dependance of the stability of the polymer-supported catalysts on their palladium precursor was observed with palladium acetate-based polymeric NHC catalysts being the most stable. Finally, the reactivity of the supported NHC ruthenium complexes as catalysts for ring-closing metathesis was studied. Again, in all cases good conversions were observed with comparable activities to other supported NHC-ruthenium catalysts. Lastly, the ruthenium catalyst was removed from the solution quantitatively demonstrating the possibility of metal removal.

5.1. Introduction

Following the results reported in chapters 3 and 4 demonstrating the instability of supported Pd-pincer complexes, different organometallic complexes reported to be stable and performant during catalysis were evaluated. Some of the most stable complexes that were found are Pd-NHC and Ru-NHC complexes. Furthermore, organometallic NHC complexes have shown great performances in a wide variety of reactions, demonstrating their usefulness in the synthesis of complex molecules that have applications ranging from drug precursors to polymers. These vital applications make the NHC ligand a perfect candidate to be supported. However, it must be demonstrated that the catalytic activity of the supported NHC complexes does not change with the nature of the support. Several research groups have made significant contributions towards the synthesis of supported NHC complexes and shown that the catalytic activity is indeed maintained.^[1-4] Over the past five years, NHCs have been grafted onto different supports ranging from monolithic supports to soluble poly(styrene)s.^[1, 2, 4-15] While often successful, metal leaching and low metal loadings remain a major shortcoming for most supported catalysts. In particular the use of a soluble polymer support to immobilize *N*-Heterocyclic carbene metal complexes has often been limited to one catalytic moiety per polymer chain.^[6, 14, 16-18] One exception to this is the work by Buchmeiser *et al.*, whose group reported the functionalization of insoluble monolithic polymer discs with a variety of ruthenium catalysts using elegant postpolymerization functionalization.^[19] In this chapter, the synthesis of supported NHCs using poly(norbornene) as soluble polymer support is reported.

5.2. Results and Discussion

To demonstrate the versatility of this strategy for preparing supported catalysts, I investigated the catalytic activity of this novel polymer supported catalysts in i) the Suzuki-Miyaura coupling of a library of aryl halides with phenylboronic acid, ii) the Sonogashira coupling of ethynyl trimethyl silane or 1-phenyl-trimethylacetylene with bromo-benzenes, iii) the Heck reaction of *n*-butyl acrylate with benzyl halides and iv) the ring-closing metathesis of diethyldiallyl malonate.

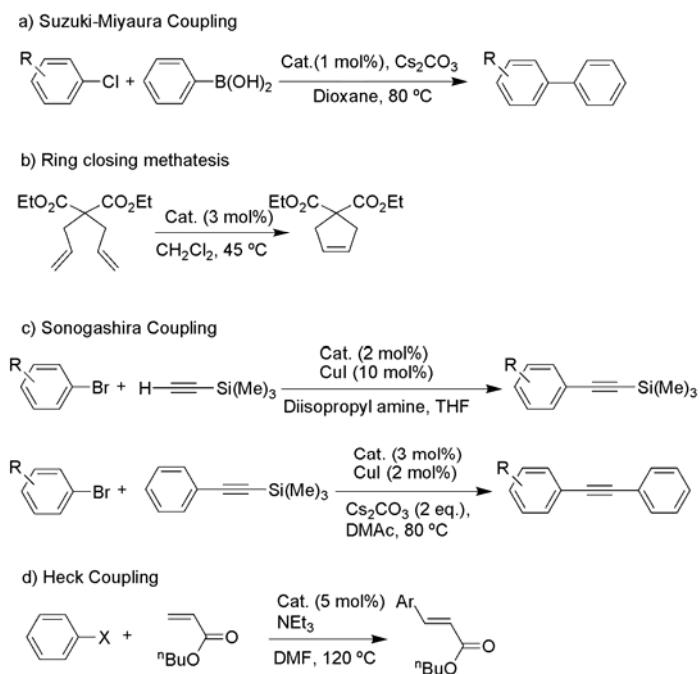


Scheme 5.1. Synthesis of the polymer supported NHC-based catalysts **6**, **7** and **9** utilized in this study.

The synthesis of the four supported catalysts (Scheme 5.1) commences with the formation of **2** that was synthesized by reacting **1** with *N*-mesityl imidazole. The poly(norbornene)-supported Pd-NHC catalysts (**6** and **7**) were synthesized by treating **2** with silver oxide yielding **3**, followed by the addition of either Pd(OAc)₂, Pd₂dba₃, or Pd₂allyl₂chloride₂ to yield **5a – c**. Monomers **5a – c** and **4** were then co-polymerized in

ratios of 1:4 and 1:0 respectively using the first generation Grubbs catalyst **10** to yield copolymers **6a – c** and **7a – c** respectively. For the synthesis of the poly(norbornene)-supported catalysts **9**, **2** and **4** were co-polymerized in ratios of 1:9 with **10**. A ruthenium monomer precursor for **9** could not be synthesized since the ring-opening metathesis polymerization would dominate when mixing the deprotonated form of **2** with **10**.

All catalytic reactions (Scheme 5.2) were carried out under an inert atmosphere using screw-cap vials and were repeated at least three times. The products were characterized by GC-MS and ^1H and ^{13}C NMR spectroscopy.



Scheme 5.2. The catalytic reactions that have been employed to evaluate catalysts **6**, **7** and **9**.

First, the activity of the palladium-supported catalysts in the Suzuki-Miyaura transformation was investigated. The Suzuki-Miyaura transformation is an important tool for the synthesis of complex molecules with applications ranging from supramolecular chemistry^[20] to natural product synthesis.^[21, 22] To evaluate the generality of the supported catalysts, aryl chlorides with electron-donating or electron-withdrawing groups as well as sterically hindered aryl chlorides were employed as reactants and coupled to phenylboronic acid. Suzuki-Miyaura coupling reactions were carried out with all six different supported palladium catalysts (**6a – c** and **7a – c**) using a variety of reaction conditions to evaluate the different catalysts and to optimize reaction conditions.

The first system investigated consisted of a mixture of Pd₂(dba)₃ and **8**, with the carbene and ultimately the catalyst generated *in-situ*. Cs₂CO₃ was used as the base and the reaction was carried out in dioxane at 80 °C using 4-chlorotoluene and phenylboronic acid as reactants. For all substrates, the Suzuki-Miyaura catalysis was complete within three hours with greater than 85 % of products isolated for all transformations, demonstrating the catalytic activity of our *in-situ* generated catalyst. Control experiments using the same reaction conditions in the absence of either the palladium precursor or **8** did not result in the formation of any product.

Table 5.1. Results for the catalytic Suzuki-Miyaura coupling reaction.


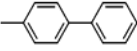

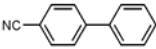
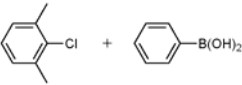
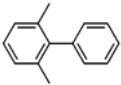
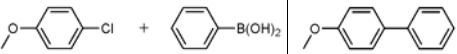
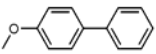
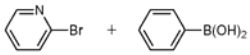
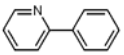
Entry	Substrates	Product	Catalyst	Time (min)	Yield (%)
1			6a	30	99
			6b	30	97
			6c	30	99
			7a	45	99
			7b	45	94
			7c	45	97
2			6a	30	100
			6b	30	99
			6c	30	99
			7a	30	95
			7b	30	97
			7c	30	98
3			6a	130	93
			6b	130	88
			6c	130	84
			7a	130	90

Table 5.1. continued

			7b	130	88
			7c	130	81
4			6a	120	92
			6b	120	88
			6c	120	85
			7a	120	92
			7b	120	86
			7c	120	85
5			6b	180	84

The second Suzuki-Miyaura system studied employed the fully palladated and characterized polymers **6** and **7**. I investigated these supported catalysts in the coupling of phenyl boronic acid to a small library of chloro-aryl compounds. The chloro-aryl compounds were chosen to investigate the influence of electron-donating/withdrawing groups as well as bulky substrates on the catalytic activity of **6** and **7**. Initially, potassium *tert*-butoxide was used as the base and isopropanol as the solvent. When the reactions were carried out at room temperature, 70% conversion was observed after 24 hours. Switching to cesium carbonate as the base and dioxane as the solvent and increasing the reaction temperature to 80° C allowed me to optimize the isolated yields. The catalytic results of these transformations are compiled in Table 5.1. For all substrates, isolated

yields of 80-99% with the vast majority of reactions above 90% yields were obtained within hours.

The different functional groups on the phenyl chlorides affect the conversions only slightly. Substrates containing electron-withdrawing groups such as CN have slightly faster conversions. In contrast, electron-donating groups such as methoxy on the substrates slow down the conversions. Nevertheless, even with substrates containing electron-donating groups, quantitative conversions were still obtained within two to three hours. The sterically bulky substrates such as dimethyl bromobenzene slowed down the reaction and quantitative conversions could not be obtained with any of the catalytic species.

Reactions using copolymers **7** yielded very similar results to the homopolymers suggesting that the spacing of the metal complex does not affect its activity. Overall the different polymer supported catalysts showed very similar conversions compared to their small molecules analogues with catalysts **6a** and **6b** being the most active.

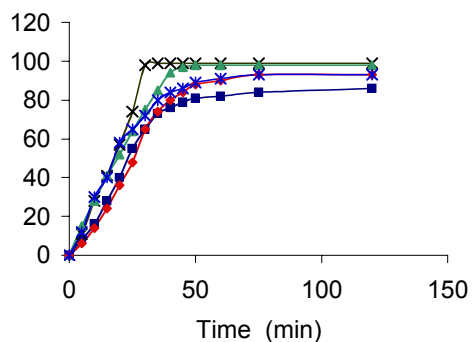
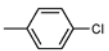
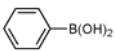
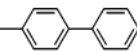
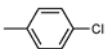
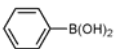
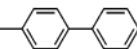
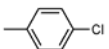
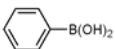
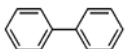
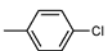
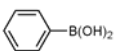
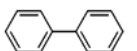
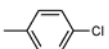
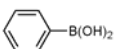
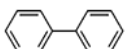
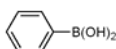
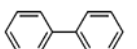
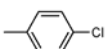
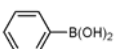
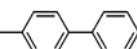
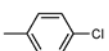
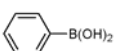
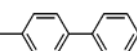
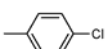
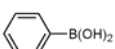
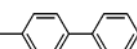


Figure 5.1. Kinetic Study for a) the Suzuki-Miyaura reaction with **6a** (×), b) the Sonogashira reaction with **6a** (▲), c) the Suzuki-Miyaura reaction with **6a** in the presence of QuadraPure[®] (■), d) the Sonogashira reaction with **6a** in the presence of QuadraPure[®] (◆), and e) the Suzuki-Miyaura reaction with **6a** with the addition of QuadraPure[®] after 20 minutes (*).

To investigate the catalytic system further, I performed kinetic studies of the most active polymer supported catalyst, **6a**, using chlorotoluene and phenyl boronic acid as substrates. Samples of the reaction mixtures were taken every five minutes until complete conversion. The kinetic data are outlined in Figure 5.1. The data clearly show that no induction period is present.

Table 5.2. Leaching test results.

Entry	Substrates	Products	Catalyst	Poison	Yield (%)
1	 + 		6a	PVPy (500 mol%)	<15
2	 + 		6a	Poly(styrene) (500 mol%)	<15
3	 + 		6a	Mercury (500 mol%)	95
4	 + 		None	Mercury (500 mol%)	0
5	 + 		Pd(0)	Mercury (500 mol%)	0
6			6a	Mercury (500 mol%)	98
7	 + 		6a	Quadra-Pure 2 eq	89
8	 + 		6b	Quadra-Pure 2 eq	79
9	 + 		6c	Quadra-Pure 2 eq	0

Over the past two years, a variety of supported palladium catalysts have been shown to leach palladium during the catalysis.^[12, 23-26] Chapter 3 and 4 demonstrated that the supported palladium species does not catalyze any carbon-carbon bond formations but that the leached palladium species are the sole catalytically active species.^[23-26] To identify if the same restrictions are true for the poly(norbornene)-supported NHC palladium complexes, I investigated whether or not palladium leaches during the reaction and if the polymer supported species is active during the catalysis. To identify the nature of the catalytic species, three catalyst poisons were used: a) highly cross-linked insoluble poly(vinyl pyridine) (PVPy), b) Quadra-Pure[®], a microporous resin metal scavenger that is especially sensitive to palladium, and c) mercury(0).^[61-63]

Leaching test for the Suzuki couplings was carried out using the same reaction conditions as outlined above. When carrying out the PVPy poisoning test (a ratio of 1:500 of Pd to PVPy was used) with catalyst **6a**, a decrease in activity was observed, with only 15% conversion after 24 hours (Table 5.2, Entry 1). Nevertheless, the catalyst stayed active during the whole experiment. To test if this decrease was due to palladium leaching off the supported NHC ligands or due to the lack of accessibility of the reactants to the catalyst sites, the same reaction using cross-linked poly(styrene) ($M_w = 25,000$) was carried out. Poly(styrene) is not able to coordinate to leached palladium and should therefore not inhibit the catalysis from leached metal species. When carrying out the catalysis in the presence of 500 equivalents of poly(styrene) for each catalytic moiety, a dramatic drop in catalyst activity was observed, with a conversion of approximately 15 % after 24 hours (Table 5.2, Entry 2), *i.e.* the same drop in activity was observed as described above for the poly(vinyl pyridine) poisoning experiment. This result suggests

that the reduced activity in the poly(vinyl pyridine) leaching test is most likely not due to metal leaching during the catalysis but reduced accessibility of the active sites in this case.

When carrying out the mercury test with the polymer supported palladium NHC catalyst **6a**, 90% conversion of the phenylboronic acid to the corresponding biphenyl, the homocoupling product, was observed (Table 5.2, Entry 3). To investigate this result, a series of control experiments were carried out. First, the reaction without the supported palladium complex was carried out, *i.e.* only the reactants and the mercury (Table 5.2, Entry 4) were added to the reaction flask. No conversions were observed. When using a non-supported Pd(0) source as catalyst, either Pd on carbon or Pd₂(dba)₃, and mercury (Table 5.2, Entry 5) no conversion was observed. This proves that Pd(0) metal is not active in the presence of mercury. In the literature a variety of reductants including mercury(0) are described to catalyze the homocouplings of aryl boronic acids as well as aryl iodides or bromides.^[27-30] To investigate if the mercury acts as a reductant in the poisoning tests, I carried out the catalytic reaction without the addition of chlorotoluene, *i.e.* only phenyl boronic acid, the supported catalyst and mercury were present during the reaction. This experiment resulted in 95% conversion (Table 5.2, Entry 6) of the phenyl boronic acid to the corresponding biphenyl. These results suggest that the mercury acts as a reductant in our poisoning tests but also that the supported palladium catalyst seems to be stable during the poisoning test and that no palladium leaches out. If leaching would have occurred and the catalysis (homocoupling) would have been due to a leached Pd species, the Hg should have amalgamized the leached Pd species resulting in no catalysis. Based on the PVPy and Hg(0) poisoning tests, no definite conclusions can be

drawn regarding the stability and the potential palladium leaching of the polymer supported catalyst **6a**. Following these results no further PVPy or Hg(0) leaching tests were carried out on any other supported catalysts **6b**, **c** or **7a-c**.

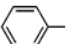

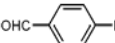
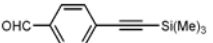
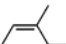

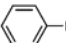


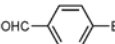

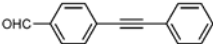
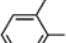
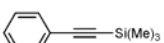

The next leaching tests that were carried out used QuadraPure[®] to trap leached palladium. QuadraPure[®] is a microporous resin that scavenges different metals and is especially efficient for trapping palladium.^[31] When carrying out the Suzuki-Miyaura coupling reaction in the presence of QuadraPure[®], 89% and 79% conversions were observed after 120 minutes (in comparison, the reactions without the addition of QuadraPure[®] gave 99% yields after 30 minutes) with **6a** and **6b** respectively while no conversions were obtained when using **6c** as catalyst. Kinetic studies using **6a** and QuadraPure[®] (Figure 5.1 blue squares and stars) showed that the presence of QuadraPure slows the reaction but does not inhibit conversion. The conversion obtained was 86% within 120 minutes. The presence of QuadraPure[®] slowed down the conversion but the kinetic curve looks very similar to the one without the poison present. By comparing the kinetic data with and without QuadraPure[®] present during the catalysis, one can clearly see that the poison, while slowing down the catalysis, does not prevent the catalytic transformation, suggesting that the active species for the catalysis is, at least in part, the polymer-supported palladium complex.

In summary, the poisoning studies show that **6c** leaches under the Suzuki-Miyaura reaction conditions and that the polymer supported **6c** is not catalytically active. Rather the catalytic species is a leached palladium species. In contrast, while these leaching studies cannot exclude small amounts of leached species for **6a** and **6b**, they show that

QuadraPure[®] does not shut down the catalysis proving that both polymers are catalytically active in the Suzuki-Miyaura coupling.

Recycling experiment were carried out for the Suzuki-Miyaura coupling of chloro-benzene with phenyl-boronic acid using similar conditions as described above. After complete reaction (confirmed by GC), the reactants and products were distilled off and the resulting polymeric residue dried. The polymeric residue was then reused for the same catalytic transformation using the exact same reaction conditions. The polymer became less soluble after this first cycle yielding 80% conversion after 90 minutes. Following the same isolation procedure after the second cycle, the polymer became only slightly soluble in DMF for the third reuse and yielded only 44% conversion after 90 minutes. I have observed the same solubility problems with other poly(norbornene)-based catalyst supports^[32] and investigations are currently being carried out to characterize the reason for the decrease in solubility.

Table 5.3. Catalytic results for the Sonogashira coupling reaction.

Entry	Substrates	Products	Catalyst	Time (min)	Yield (%)
1	 + $\text{H}-\text{C}\equiv\text{C}-\text{Si}(\text{Me})_3$		6a	150	100
2	 + $\text{H}-\text{C}\equiv\text{C}-\text{Si}(\text{Me})_3$		6a	120	100
3	 + $\text{H}-\text{C}\equiv\text{C}-\text{Si}(\text{Me})_3$		6a	150	83
4	 + 		6a	45	96
5	 + 		6a	25	99
6	 + 		6a	60	95

To expand the scope of the catalysts, the Sonogashira coupling using the most active polymeric catalysts **6a** was investigated. Because of the importance of alkyne functionalities for a wide range of natural compounds as well as in the synthesis of highly conducting materials,^[33-37] the Sonogashira reaction between an alkylhalide and a terminal alkyne is the method of choice to incorporate alkyne functionalities in aromatic systems. The reaction was developed in 1975 by Sonogashira using a mixture of palladium and copper iodide as the catalyst and has been improved steadily over the past 30 years.^[38-41] In this chapter, two types of Sonogashira reactions were investigated. The

first one consisted of the coupling of a silyl terminated acetylene to an aryl bromide. As reactants, I employed a silane protected acetylene and a small library of aryl bromides. Diisopropylamine (ten equivalents) was used as the base and tetrahydrofuran as the solvent. The base, solvent and CuI (10 mol%) were added to the reaction vessel at room temperature. When subjected to these conditions, all aryl halides were converted to the corresponding products in 83-100% isolated yields in 120-150 minutes (Table 5.2). As expected, the reaction using bromobenzaldehyde as reactant was the fastest with 100% conversion in 120 minutes. The more sterically hindered 2-bromotoluene reacted in 83% conversion within 150 minutes compared to the non-hindered bromobenzene which had quantitative conversion within the same time.

The second Sonogashira reaction consisted of the *in-situ* deprotection of a silane protected acetylene and the coupling of the resulting acetylene with different aryl bromide.^[42] Cesium carbonate (two equivalents) which was employed as the base and deprotection agent, dimethylacetate, and CuI (2 mol%) were added to a screw cap vial and stirred at 80 °C. Similar yields but faster reaction rates compared to method A were obtained. The 4-bromo benzaldehyde showed quantitative conversions within 25 minutes while the bromo-benzene and the 2-bromotoluene had 96% and 95% conversion within 45 and 60 minutes respectively. These results compare favorably with those reported by Nolan *et al.* using the small molecule analog to **6a**.^[42]

To verify the robustness of our catalysts in the Sonogashira coupling reactions, leaching tests were carried out using **6a** and QuadraPure[®] as the poison. I employed benzylbromide and silane protected acetylene as reactants, CuI (10 mol%), diisopropylamine (ten equivalents) as the base and THF as solvent. After 24 hours, 100%

conversion was observed. The second Sonogashira reaction tested consisted of bromobenzene and trimethyl(phenylethynyl) silane as reactants, cesium carbonate (2 equivalents) as a base, CuI (2 mol%) and dimethylacetate. Again, the reaction yielded 100% conversion after 24 hours. To determine the activity of **6a** in the presence of QuadraPure[®] in more detail, I carried out kinetic studies with and without the poison. The results are shown in Figure 5.1. As it was the case for the Suzuki coupling poisoning studies, the Sonogashira reaction slows down slightly in the presence of QuadraPure[®]. The transformation takes 35 minutes to reach 80% conversion without the poison while in the presence of the poison the same conversions are obtained after 50 minutes. Therefore, in analogy to the Suzuki studies outlined above, the Sonogashira poisoning studies demonstrate the stability of our catalyst under Sonogashira reaction and suggest that the active species for the catalysis is at least partially the polymer-tethered palladium complex.

The third palladium-catalyzed transformation studied was the Heck coupling reaction. This reaction has been widely studied since its first report in the early 70's.^[43, 44] Again, I employed the best catalyst, **6a** (2 mol%), for all studies. I used triethylamine (two equivalents) as base and iodobenzene (one equivalent) and *n*-butylacrylate (1.5 equivalents) as substrates. At 120 °C, the catalysis proceeded in 30 minutes with 99% conversions. However, after the reaction, some palladium black was observed at the bottom of the flask indicating leaching of palladium from the complex. As these results clearly showed metal leaching, I wanted to investigate if the polymer-supported catalyst is catalytically active or if all activity stems from the leached palladium species. I carried out a Heck catalysis experiment in the presence of the QuadraPure[®] poison. The reaction

conditions were: iodobenzene and *n*-butylacrylate as reactants, triethylamine (two equivalents) as the base and DMF as solvent. The reaction yielded 44% conversion after 24 hours. While this result is inconclusive, the observed palladium black formation during the catalysis in combination with the lower conversions suggests that the vast majority of catalytic activity stems from leached palladium species and not from **6a**.

The second metal that was supported on the poly(norbornene) NHC polymers was ruthenium. The resulting polymer supported ruthenium complex (**9**) was investigated as active catalysts for olefin metathesis, in particular ring-closing metathesis (RCM).^[45] To study the activity of these supported catalysts, the RCM of diethyl diallyl malonate in methylene chloride at 45 °C was investigated.^[10, 46, 47] Under these reaction conditions, diethyl diallyl malonate was converted in 95% yield to its corresponding RCM product, cyclopent-3-ene-1,1-dicarboxylic acid diethyl ester, within 20 minutes using 5.0 mol% of **9** (Table 5.1, Entry 15). This activity is comparable to other supported Grubbs catalyst analogues of **10** that convert diethyl diallyl malonate using similar catalyst loadings with the same conversions in the same time frame,^[10, 46, 47] demonstrating that the supported catalyst is an active olefin metathesis catalyst.

The polymeric catalyst **9** can be removed from the reaction mixture after complete catalysis using basic precipitation methods. To elucidate whether any ruthenium leached into the reaction solution and if the polymeric catalysts can be removed quantitatively, ICP-MS and elemental analyses of the reaction solutions after the removal of the polymeric catalysts were carried out. The analyses showed no traces of ruthenium in the reaction solution demonstrating the quantitative recovery of the polymer and thereby the quantitative removal of the metal species from the reaction mixture.

5.3. Conclusion

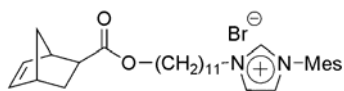
This chapter describes the synthesis of a new class of polymer-supported *N*-heterocyclic carbene ligands, their metalation, before and after polymerization, and their use as supported catalysts for a variety of carbon-carbon bond formations. I demonstrated the versatility of our supported catalysts by investigating the catalytic activity of all complexes in a wide array of reactions ranging from RCM to Suzuki couplings. For all transformations studied, the catalysts showed high activities that were comparable to their small molecule analogous. We have shown by using poisoning studies that the stability of the palladium-based polymeric catalysts depended on the ligands around the palladium center. While for the polymer supported palladium acetate-based NHC complexes the catalytic activity in the Suzuki and Sonogashira couplings stems mainly from the polymer-tethered complexes, palladium dba-based NHC complexes decompose under these reaction conditions. Finally, for the ring-closing metathesis I demonstrated the ability to remove the polymeric catalysts from the reaction mixture thereby ensuring the removal of any undesirable metal species from the product obviating extensive purification steps.

5.4. Experimental section

General Experimental Conditions. All reactions with air- and moisture sensitive compounds were carried out under a dry nitrogen/argon atmosphere using an MBraun UniLab 2000 dry box and/or standard Schlenk line techniques. THF, CH₂Cl₂, toluene, 1,4 dioxane and hexanes were distilled from sodium and benzophenone. Benzyl alcohol and methyl acetate were distilled from calcium hydride. Pd(OAc)₂, first generation

Grubbs catalyst, and all bases were obtained from commercial sources and generally used without further purification. The syntheses of mesityl imidazole and **1** were carried out following published procedures.^[48, 49] Gas-chromatographic analyses were performed on a Hewlett Packard G1800A GCD system GC-MS. ¹H (300 MHz) and ¹³C NMR (75 MHz) spectra were recorded on a Varian Mercury VX instrument. All spectra were referenced to residual proton solvent. Mass spectral analyses were provided by the Georgia Tech MassSpectrometry Facility using a VG-70se spectrometer. Gel-permeation chromatography (GPC) analyses were carried out using a Waters 1525 binary pump coupled to a Waters 2414 refractive index detector. The GPC was calibrated using poly(styrene) standards on a Styragel[®] HR 4 and HR 5E column set with CH₂Cl₂ as an eluent. All GPC experiments were carried out with a flow rate of 1 mL/min. Elemental analyses were carried out by either Atlantic Microlabs, Norcross GA (CHN analyses) or Galbraith Laboratories, Inc., TN (determination of the metal content).

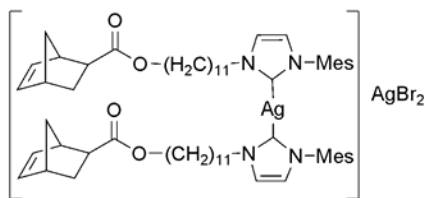
Synthesis of *exo*-1-[11-(bicyclo[2.2.1]hept-5-ene-2-carbonyloxy)-undecyl]-3-(2,4,6-trimethyl-phenyl)-3H-imidazol-1-ium (2)



In a round bottom flask equipped with a condenser, mesityl imidazole (950 mg, 5.1 mmol), **1** (1.9 g, 5.1 mmol) and toluene (50 mL) were added. The reaction was

refluxed for 72 hours. The solvent was removed yielding a brown oil which was purified using column chromatography (eluent: 1:20 \Rightarrow 1:1 ethanol : hexanes) to yield a yellow oil (1.6 g, 68%). ^1H NMR (CDCl_3): δ = 10.57 (s, 1H), 7.47 (s, 1H), 7.12 (s, 1H), 6.99 (s, 2H), 6.10 (m, 2H), 4.07 (t, J = 6.6 Hz, 2H), 3.03 (m, 1H), 2.33 (s, 5H), 2.07 (s, 9H), 1.91 (m, 1H), 1.75-1.58 (m, 5H), 1.54 (m, 1H), 1.51 (m, 1H), 1.46-1.19 (m, 14H). ^{13}C NMR (CDCl_3): δ = 176.2, 139.4, 138.6, 135.2, 134.5, 129.2, 64.5, 51.7, 46.2, 43.0, 41.9, 31.2, 30.3, 29.5, 28.8, 26.0, 25.5, 21.2, 17.0. MS (ESI): m/z = 477.53 (M^+ , calcd 477.35). Anal. Calcd for $\text{C}_{31}\text{H}_{45}\text{BrN}_2\text{O}_2$: C, 66.77; H, 8.13; N, 5.02. Found: C, 66.69; H, 8.15; N, 5.11.

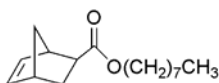
Synthesis of *exo*-Ag-di-bicyclo[2.2.1]hept-5-ene-2-carboxylic acid 11-[3-(2,4,6-trimethyl-phenyl)-2,3-dihydro-imidazol-1-yl]-undecyl ester silver dibromide (3)



In a screw cap vial **2** (306 mg, 0.54 mmol), silver oxide (64 mg, 0.27 mmol) and CH_2Cl_2 (10 mL) were combined. The solution was stirred for three hours during which a white precipitate formed. The solution was then filtered through celite and the solvent removed *in vacuo* to yield a brown oil. Yield 320 mg (89%). ^1H (CDCl_3): δ = 7.12 (m, 2H), 6.99 (s, 2H), 6.10 (m, 2H), 4.07 (t, J = 6.6 Hz, 2H), 3.03 (m, 1H), 2.33 (s, 5H), 2.07 (s, 9H), 1.91 (m, 1H), 1.75-1.58 (m, 5H), 1.54 (m, 1H), 1.51 (m, 1H), 1.46-1.19 (m,

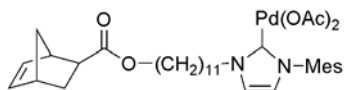
14H). ^{13}C NMR (CDCl_3): δ = 177.2, 139.4, 138.6, 135.5, 134.4, 129.2, 64.2, 51.1, 46.9, 43.5, 41.7, 31.4, 30.4, 29.0, 28.3, 26.6, 25.0, 23.5, 21.1, 17.1. MS (ESI): m/z = 1061.92 (M^+ , calcd 1061.65). Anal calcd for $\text{C}_{62}\text{H}_{90}\text{Ag}_2\text{Br}_2\text{N}_4\text{O}_4$: C, 55.95; H, 6.82; N, 4.21. Found: C, 56.03; H, 6.85; N, 4.42.

Synthesis of *exo*-bicyclo[2.2.1]hept-5-ene-2-carboxylic acid octyl ester (4)



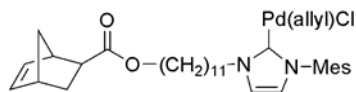
In a round bottom flask equipped with a condenser, *exo*-bicyclo[2.2.1]hept-5-ene-2-carboxylic acid (2.44 g, 17.6 mmol), 1-octanol (2.8 mL, 17.6 mmol), dicyclohexyl diamine (3.6 g, 17.6 mmol), a catalytic amount of diaminopyridine (100 mg) and CH_2Cl_2 (20 mL) were combined and refluxed overnight. The solution was then filtered through celite and the solvent removed under vacuum to yield a yellow solution which was further purified using column chromatography (eluent: hexanes) to yield 3.74 g of a colorless oil (85%). ^1H NMR (CDCl_3): δ = 6.12 (m, 2H), 4.07 (t, 2H, J = 6.6 Hz), 3.03 (m, 1H), 2.92 (m, 1H), 2.21 (m, 1H), 1.68-1.49 (m, 3H), 1.41-1.24 (m, 12H), 0.88 (t, 3H, J = 7.1 Hz). ^{13}C NMR (CDCl_3): δ = 176.2, 137.8, 135.6, 46.8, 46.2, 43.2, 41.5, 33.9, 29.2, 28.9, 28.5. MS (ESI): m/z = 250.20 (M^+ , calcd 250.38). Anal. Calcd for $\text{C}_{16}\text{H}_{26}\text{O}_2$: C, 76.75; H, 10.47; Found: C, 76.69; H, 10.51.

Synthesis of *exo*-Pd(OAc)₂-bicyclo[2.2.1]hept-5-ene-2-carboxylic acid 11-[3-(2,4,6-trimethyl-phenyl)-2,3-dihydro-imidazol-1-yl]-undecyl ester (5a)



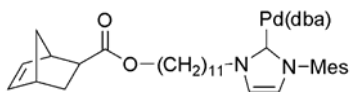
Under inert atmosphere, in a screw cap vial, **3** (200 mg, 0.4 mmol), Pd(OAc)₂ (141 mg, 0.6 mmol) and CH₂Cl₂ (10 mL) were added. The solution was stirred overnight yielding a silver solid. The reaction mixture was filtered through celite to yield a yellow solution. The solvent was removed and the resulting yellow oil was further purified *via* column chromatography (eluent 1:1 hexanes:ethylacetate) to yield a yellow solid. Yield 190 mg (60%). ¹H NMR (CDCl₃): δ = 6.88 (s, 2H), 6.10 (m, 2H), 4.07 (t, *J* = 6.6 Hz, 2H), 3.03 (m, 1H), 2.33 (s, 5H), 2.07 (s, 9H), 1.91 (m, 1H), 1.75-1.58 (m, 5H), 1.54 (m, 1H), 1.51 (m, 1H), 1.46-1.19 (m, 20H). ¹³C NMR (CDCl₃): δ = 220.2, 176.2, 139.7, 137.9, 135.1, 134.4, 129.6, 64.1, 51.2, 46.7, 43.4, 41.5, 31.6, 30.5, 29.9, 28.2, 26.4, 25.6, 21.5, 17.0. MS (ESI): *m/z* = 701.3 (*M*⁺, calcd 700.27). Anal. Calcd for C₃₅H₅₀N₂O₆Pd: C, 59.95; H, 7.19; N, 4.00. Found C 60.21; H, 7.23; N, 3.92.

Synthesis of *exo*-Pd(allyl)Cl-bicyclo[2.2.1]hept-5-ene-2-carboxylic acid 11-[3-(2,4,6-trimethyl-phenyl)-2,3-dihydro-imidazol-1-yl]-undecyl ester (5b)



Under inert atmosphere, in a screw cap vial, **3** (57 mg, 0.04 mmol), Pd₂(allyl)₂Cl₂ (16 mg, 0.04 mmol) and THF (5 mL) were combined. The solution was stirred for five hours forming a silver precipitate. The reaction mixture was filtered through celite to yield a yellow solution. The solvent was removed *in vacuo* to yield yellow oil. The oil was washed three times with hexanes and dried under *vacuo* forming yellow foam. Yield 16 mg (64%). ¹H NMR (CDCl₃): δ = 7.06 (d, 2H), 6.85 (m, 2H), 6.12 (m, 2H), 4.52 (m, 4H), 4.06 (t, *J* = 6.5 Hz, 2H), 3.71 (m, 1H), 3.06 (d, 1H), 3.02 (m, 1H), 2.72 (d, 1H), 2.33 (s, 5H), 2.07 (s, 9H), 1.91 (m, 1H), 1.75-1.55 (m, 6H), 1.54 (m, 1H), 1.51 (m, 1H), 1.46-1.16 (m, 14H). ¹³C NMR (CDCl₃): δ = 180.1, 174.5, 139.8, 136.7, 135.2, 132.6, 122.4, 121.5, 114.8, 68.5, 64.3, 49.5, 43.2, 42.4, 30.9, 29.4, 29.1, 28.5, 26.3, 25.9, 25.8, 25.5, 21.0. MS (ESI): *m/z*: 660.35 (M⁺, calcd 660.27). Anal. Calcd for C₃₄H₅₁ClN₂O₂Pd: C, 61.72; H, 7.77; N, 4.23. Found C 61.03; H 7.74; N 4.95.

Synthesis of *exo*-Pddba-bicyclo[2.2.1]hept-5-ene-2-carboxylic acid 11-[3-(2,4,6-trimethyl-phenyl)-2,3-dihydro-imidazol-1-yl]-undecyl ester (5c)



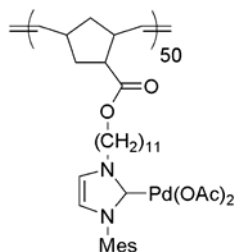
Under inert atmosphere, in a screw cap vial, **3** (76 mg, 0.06 mmol), Pd₂dba₃ (52 mg, 0.06 mmol) and THF (5 mL) were combined. The solution was stirred for five hours forming a black precipitate. The reaction mixture was filtered through celite to yield a black solution. The solvent was removed *in vacuo* to yield a black solid. The solid was washed three times with hexanes and dried under *vacuo* to yield a brown solid. Yield 21 mg (45%). ¹H NMR (CDCl₃): δ = 7.65 (d, 4H), 7.31 (m, 6H), 7.12 (d, 2H), 6.95 (m, 2H), 6.86 (m, 2H), 6.82 (m, 2H), 6.11 (m, 2H), 4.08 (t, *J* = 6.4 Hz, 2H), 3.05 (m, 1H), 2.33 (s, 5H), 2.07 (s, 9H), 1.93 (m, 1H), 1.75-1.58 (m, 5H), 1.55 (m, 1H), 1.51 (m, 1H), 1.46-1.20 (m, 14H). ¹³C NMR (CDCl₃): δ = 189.1, 179.7, 145.8, 139.3, 136.2, 135.8, 135.3, 132.1, 129.5, 127.9, 125.3, 122.1, 115.4, 71.8, 50.8, 46.9, 43.2, 39.8, 36.3, 30.8, 30.0, 29.6, 25.3, 24.1. MS (ESI): *m/z* 818.30 (M⁺, calcd 818.41). Anal. Calcd for C₄₈H₅₉N₂O₃Pd: C, 70.44; H, 7.27; N, 3.42. Found C, 70.33; H 7.32; N, 3.15.

General polymerization procedure for the synthesis of polymers 5 - 9

The respective monomer was dissolved in CDCl₃ followed by the addition of the desired amount of catalyst. The polymerization was monitored by NMR spectroscopy. After complete polymerization a few drops of ethyl vinyl ether were added to terminate

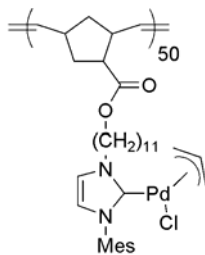
the polymerization. The polymer was purified by repeated precipitations into cold methanol followed by centrifugation at 400 rpm for ten minutes. The purification procedure was repeated until the resulting methanol solution became colorless. The methanol was decanted and the resulting polymer dried *in vacuo*.

Polymer 6a.



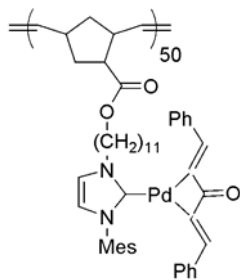
^1H NMR (CDCl_3): δ = 6.89-6.85 (br s, 2H), 5.53-5.21 (br m, 2H), 4.07-3.99 (br m, 2H), 3.03 (m, 1H), 2.33-2.30 (br s, 5H), 2.07-1.99 (br s, 9H), 1.91 (m, 1H), 1.75-1.58 (br m, 5H), 1.54 (m, 1H), 1.51 (m, 1H), 1.46-1.19 (br m, 20H). ^{13}C NMR (CDCl_3): δ = 184.0, 175.2, 175.0, 169.2, 145.5, 143.9, 137.4, 136.2, 128.4, 126.3, 126.0, 122.2, 114.4, 104.5, 50.2, 47.1, 43.1, 40.9, 36.4, 30.8, 29.7, 29.4, 25.2, 14.4, 9.2.

Polymer 6b.



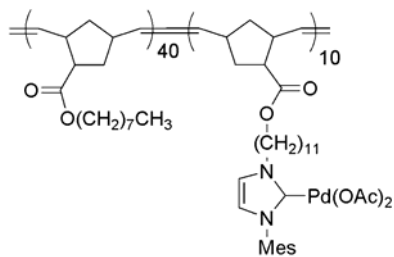
¹H NMR (CDCl₃): δ = 7.06-7.03 (br m, 2H), 6.88-6.83 (br m, 2H) 5.55-5.20 (br m, 2H), 4.52-4.50 (br m, 4H), 4.07-4.02 (m, 2H), 3.71 (m, 1H), 3.07-3.05 (m, 1H), 3.02 (m, 1H), 2.74 (m, 1H), 2.33-2.28 (br s, 5H), 2.05 (br s, 9H), 1.91 (m, 1H), 1.75-1.53 (m, 6H), 1.52 (m, 1H), 1.50-1.48 (br m, 1H), 1.44-1.13 (br m, 14H). ¹³C NMR (CDCl₃): δ = 180.1, 139.0, 136.4, 135.8, 135.5, 132.1, 128.9, 122.0, 121.1, 114.4, 73.2, 50.3, 47.4, 43.4, 40.2, 36.4, 30.2, 29.8, 29.4, 25.4, 14.3, 8.9.

Polymer 6c.



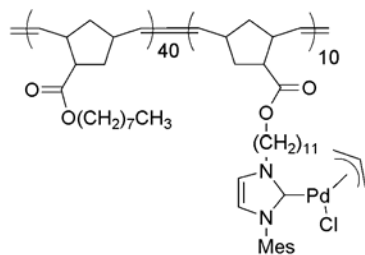
^1H NMR (CDCl_3): δ = 7.67-7.64 (br m, 4H), 7.34-7.30 (br m, 6H), 7.12-7.10 (br m, 2H), 6.95 (m, 2H), 6.86 (m, 2H), 6.84-6.81 (br m, 2H), 5.61-5.54 (br m, 2H) 4.10 (m, 2H), 3.05 (m, 1H), 2.33-2.29 (br s, 5H), 2.09-2.06 (br s, 9H), 1.95-1.93 (br m, 1H), 1.75-1.58 (m, 5H), 1.55-1.53 (m, 1H), 1.51-1.49 (m, 1H), 1.45-1.16 (m, 14H). ^{13}C NMR (CDCl_3): δ = 189.1, 179.8, 145.8, 139.2, 136.8, 135.8, 135.3, 132.1, 129.5, 128.9, 125.3, 122.1, 114.4, 71.2, 50.8, 46.9, 43.2, 39.8, 36.3, 30.8, 30.0, 29.6, 25.3, 13.5, 8.9.

Polymer 7a.



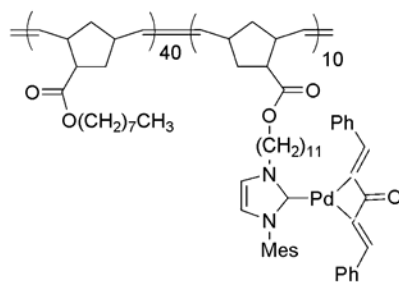
^1H NMR (CDCl_3): δ = 6.89-6.85 (br s, 2H), 5.53-5.21 (br m, 10H), 4.07-3.99 (br m, 10H), 3.03 (m, 5H), 2.33-2.26 (br s, 25H), 2.07-1.92 (br s, 45H), 1.91 (m, 4H), 1.75-1.58 (br m, 5H), 1.56-1.52 (m, 5H), 1.51-1.49 (m, 5H), 1.46-0.63 (br m, 100H). ^{13}C NMR (CDCl_3): δ = 184.0, 175.2, 175.0, 169.2, 151.8, 145.5, 143.9, 137.4, 136.2, 128.4, 126.5, 126.2, 122.2, 114.4, 104.8, 113.7, 64.8, 50.0, 48.7, 47.1, 43.1, 40.9, 36.4, 30.8, 29.7, 29.4, 26.3, 25.2, 14.4, 9.1.

Polymer 7b.



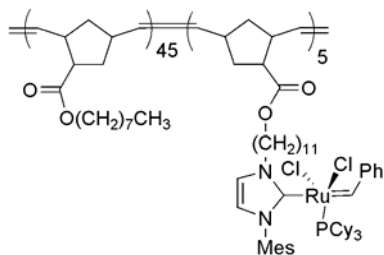
^1H NMR (CDCl_3): δ = 7.08-7.03 (br m, 2H), 6.89-6.80 (br m, 2H) 5.55-5.22 (br m, 2H), 4.52-4.50 (br m, 4H), 4.07-4.02 (m, 10H), 3.71 (m, 1H), 3.07-3.03 (m, 5H), 2.33-2.23 (br m, 25H), 2.05-1.89 (br m, 49H), 1.75-1.49 (br m, 6H), 1.48-1.43 (br m, 5H), 1.41-0.59 (br m, 100H). ^{13}C NMR (CDCl_3): δ = 180.1, 139.0, 136.4, 135.8, 135.5, 132.1, 128.9, 122.0, 121.1, 114.4, 73.2, 50.3, 48.3, 47.4, 43.4, 40.8, 40.2, 36.4, 31.1, 30.2, 29.8, 29.4, 26.7, 25.4, 14.3, 8.9, 8.6.

Polymer 7c.



^1H NMR (CDCl_3): δ = 7.67-7.64 (br m, 4H), 7.35-7.30 (br m, 6H), 7.12-7.10 (br m, 2H), 6.98-6.94 (br m, 2H), 6.86 (m, 2H), 6.84-6.81 (br m, 2H), 5.61-5.54 (br m, 2H) 4.10-4.01 (br m, 11H), 2.33-2.21 (br s, 25H), 2.09-1.98 (br s, 49H), 1.75-1.52 (m, 7H), 1.45-0.86 (m, 100H). ^{13}C NMR (CDCl_3): δ = 189.1, 179.8, 145.8, 139.2, 136.8, 135.8, 135.3, 132.1, 129.5, 128.9, 125.3, 122.1, 114.4, 71.2, 50.8, 46.9, 42.1, 43.2, 39.8, 37.3, 36.3, 35.2, 32.1, 31.4, 30.8, 30.0, 29.6, 28.4, 27.6, 25.3, 20.1, 13.5, 9.2, 8.7.

Polymer 9.



^1H NMR (CDCl_3): δ = 7.20-7.03 (br m, 4H), 6.86-6.82 (br m, 2H) 5.53-5.21 (br m, 2H), 4.55-4.50 (br m, 4H), 4.10-4.02 (m, 10H), 3.71 (m, 1H), 3.12-3.05 (m, 5H), 2.45-2.23 (br m, 25H), 2.04-0.59 (br m, 184H). ^{13}C NMR (CDCl_3): δ = 190.4, 150.1, 139.0, 136.4, 135.8, 135.5, 132.1, 128.9, 126.4, 123.4, 122.2, 121.1, 114.4, 73.1, 52.3, 49.1, 47.3, 42.7, 40.5, 40.1, 31.5, 30.1, 29.9, 29.4, 28.7, 25.1, 11.3, 9.3, 8.2.

Characterization of the products from table 5.1

Product 1: ^1H NMR (CDCl_3): δ = 7.76 (m, 2H, o- CH_3), 7.67 (m, 2H, m- CH_3), 7.54 (m, 2H, o-Bn), 7.45 (m, 2H, m-Bn), 7.34 (m, 1H, p-Bn), 2.37 (s, 3H, CH_3).

Product 2: ^1H NMR (CDCl_3): δ = 7.75 (m, 2H, o-CN), 7.53 (m, 2H, o-Bn), 7.46 (m, 2H, m-CN), 7.40 (m, 2H, m-Bn), 7.37 (m, 1H, p-Bn).

Product 3: ^1H NMR (CDCl_3): δ = 7.52 (m, 1H, p-Mes), 7.31 (m, 2H, m-Mes), 7.22 (m, 1H, p-Bn), 7.18 (m, 2H, o-Mes), 7.12 (m, 2H, m-Bn), 2.71 (s, 6H, CH_3).

Product 4: ^1H NMR (CDCl_3): δ = 7.58 (m, 2H, p-OMe), 7.55 (m, 2H, o-Bn), 7.36 (m, 2H, m-Bn), 7.32 (m, 1H, p-Bn), 6.98 (m, 2H, o-OMe), 3.88 (s, 3H, O- CH_3).

Product 5: ^1H NMR (CDCl_3): $\delta = 8.56$ (m, 1H, **CH-N**), 7.98 (m, 2H, o-Py), 7.55 (m, 1H, **N=C-CH**), 7.48 (m, 1H, Py), 7.34 (m, 2H, m-Py), 7.26 (m, 1H, p-Py), 6.99 (m, 1H, Py).

Characterization of the products from table 5.2

Product 1: See table 5.1 product 1

Product 2: ^1H NMR (CDCl_3): $\delta = 7.52$ (m, 4H, o-Bn), 7.34 (m, 4H, m-Bn), 7.25 (m, 2H, p-Bn)

Characterization of the products from table 5.3

Product 1: ^1H NMR (CDCl_3): $\delta = 7.47$ (m, 2H, m), 7.38 (m, 2H, o), 7.26 (m, 1H, p), 0.22 (s, 9H, $\text{Si}(\text{CH}_3)_3$).

Product 2: ^1H NMR (CDCl_3): $\delta = 9.82$ (s, 1H, **O=C-H**), 7.96 (m, 2H, o-aldehyde), 7.61 (m, 2H, o-Si), 0.24 (s, 9H, $\text{Si}(\text{CH}_3)_3$).

Product 3: ^1H NMR (CDCl_3): $\delta = 7.42$ (m, 1H, o-Si), 7.28 (m, 1H, p-Si), 7.26 (m, 1H, o- CH_3), 7.24 (m, 1H, p- CH_3), 2.34 (s, 3H, CH_3), 0.29 (s, 9H, $\text{Si}(\text{CH}_3)_3$).

Product 4: ^1H NMR (CDCl_3): $\delta = 7.48$ (m, 4H, o), 7.23-7.20 (m, 6H).

Product 5: ^1H NMR (CDCl_3): $\delta = 10.01$ (s, 1H, **O=C-H**), 7.85 (m, 2H, o-aldehyde), 7.62 (m, 2H, m-aldehyde), 7.48 (m, 2H, o), 7.23 (m, 2H, m), 7.20 (m, 1H, p).

Product 6: ^1H NMR (CDCl_3): $\delta = 7.60$ (m, 1H, o-alkyne), 7.46 (m, 2H, o), 7.37 (m, 1H, p- CH_3), 7.32 (m, 1H, m- CH_3), 7.24 (m, 2H, m), 7.20 (m, 1H, p), 7.14 (m, 1H, o- CH_3), 2.33 (s, 3H, CH_3).

General procedure for the Suzuki-Miyaura reaction

Under an atmosphere of nitrogen, a screw cap vial was loaded with the desired catalyst, phenylboronic acid, chlorotoluene and DMF. After stirring for ten minutes, the cesium carbonate was added in one portion. The solution was heated to 80 °C until completion of the reaction. The product was then purified via column chromatography.

General procedure for the Sonogashira reaction (A)

Under an inert atmosphere, a screw cap vial was loaded with the desired catalyst, bromobenzene, ethynyltrimethyl silane, CuI, diisopropylamine and THF. The solution was stirred at room temperature until completion of the reaction. The product was purified *via* column chromatography.

General procedure for the Sonogashira reaction (B)

Under an inert atmosphere, a screw cap vial was loaded with the desired catalyst, bromobenzene, trimethyl(phenylethynyl)silane, CuI, cesium carbonate and dimethylacetate. The solution was stirred at 80 °C until completion of the reaction. The product was purified *via* column chromatography.

General procedure for the Heck reaction

Under an inert atmosphere, a screw cap vial was loaded with the desired catalyst, iodobenzene, *n*-butylacrylate, triethylamine and DMF. The solution was stirred at 120 °C until completion of the reaction. The product was purified *via* column chromatography.

General procedure for the ring-closing metathesis reaction

Under an inert atmosphere, a screw cap vial was loaded with **9**, diethyldiallyl malonate and CH_2Cl_2 . The solution was stirred at 45 °C until completion of the reaction. The product was purified *via* column chromatography.

General procedure for the leaching tests using QuadraPure[®]. Example: Suzuki-Miyaura reaction.

Under an inert atmosphere, a screw cap vial was loaded with the desired catalyst (1 mol%), phenylboronic acid (1.2 equivalent), chlorotoluene (1 equivalent), QuadraPure[®] (2 mol%) and DMF. After stirring for 10 minutes, the cesium carbonate (1.5 equivalents) was added in one portion to the reaction mixture. The solution was heated to 80 °C and samples for GC analysis were taken every 5 minutes for the first 60 minutes, then every 30 minutes for the next 120 minutes.

General procedure for the leaching tests using PVPy or mercury. Example: Suzuki-Miyaura reaction.

Under an inert atmosphere, a screw cap vial was loaded with the desired catalyst (1 mol%), phenylboronic acid (1.2 equivalent), chlorotoluene (1 equivalent), poison (500 equivalent) and DMF. After stirring for 10 minutes, the cesium carbonate (1.5 equivalents) was added in one portion to the reaction mixture. The solution was heated to 80 °C and samples for GC analysis were taken every 5 minutes for the first 60 minutes, then every 30 minutes for the next 120 minutes.

General procedure for precipitation process

The precipitation of the polymer consists on reducing the amount of solvent to a minimum and adding cold methanol. The formed precipitate is then centrifuged for 10 minutes and the remaining solution decanted.

5.6. References

- [1] M. R. Buchmeiser, *New J. Chem.* **2004**, 28, 549.
- [2] M. R. Buchmeiser, *Catal. Today* **2005**, 105, 612.
- [3] A. H. Hoveyda, D. G. Gillingham, J. J. V. Veldhuizen, O. Kataoka, S. B. Garber, J. S. Kingsbury, J. P. A. Harrity, *Org. Biomol. Chem.* **2004**, 2, 8.
- [4] S. C. Schürer, S. Gessler, N. Buschmann, S. Blechert, *Angew. Chem., Int. Ed. Engl.* **2000**, 39, 3898.
- [5] B. Karimi, D. Enders, *Org. Lett.* **2006**, 8, 1237.
- [6] D. Schönfelder, K. Fischer, M. Schmidt, O. Nuyken, R. Weberskirch, *Macromolecules* **2005**, 38, 254.
- [7] B. Çetinkaya, N. Gürbüz, T. Seçkin, I. Özdemir, *J. Mol. Catal.* **2002**, 184, 31.
- [8] M. Ahmed, A. G. M. Barrett, D. C. Braddock, S. M. Cramp, P. A. Procopiou, *Synlett* **2000**, 7, 1007.
- [9] L. Jafarpour, S. P. Nolan, *Org. Lett.* **2000**, 2, 4075.
- [10] M. Mayr, B. Mayr, M. R. Buchmeiser, *Angew. Chem., Int. Ed. Engl.* **2001**, 40, 3839.
- [11] M. Mayr, B. Mayr, M. R. Buchmeiser, *Stud. Surf. Sci. Catal.* **2002**, 143, 305.
- [12] J. Schwarz, V. P. W. Böhm, M. G. Gardiner, M. Grosche, W. A. Herrmann, W. Hieringer, G. Raudaschl-Sieber, *Chem. Eur. J.* **2000**, 6, 1773.
- [13] Q. Yao, *Angew. Chem., Int. Ed. Engl.* **2000**, 39, 3896.

- [14] Q. Yao, M. Rodriguez, *Tetrahedron Lett.* **2004**, 45, 2447.
- [15] M. T. Zarka, M. Bortenschlager, K. Wurst, O. Nuyken, R. Weberskirch, *Organometallics* **2004**, 23, 4817.
- [16] J.-H. Kim, B.-H. Jun, J.-W. Byun, Y.-S. Lee, *Tetrahedron Lett.* **2004**, 45, 5827.
- [17] J.-H. Kim, J.-W. Kim, M. Shokouhimehr, Y.-S. Lee, *J. Org. Chem.* **2005**, 70, 6714.
- [18] P. D. Stevens, G. Li, J. Fan, M. Yen, Y. Gao, *J. Chem. Soc., Chem. Commun.* **2005**, 4435.
- [19] M. Mayr, M. R. Buchmeiser, *Macromol. Rapid Commun.* **2004**, 25, 231.
- [20] J. Roncali, *Chem. Rev.* **1992**, 92, 711.
- [21] K. B. G. Torssell, *Natural product chemistry : a mechanistic and biosynthetic approach to secondary metabolism* Wiley, Chichester, **1983**.
- [22] O. Baudoin, M. Cesario, D. Guenard, F. Gueritte, *J. Org. Chem.* **2002**, 67, 1199.
- [23] D. E. Bergbreiter, P. L. Osburn, J. Frels, *Adv. Synth. Catal.* **2004**, 347, 172.
- [24] K. Yu, W. Sommer, C. W. Jones, M. Weck, *Adv. Synth. Catal.* **2004**, 347, 161.
- [25] K. Yu, W. Sommer, M. Weck, C. W. Jones, *J. Catal.* **2004**, 226, 101.
- [26] W. J. Sommer, K. Yu, J. Sears, Y. Ji, X. Zheng, R. Davis, C. D. Sherrill, C. W. Jones, M. Weck, *Organometallics* **2005**, 24, 4351.
- [27] W. M. Seganish, M. E. Mowery, S. Riggleman, P. DeShong, *Tetrahedron* **2005**, 61, 2117.
- [28] Y. M. Chang, S. H. Lee, M. Y. Cho, B. W. Yoo, H. J. Rhee, S. H. Lee, C. M. Yoon, *Synth. Commun.* **2005**, 35, 1851.
- [29] S. Punna, D. D. Díaz, M. G. Finn, *Synlett* **2004**, 13, 2351.

- [30] R. Nakajima, M. Kinosada, T. Tamura, T. Hara, *Bull. Chem. Soc. Jpn.* **1983**, *56*, 1113.
- [31] C. Davis, <http://www.reaxa.com/quadrapure.pdf>, **2005**.
- [32] M. Holbach, M. Weck, *J. Org. Chem.* **2006**, *71*, 1825.
- [33] K. C. Nicolaou, E. J. Sorensen, *Classics in total synthesis*, Wiley-VCH, Weinheim, **1996**.
- [34] P. J. Stang, F. Diederich, *Modern acetylene chemistry* VCH, Weinheim, **1995**.
- [35] U. Ziener, A. Godt, *J. Org. Chem.* **1997**, *62*, 6137.
- [36] V. Francke, T. Mangel, K. Mullen, *Macromolecules* **1998**, *31*, 2447.
- [37] A. Nagy, Z. Novák, A. Kotschy, *J. Organomet. Chem.* **2005**, *690*, 4453.
- [38] K. Sonogashira, *J. Organomet. Chem.* **2002**, *653*, 46.
- [39] K. Sonogashira, Y. Tohda, N. Hagihara, *Tetrahedron Lett.* **1975**, *16*, 4470.
- [40] E.-i. Negishi, L. Anastasia, *Chem. Rev.* **2003**, *103*, 1979.
- [41] R. R. Tykwinski, *Angew. Chem., Int. Ed.* **2003**, *42*, 1566.
- [42] C. Yang, S. P. Nolan, *Organometallics* **2002**, *21*, 1020.
- [43] T. Mizoroki, K. Mori, A. Ozaki, *Bull. Chem. Soc. Jpn.* **1971**, *44*, 581.
- [44] R. F. Heck, J. P. Nolley, *J. Org. Chem.* **1972**, *37*, 2320.
- [45] R. H. Grubbs, S. J. Miller, G. C. Fu, *Acc. Chem. Res.* **1995**, *28*, 446.
- [46] D. Fischer, S. Blechert, *Adv. Synth. Catal.* **2005**, *347*, 1329.
- [47] M. Mayr, D. Wang, R. Kröll, N. Schuler, S. Prühs, A. Fürstner, M. R. Buchmeiser, *Adv. Synth. Catal.* **2005**, *347*, 484.
- [48] M. G. Gardiner, W. A. Herrmann, C.-P. Reisinger, J. Schwarz, M. Spiegler, *J. Organomet. Chem.* **1999**, *572*, 239.

[49] J. M. Pollino, M. Weck, *Synthesis* **2002**, 9, 1277.

CHAPTER 6

GOLD NANOPARTICLES AS A SUPPORT

Abstract

A new synthetic method was introduced allowing for the functionalization of gold nanoparticles. This new method allows for the introduction of a wide variety of functions that were not available before due to the synthetic challenges of making terminated thiol compounds. This functionalization method uses “click” chemistry to add the desired functions onto the gold nanoparticles. It consist on using 5-40 mol% of CuSO₄ and 10-40 mol% of sodium ascorbate along with the terminated alkyne function and the alkyl azide coated MPC. The reactants are combined and reacted in a microwave resulting in 80-100% conversion of the azide. This facile functionalization of gold nanoparticles opens new opportunities to scientist to add functionalities that were not available before.

Using this newly developed method, the introduction of catalysts was investigated. Gold nanoparticles were functionalized with N-heterocyclic carbene palladated complex. These palladium complexes have proved to be very efficient catalyst for a wide variety of catalytic reactions, one of interest in particular, the Suzuki-Miyaura coupling. To investigate the newly synthesized system, a variety of functionalized aryl chlorides were reacted with phenylboronic acid. The functions included electron donating as well as electron withdrawing functions. The reaction was setup in a microwave reactor and yielded 85%-100% conversion of the aryl chloride. The role of the base was also investigated, with a variety of inorganic and organic bases. The results of this screening resulted in Na^tOBu as being the best base for our coupling reaction. The first gold

nanoparticles supported palladium complex for Suzuki coupling chemistry was synthesized. The conversions obtained with this new system were similar to the one obtain with the small molecule analogues.

6.1. Introduction

The investigations of polymer supported Pd-pincer complexes and Pd *N*-Heterocyclic carbene complexes lead me to examine other supports. This new support should be soluble under reaction condition but also easily recoverable. It should also be modifiable and easy to synthesize. A potential support that meets several of the described criteria was identified, gold nanoparticles. Gold nanoparticles are among the most studied metallic nanoparticles since they have the potential to play a key role in catalysis, imaging, disease diagnostics, and gene expression.^[1-7] For example, gold nanoparticles have been identified as key materials in bionanotechnology.^[1, 4, 5, 8-10] One example is the grafting of carcinoembryonic antigen antibodies onto gold nanoparticles followed by the immobilization of the functionalized particles to a gold electrode thereby enhancing the selectivity of immunoassay electrodes.^[11] A second application is in catalysis. One interesting report in this area describes the use of *N*-imidazole functionalized thiolate gold nanoparticles for the cleavage of 2,4-dinitrophenyl acetate.^[12] The underlying methodology that is crucial to these applications is the easy and high yielding functionalization of gold nanoparticles with any compound of interest. Unfortunately, such modification methodologies for gold nanoparticles are scarce and remain a challenge for scientists presenting a roadblock for further research. Herein, a

straightforward functionalization strategy to overcome these shortcomings using 1,3 dipolar cycloadditions is presented.

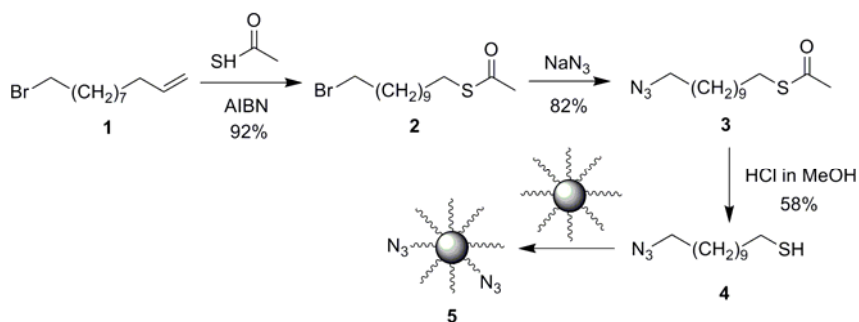
6.2. Results and discussion

This methodology is based on the synthesis of alkylthiol protected gold nanocluster using phase transfer chemistry developed by Brust *et al.*^[13] The Brust strategy allows for full control over the size and the solubility of the particles and has been employed in the synthesis of alkylthiol monolayer protected gold clusters using a library of alkanethiolates.^[2, 6, 7, 14-17] Furthermore, it was demonstrated that alkyl thiols can be exchanged on the gold cluster allowing for the introduction of functionalized thiols into the alkylthiol monolayer of gold clusters^[14] by simply stirring a solution of the desired functionalized thiols with the gold nanoparticles for extended periods.^[18-21] Unfortunately, this method lacks any control during the exchange process. The ideal functionalization strategy should allow for full control during the functionalization step without the tedious synthesis of thiolated ligands. The employment of 1,3-dipolar cycloaddition is suggested as a key synthetic step fulfills this requirement.

The 1,3-dipolar cycloaddition combines an alkyne and an azide to form a triazole ring.^[22, 23] In 2001, Sharpless introduced a copper-catalyzed version that often results in quantitative yields at very mild reaction conditions.^{[24-26], [27]} Since then, copper-catalyzed 1,3 dipolar cycloadditions have been reported as the key functionalization step for a variety of materials ranging from polymers to peptides.^[26, 28] It has also been recognized as an important tool for gold nanoparticle functionalization. In 2006, Fleming *et al.* reported the functionalization of gold nanoparticles with thiols bearing azides.^[29]

While this contribution was an important step forward, it was limited to the use of activated ethynyl compounds, required long reaction times (24 to 96 hours), and resulted in low yields. Brennan *et al.* presented a similar method using the standard ‘Sharpless conditions’ to introduce lipases onto gold nanoparticles.^[30] However, long reaction times (96 hours), a 10^6 molar excess of catalysts in comparison to the azide, and extensive purifications to remove the excess alkyne and catalyst limited the applicability of the procedure. While these contributions demonstrate the potential of 1,3-dipolar cycloadditions in nanoparticle functionalization, a general functionalization scheme that allows for fast and quantitative attachment of any compound onto gold nanoparticles in a modular fashion is still an unfulfilled goal. Such a methodology is introduced by describing a general and high yielding recipe to react a library of alkynes with alkylthiol functionalized gold nanoparticles. The yields are very high and the purification of the functionalized gold nanoparticles can be carried out via simple extraction and precipitation.

The azide functionalized gold nanoparticle (**5**) is the key reagent to the strategy. The synthesis of **5** is described in Scheme 6.1. 11-Bromo-1-undecene (**1**) was reacted with thioacetic acid followed by the reaction with sodium azide to yield 11-azidoundecyl ethanethiolate (**3**). Compound **3** was then reacted with HCl in MeOH to generate 11-azidoundecane-1-thiol (**4**) which was mixed with the alkyl thiol protected gold nanoparticle^[13] to yield **5**.



Scheme 6.1. Synthesis of the azide functionalized gold nanoparticles.

The characterization of the azide-functionalized nanoparticles was carried out using TEM, UV, FT-IR and NMR spectroscopy. TEM images showed that the gold nanoparticles are between 2 nm and 5 nm. The presence of the azide functionality on the gold nanoparticles was confirmed by IR and NMR spectroscopies. The FT-IR spectra displayed a stretch around 2100 cm^{-1} characteristic of the azide functionality, while the NMR spectrum of **5** in CDCl_3 showed a signal at 3.24 ppm characteristic of the CH_2 group adjacent to the azide. Quantification of the azide loading on the nanoparticle was not possible using NMR spectroscopy because of the broadness of all signals and the subsequent problems with the integration of overlapping signals. Therefore, the alkanethiols were cleaved off the gold nanoparticles by reacting the particles with I_2 .^[31, 32] The resulting “free” alkyl thiols were then analyzed via NMR spectroscopy giving an azide loading of 38%.

Next, the dipolar 1,3-cycloaddition of the azide functionalized nanoparticles with a library of alkynes was investigated. First, to assure the stability of the gold nanoparticles under reaction conditions, we carried out a test reaction with **5** using the

standard 1,3 dipolar cycloaddition reaction conditions: a mixture of DMSO, ^tBuOH and H₂O as solvents and a catalyst mixture of 20 mol% of CuSO₄ and 40 mol% of sodium ascorbate.^[24, 25, 28] To minimize reaction times, a microwave reactor as reaction vessel was employed. Several groups have reported on the use of microwave-assisted 1,3 dipolar cycloadditions and have demonstrated that it shortens the reaction times to 5-10 minutes while optimizing yields.^[33-35] The reaction was carried out for 10 minutes in the microwave reactor with a reaction vessel shut off temperature of 100 °C. The treated functionalized gold nanoparticles were characterized using UV, IR, and NMR spectroscopies and TEM to investigate if any decomposition took place or if any undesired side reactions did occur. The gold nanoparticles showed no changes when investigated by any of these characterization methods demonstrating the stability of gold nanoparticles to our reaction conditions. Noticeable nanoparticle decomposition was observed when the particles were treated for periods of time in excess of 15 minutes.

Next, the reaction protocol for the gold nanoparticle functionalization was optimized. To determine the best reaction conditions for the functionalization of **5** via 1,3 dipolar cycloadditions, we employed phenylacetylene as the alkyne of choice. The catalyst loading, reaction time and temperature were varied during the optimization process (Table 6.1). The solvent mixture of ^tBuOH and water, typically used for 1,3-dipolar cycloadditions, was not the ideal choice for our studies due to limited solubility of the gold nanoparticles in these solvents and a variety of solvent mixtures were evaluated. The optimization experiments are described in detail in Table 6.1. To characterize the yields of all reactions, the thiols were cleaved using I₂ and analyzed via mass spectrometry and NMR spectroscopy by the disappearance of the signal at 3.24 ppm and

the appearance of a new signal at 4.2 ppm which is characteristic to the methylene group located next to the newly formed triazole ring. The optimal conversions for phenylacetylene were determined to be: 10 mol% CuSO₄, 20 mol% sodium ascorbate, either a mixture of dioxane and ^tBuOH or THF as solvents, and 10 equivalents of phenylacetylene (Entries 10 and 13, Table 6.1). Purification of the functionalized gold nanoparticles was straightforward. Addition of methylene chloride to the reaction mixture induced a phase separation between the organic layer and the water layer. The organic layer was separated, the solvent evaporated and the gold nanoparticles residue precipitated several times into methanol to insure full removal of excess alkyne.

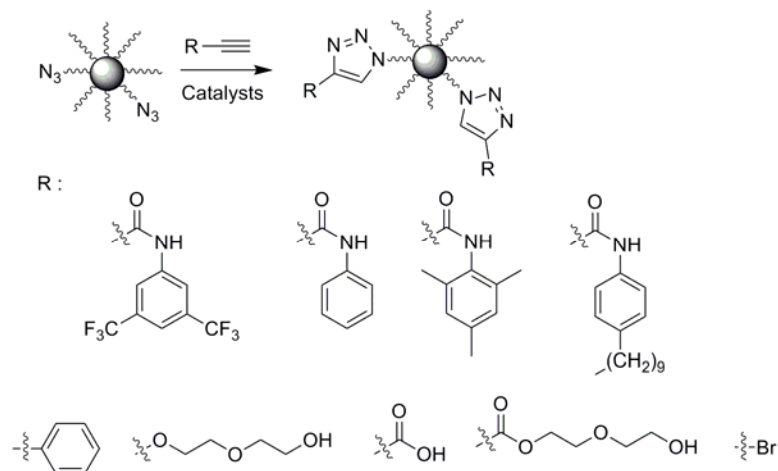
Table 6.1. Optimization of 1,3 dipolar cycloaddition conditions for gold nanoparticle functionalization.

Entry	CuSO ₄ Loading (mol%)	NaAsc Loading (mol%)	Power Setting (W)	Reaction Time (min)	Shut- off Temp. (°C)	Solvent Mixture	Yield (%)
1	1	2	100	3	50	DMSO/ ^t BuO H/H ₂ O:1/1/0. 5	0
2	5	10	100	3	50	DMSO/ ^t BuO H/H ₂ O:1/1/0. 5	45
3	10	20	100	3	50	DMSO/ ^t BuO H/H ₂ O:1/1/0. 5	74
4	5	10	100	5	50	DMSO/ ^t BuO H/H ₂ O:1/1/0. 5	77

Table 6.1. continued

5	5	10	150	3	50	DMSO/ ^t BuO H/H ₂ O:1/1/0. 5	75
6	5	10	150	5	50	DMSO/ ^t BuO H/H ₂ O:1/1/0. 5	75
7	-	-	100	3	100	DMSO/ ^t BuO H/H ₂ O:1/1/0. 5	0
8	5	10	100	3	100	DMSO/ ^t BuO H/H ₂ O:1/1/0. 5	82
9	10	20	100	3	100	DMSO/ ^t BuO H/H ₂ O:1/1/0. 5	88
10	10	20	100	10	100	DMSO/ ^t BuO H/H ₂ O:1/1/0. 5	100
11	1	2	100	10	100	THF	55
12	5	10	100	10	100	THF	82
13	10	20	100	10	100	THF	100
14	5	10	100	20	100	THF	78
15	5	10	100	20	100	THF	71

After the determination of the optimal reaction conditions for the functionalization of gold nanoparticles, we investigated the versatility of the transformation using a library of alkynes. The alkynes that were employed for this study are shown in Scheme 2 and include both activated and non-activated alkynes as well as aromatic and aliphatic ones.



Scheme 6.2. Library of alkynes used as substrates in the 1,3 dipolar cycloadditions and the functionalized nanoparticles before and after the transformation.

The results from the different nanoparticle functionalizations are described in Table 2. In general, with yields ranging from 78% to 100%, activated alkynes are more reactive, requiring less catalyst loading and time than their non-activated analogues. While different catalyst loadings were needed for different alkynes, we were still able to determine a general recipe for each “family” of functionalities. For aromatic non-activated alkynes, 10 mol% of CuSO_4 and 20 mol% of sodium ascorbate are required. In contrast, for alkyl-based non-activated alkynes, only 5 mol% of CuSO_4 and 10 mol% of sodium ascorbate are required for near quantitative conversions. However, when heteroatoms such as oxygen are adjacent to the alkyne, higher catalyst loadings are needed while only moderate to good yields were observed. In comparison, activated

alkynes, such as propiolamide, require only 5 mol% CuSO₄ and 10 mol% of sodium ascorbate to yield quantitative conversions.

Table 6.2. Yields of 1,3 dipolar cycloadditions on gold nanoparticles using the library of alkynes.

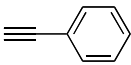
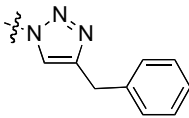
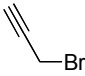
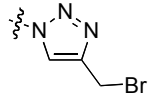
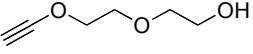
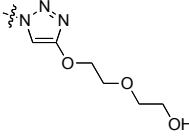
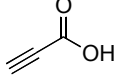
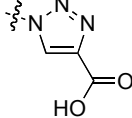
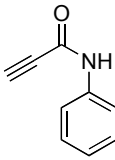
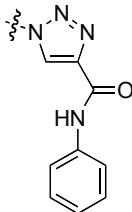
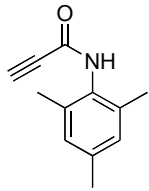
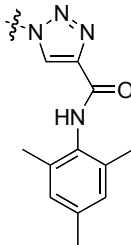
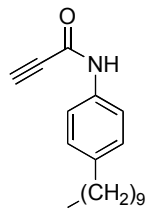
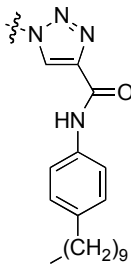
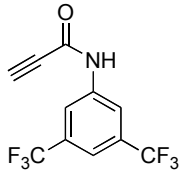
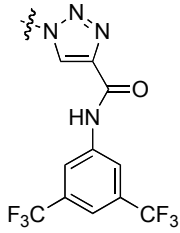
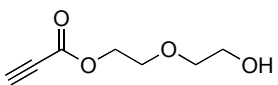
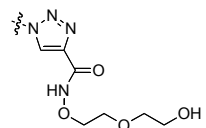
Entry	Substrate	Product	CuSO ₄ Loading (mol%)	Yield (%)
1			10	100
2			5	98
3			15	78
4			5	89
5			5	94

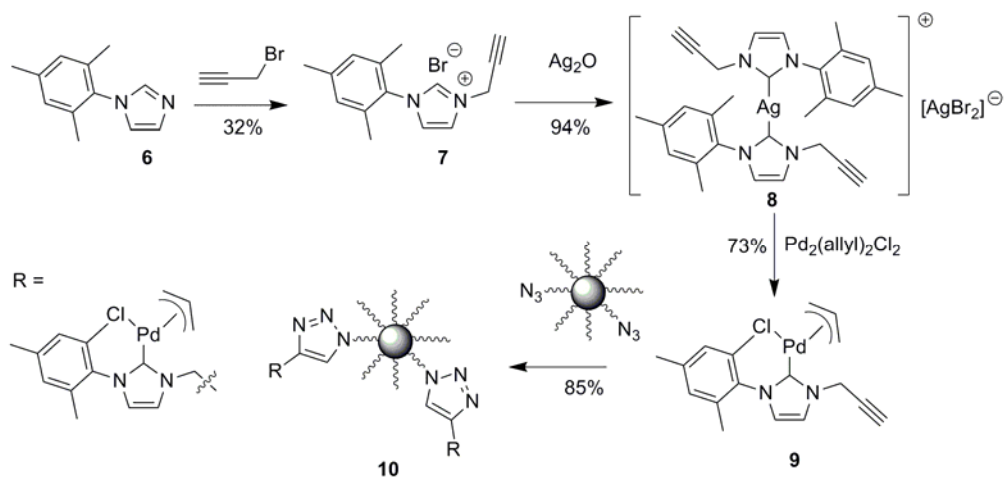
Table 6.2. continued

6			5	85
7			5	92
8			5	97
9			10	81

Using this newly developed synthetic protocol, the possibility of using gold nanoparticles as support for homogeneous catalysis by adding an organometallic complex onto the gold nanoparticles as a proof of principle for the applicability of our methodology was investigated. The catalytic activities of several polymer-supported catalysts containing Pd-*N*-heterocyclic carbene complexes were previously

investigated.^[36] The intrinsic characteristic of gold nanoparticles, such as tunable (i) solubility in common organic and aqueous solvents and (ii) size of the particle, makes this system interesting as potential support in catalysis. *N*-heterocyclic carbene (NHC) palladium complexes were grafted onto the gold nanoparticles and the catalytic activity of the resulting supported complexes was investigated. Palladium NHC complexes are well-known catalysts for C-C coupling reactions, an important class of catalytic reactions with application in polymer science as well as fine chemical and pharmaceutical industries.^[37, 38]

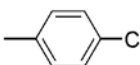
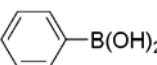
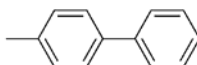
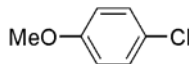
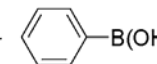
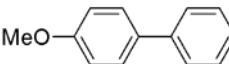
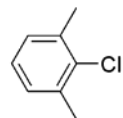
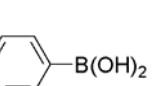
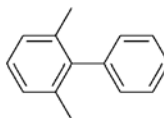
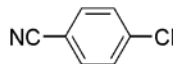
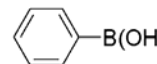
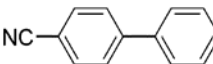
First, an alkyne containing a *N*-heterocyclic ligand was synthesized. *N*-mesityl imidazole was refluxed with propargyl bromide in toluene for 16 hours to yield the desired alkyne containing NHC ligand (**7**). 1-Mesityl-3-(prop-2-ynyl)-1H-imidazol-3-ium bromide was then reacted with silver oxide to form the silver complex **8** in close analogy to literature procedures^[39] which was then treated with palladium allyl chloride to form **9**. Finally, using the newly developed methodology, **9** was “clicked” onto the gold nanoparticles with a yield of 85 % using sodium ascorbate and CuSO₄ as catalysts.



Scheme 6.3. Synthesis of the palladium complex supported gold nanoparticles

The newly supported Palladium complex **10** was then tested in the Suzuki coupling of a series of aryl chloride with phenyl boronic acid (Table 6.3).

Table 6.3. Results of Suzuki-Miyaura reaction using **10**.

Entry	Substrates	Product	Yield
1	 + 		99%
2	 + 		99%
3	 + 		85%
4	 + 		88%

Due to the sensitivity of gold nanoparticles to heat the catalytic reactions were carried out in a microwave reactor.^[40] The power was set to 100W for 6 minutes. The catalyst loading for all catalytic transformations was 0.5 mol% (based on palladium), the base Na^tOBu and the solvent dioxane. Yields of 85-99% were observed for all four test reaction. These values are very similar to the ones reported in the literature for the homogeneous palladium *N*-heterocyclic carbene analogue.^[41] These results demonstrate that our newly developed methodology can be employed as key step in the synthesis of supported catalysts and that the resulting catalysts retain their activity when compared to their small molecule analogues.

6.3. Conclusion

In summary, a synthetic protocol for the facile addition of different functionalities onto the gold nanoparticles in high yields within minutes was developed. The versatility of the method was demonstrated with conversions of 80% or higher for the library of alkynes studied. This methodology has a variety of advantages over current gold nanoparticles functionalization methods including (i) more synthetic flexibility for the synthesis of desired functionalities on gold nanoparticles (ii) reduced reaction times, and (iii) easy purification methods. To demonstrate the versatility of the newly developed methodology as well as its applicability, we attached palladium NHC complexes to the gold nanoclusters and investigated their potential as catalysts for Suzuki couplings. The yields obtained for the Suzuki couplings were comparable to the ones obtained with the small molecule analogues. This example demonstrates the potential of this newly developed methodology.

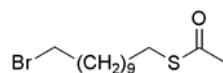
6.4. Experimental Section

All reactions with air- and moisture sensitive compounds were carried out under a dry nitrogen/argon atmosphere using an MBraun UniLab 2000 dry box and/or standard Schlenk line techniques. CH_2Cl_2 and toluene were distilled from sodium and benzophenone. $\text{Pd}(\text{allyl})_2\text{chloride}$ and all bases were obtained from commercial sources and used without further purification. The syntheses of mesityl imidazole and monolayer protected clusters with octanethiols were carried out following published procedures.^{[13,}

^{42]} Gas-chromatographic analyses were performed on a Hewlett Packard G1800A GCD

system GC-MS. ^1H (300 MHz) and ^{13}C NMR (75 MHz) spectra were recorded on a Varian Mercury VX instrument. All spectra were referenced to residual proton solvent. Mass spectral analyses were provided by the Georgia Tech MassSpectrometry Facility using a VG-70se spectrometer. Elemental analyses were carried out by either Atlantic Microlabs, Norcross GA (CHN analyses) or Galbraith Laboratories, Inc., TN (determination of the metal content).

Synthesis of S-10-bromodecyl ethanethioate (2)

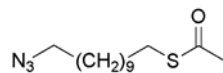


In a round bottom flask, 11-bromo-1-undecene (2.12 mL, 8.5 mmol), thioacetic acid (3 mL, 42.8 mmol), AIBN (700 mg) and toluene (100 mL) were combined. A flow of argon was bubbled through the reaction for 20 minutes before refluxing the reaction for 4 hours. The reaction was then allowed to cool before the removal of the solvent under vacuum. The resulting orange slurry was dissolved in CH_2Cl_2 (100 mL) and washed with NaHCO_3 (50 mL) and NaCl (50 mL). The organic layer was dried over MgSO_4 and the solvent removed under vacuum to yield a yellow solid. The product was further purified via column chromatography (1:2, CH_2Cl_2 :Hexanes) to yield a colorless oil. Yield: 9.36 g (95%). ^1H NMR (CDCl_3 , 300 MHz): δ = 3.38 (t, 2H, J = 6.9 Hz, $\text{CH}_2\text{-Br}$), 2.84 (t, 2H, J = 7.2 Hz, $\text{CH}_2\text{-S}$), 2.30 (s, 3H, CO-CH_3), 1.83 (q of t, 2H, J = 7.8 Hz, $\text{Br-CH}_2\text{-CH}_2$), 1.55 (m, 2H, $\text{S-CH}_2\text{-CH}_2$), 1.25 (m, 14H). ^{13}C (CDCl_3 , 300 MHz): δ = 195.9, 33.8, 32.8, 30.4, 29.6, 29.3, 28.7, 28.5, 28.3, 28.2, 27.3. HRMS(ESI): m/z calcd for

C₁₃H₂₅BrOS 308.0809 found 308.0823. Anal. Calcd for C₁₃H₂₅BrOS: C, 50.48; H, 8.15.

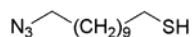
Found C, 51.20; H, 8.01.

Synthesis of S-10-azidodecyl ethanethioate (**3**)



In a round bottom flask, **2** (100 mg, 0.3 mmol), sodium azide (179 mg, 2.7 mmol) and DMF (5 mL) were combined. The mixture was heated to 60 °C for 10 hours. The DMF was removed under vacuum and the resulting crude mixture was dissolved in CH₂Cl₂ and washed with water (3 × 50 mL) and brine (50 mL). The organic layer was dried over MgSO₄ and the solvent removed under vacuum to yield an off-white oil. Yield: 52 mg (73 %). ¹H NMR (CDCl₃, 300 MHz): δ = 3.24 (t, 2H, *J* = 8.8 Hz, CH₂-N₃), 2.82 (t, 2H, *J* = 7.2 Hz, CH₂-S), 3.29 (s, 3H, CO-CH₃), 1.54 (m, 2H, CH₂-CH₂-S), 1.24 (m, 16H). ¹³C (CDCl₃, 300 MHz): δ = 196.0, 51.5, 30.6, 29.4, 29.3, 29.1, 29.0, 28.8, 28.7. HRMS(ESI): *m/z* calcd for C₁₃H₂₅N₃OS 271.1718 found 271.1711.

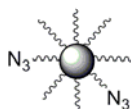
Synthesis of 10-azidodecane-1-thiol (**4**)



To an ice-cold solution of dry MeOH (50 mL) acetyl chloride was added dropwise. The solution was stirred for 5 minutes before the addition of **3** (500 mg, 1.8

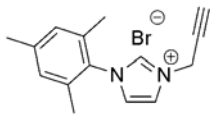
mmol). The solution was stirred for 3 hours under Ar. The reaction was then poured into degassed water and the organic layer extracted with hexanes (2×20 mL). The combined organic layers were washed with water (2×50 mL), dried over MgSO_4 and the solvent removed under vacuum to yield a colorless oil. Yield 370 mg (90 %). ^1H NMR (CDCl_3 , 300 MHz): δ = 3.23 (t, 2H, J = 6.8 Hz, $\text{CH}_2\text{-N}_3$), 2.51 (q, 2H, J = 7.3 Hz, $\text{CH}_2\text{-S}$), 1.54 (m, 6H), 1.25 (m, 16H). ^{13}C (CDCl_3 , 300 MHz): δ = 51.5, 34, 29.6, 29.5, 29.2, 28.6, 28.2, 27.8, 27.1. HRMS(ESI): m/z calcd for $\text{C}_{11}\text{H}_{23}\text{N}_3\text{S}$ 229.1613 found 229.1645.

Synthesis of azide functionalized gold nanoparticles (5)



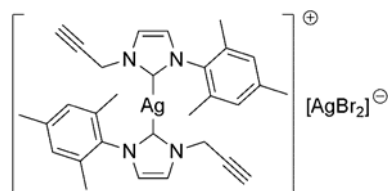
Compound **4** (150 mg) was added to a stirred solution of MPC containing an octanethiol monolayer (150 mg) in CH_2Cl_2 (5 mL). The solution was stirred for 48 hours. The solvent was then reduced to 2 mL before the addition of MeOH (50 mL). The solution was put in the freezer for 2 hours before being centrifuged. The solvent was discarded and the solid dissolved in 3–4 mL of CH_2Cl_2 before the addition of MeOH (50 mL). The process was repeated two more times to yield a black solid. ^1H NMR (CDCl_3 , 300 MHz): δ = 3.26 (br m, 2H, $\text{CH}_2\text{-N}_3$), 1.26 – 1.6 (br m, 18H), 0.9 (br m, 2H). FTIR: 3000, 2100, 1500.

Synthesis of 1-mesityl-3-(prop-2-ynyl)-1H-imidazol-3-ium bromide (7)



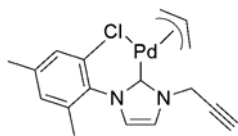
In a round bottom flask, **6** (200 mg, 1 mmol), propargyl bromide (192 mg, 1.6 mmol) and toluene (100 mL) were combined and refluxed for 16 hours. The solvent was removed under vacuum to yield a yellow solid. The product was further purified using column chromatography (1:5 hexanes:CH₂Cl₂) to yield a white solid. Yield 95 mg (32 %). ¹H NMR (CDCl₃, 300 MHz): δ = 10.50 (s, 1H, N-CH=N), 7.79 (s, 1H, Mes-N-CH=C), 7.15 (s, 1H, CH₂-N-CH=C), 7.00 (s, 2H, ArH), 5.78 (s, 2H, N-CH₂-C), 2.69 (s, 1H, C≡CH), 2.34 (s, 3H, CH-CH₃), 2.08 (s, 6H, CH-CH₃). ¹³C (CDCl₃, 300 MHz): δ = 140.8, 139.0, 138.7, 135.1, 130.1, 127.1, 121.2, 84.9, 77.4, 46.2, 20.1, 15.3. Anal. Calcd for C₁₅H₁₇BrN₂: C, 59.03; H, 5.61. Found: C, 58.89; H, 5.57.

Synthesis of bis(1-mesityl-3-(prop-2-ynyl)-1H-imidazol-2(3H)-ylidene)silver (8)



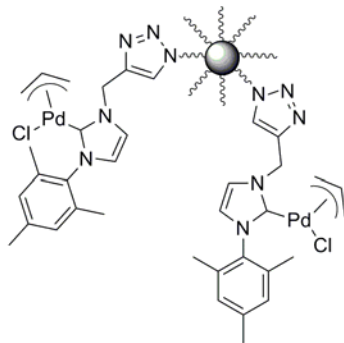
In a round bottom flask, **7** (175 mg, 0.6 mmol) and silver oxide (66 mg, 0.3 mmol) were dissolved in a 3:1 mixture of CH_2Cl_2 (6 mL) and DMF (2 mL). The solution was stirred for 10 hours before filtering it through celite. The solvent was removed under vacuum to yield an off-white solid. The product was further purified by dissolving it in CHCl_3 (2 mL) and precipitating it in an excess hexanes (20 mL). This operation was repeated twice. Yield: 157 mg (94 %). ^1H NMR (CDCl_3 , 300 MHz): δ = 7.41 (s, 1H, N-CH=C), 7.00 (m, 3H, ArH + N-CH=C), 5.12 (s, 2H, N-CH₂-C), 2.63 (s, 1H, C \equiv CH), 2.34 (s, 3H, CH-CH₃), 1.98 (s, 6H, CH-CH₃). ^{13}C (CDCl_3 , 300 MHz): δ = 142.2, 141.2, 134.9, 132.2, 130.0, 129.9, 119.3, 118.0, 113.5, 111.8, 86.1, 80.4, 79.6, 75.7, 74.6, 51.0, 44.5, 20.8, 18.8. Anal. Calcd for $\text{C}_{30}\text{H}_{32}\text{Ag}_2\text{Br}_2\text{N}_4$: C, 43.72; H, 3.91. Found: C, 43.51; H, 3.74.

Synthesis of (1-mesityl-3-(prop-2-ynyl)-1H-imidazol-2(3H)-ylidene)(prop-1-en-2-yl)palladium(II) chloride (9)



In a round bottom flask, **8** (120 mg, 0.1 mmol), palladium allyl chloride (53 mg, 0.1 mmol) and THF (5 mL) were combined. The solution was stirred for 8 hours, filtered through celite and the solvent removed under vacuum to yield an orange solid. The product was further purified by passing it through a short plug of silica yielding a yellow solid. Yield: 41.7 mg (73 %). ^1H NMR (CDCl_3 , 300 MHz): δ = 7.58 (s, 2H, N-CH=C), 6.85 (br m, 3H, ArH + N-CH=C), 5.22 (s, 2H, N-CH₂-C), 5.15 (m, 2H, CH-CH₂), 4.98 (m, 1H, CH₃-CH), 2.54 (s, 1H, C \equiv CH), 2.39 (s, 3H, CH-CH₃), 2.21 (s, 3H, CH-CH₃), 2.12 (s, 6H, CH-CH₃). ^{13}C (CDCl_3 , 300 MHz): δ = 139.8, 138.3, 134.1, 131.1, 126.7, 124.7, 117.1, 80.3, 75.8, 74.6, 43.5, 21.1, 18.6, 13.4. Anal. Calcd for $\text{C}_{18}\text{H}_{22}\text{ClN}_2\text{Pd}$: C, 52.96; H, 5.43. Found: C, 53.12; H, 5.51.

Synthesis of Pd(II) functionalized gold nanoparticles (10)



In a high-pressure tube, **5** (35 mg), **9** (10 mg), CuSO₄ (10 mol%), sodium ascorbate (20 mol%) and THF (3 mL) were combined. The mixture was placed in a microwave reactor. The reactor was set to the power level 80W and reaction time 10 minutes. The product was then extracted by adding distilled water (5 mL). The organic layer separated and the solvent was removed under vacuum. The product was dissolved in 2 mL of CH₂Cl₂ before adding an excess of methanol (50 mL). The solution was stored in the freezer for 2 hours before centrifugation. The liquid layer was discarded. The operation was repeated twice to yield a black solid. Yield (85% of Pd complex “clicked” (via NMR of decomposed gold nanoparticles)). ¹H NMR (CDCl₃, 300 MHz): δ = 7.47 (s, 1H), 7.05 (m, 3H), 5.23 (m, 1H), 5.01 (s, 2H), 2.64 (s, 1H), 2.36 (s, 3H), 1.92 (s, 6H), 1.26 – 1.6 (br m, 18H), 0.9 (br m, 2H).

General procedure for the Suzuki-Miyaura reaction

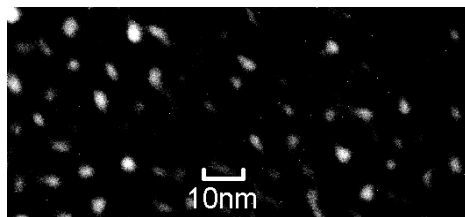
Under an atmosphere of nitrogen, a microwave high pressure tube was loaded with the Pd-NHC modified gold nanoparticles (0.5 mol% of Pd-NHC catalyst), phenylboronic acid (1.2 equivalent), the aryl chloride (1 equivalent), sodium *t*-butoxide (3 equivalents) and dioxane (2mL). The microwave was setup to 100W for 6 minutes. At the end of the reaction, water (3 mL) and CH₂Cl₂ (3 mL) were added. The organic layer was collected and the product purified via column chromatography.

Particle decomposition

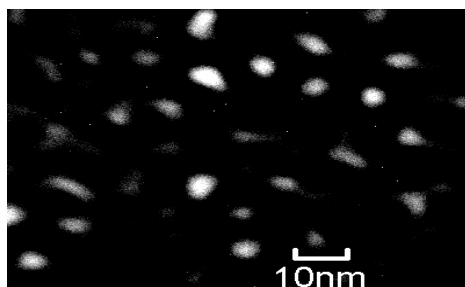
The gold nanoparticles were decomposed using the following recipe: Addition of 5 mg of I₂ to a stirred methylene chloride solution of 40 mg of particles. The solution was stirred for two hours. The solution was centrifuged and the precipitate removed. The remaining solution was dried over MgSO₄ and the solvent removed under vacuum to yield the desired disulfide.

TEM preparation

The TEM samples were prepared by drop casting a nanoparticles solution (5 mg in 2 mL of CH₂Cl₂) onto copper TEM grids coated with a layer of amorphous carbon. The images were taken on a Hitachi HF-2000 microscope.



TEM picture taken before the reaction



TEM picture taken after the reaction: CuSO₄, sodium ascorbate, in dioxane.

Characterization of the products from table 2

Characterization of product 1:

¹H NMR (CDCl₃, 300 MHz): δ = 8.37-8.34 (br s, 1H, N-CH=C), 7.58-7.53 (br m, 2H, Ar), 7.45-7.42 (br m, 2H, Ar), 4.29 (m, 2H, CH₂-CH₂-N), 2.46-2.39 (br m, CH₂-CH₂-S), 1.43-1.18 (br m).

Characterization of product 2:

¹H NMR (CDCl₃, 300 MHz): δ = 7.63-7.59 (s, 1H, N-CH=C), 4.68 (s, 2H, C-CH₂-Br), 4.36 (m, 2H, CH₂-CH₂-N), 2.43 (br m, CH₂-CH₂-S), 1.53-1.14 (br m).

Characterization of product 3:

^1H NMR (CDCl_3 , 300 MHz): δ = 6.98 (s, 1H, N-CH=C), 4.35 (m, 2H, $\text{CH}_2\text{-CH}_2\text{-N}$), 4.04 (t, 2H, J = 8Hz, C-O-CH $_2$ -C), 3.96 (t, 2H, J = 8Hz, $\text{CH}_2\text{-CH}_2\text{-OH}$), 3.76-3.74 (m, 2H, O-CH $_2$ -C), 3.65-3.62 (m, 2H, $\text{CH}_2\text{-CH}_2\text{-O}$), 2.47-2.42 (m, 2H, $\text{CH}_2\text{-CH}_2\text{-S}$), 1.57-1.14 (br m).

Characterization of product 4:

^1H NMR (CDCl_3 , 300 MHz): δ = 8.42 (s, 1H, N-CH=C), 4.44 (t, 2H, J = 12 Hz, $\text{CH}_2\text{-CH}_2\text{-N}$), 2.46-2.40 (m, 2H, $\text{CH}_2\text{-CH}_2\text{-S}$), 1.58-1.21 (br m).

Characterization of product 5:

^1H NMR (CDCl_3 , 300 MHz): δ = 10.42 (s, 1H, N-CH=C), 7.95-7.92 (m, 2H, Ar), 7.39-7.37 (m, 2H, Ar), 4.80 (m, 2H, $\text{CH}_2\text{-CH}_2\text{-N}$), 2.47-2.42 (q, 2H, J = 8 Hz, $\text{CH}_2\text{-CH}_2\text{-S}$), 1.57-1.20 (br m, 2H).

Characterization of product 6:

^1H NMR (CDCl_3 , 300 MHz): δ = 10.31 (s, 1H, N-CH=C), 6.81-6.78 (m, 2H, Ar), 4.83 (m, 2H, $\text{CH}_2\text{-CH}_2\text{-N}$), 2.49 (s, 6H, Ar-CH $_3$), 2.48-2.44 (m, 2H, $\text{CH}_2\text{-CH}_2\text{-S}$), 2.25 (s, 3H, Ar-CH $_3$), 1.57-1.22 (br m).

Characterization of product 7:

^1H NMR (CDCl_3 , 300 MHz): δ = 10.42 (s, 1H, N-CH=C), 7.73 (m, 2H, Ar), 7.13 (m, 2H, Ar), 4.82 (t, 2H, J = 8 Hz, $\text{CH}_2\text{-CH}_2\text{-N}$), 2.47-2.43 (m, 2H, $\text{CH}_2\text{-CH}_2\text{-S}$), 1.75-1.69 (m, 2H, Ar-CH $_2\text{-CH}_2\text{-C}$), 1.64-0.92 (br m).

Characterization of product 8:

^1H NMR (CDCl_3 , 300 MHz): δ = 10.21 (s, 1H, N-CH=C), 8.92 (m, 2H, Ar), 4.78 (t, 2H, J = 8 Hz, $\text{CH}_2\text{-CH}_2\text{-N}$), 2.47-2.44 (m, 2H, $\text{CH}_2\text{-CH}_2\text{-S}$), 1.57-1.20 (br m).

Characterization of product 9:

^1H NMR (CDCl_3 , 300 MHz): δ = 8.72 (s, 1H, N-CH=C), 4.45 (t, 2H, J = 10 Hz, $\text{CH}_2\text{-CH}_2\text{-N}$), 4.33 (t, 2H, J = 4 Hz, O=C-O-CH $_2$ -C), 3.70 (m, 4H), 2.46-2.41 (m, 2H, $\text{CH}_2\text{-CH}_2\text{-S}$), 1.61-1.24 (br m).

Characterization of the products from table 2 after the decomposition of the MPC

The gold nanoparticle was decomposed using the particle decomposition procedure described herein.

Characterization of product 1:

^1H NMR (CDCl_3 , 300 MHz): δ = 8.35 (s, 1H, N-CH=C), 7.56 (m, 2H, Ar), 7.51 (m, 1H, Ar), 7.45 (m, 2H, Ar), 4.29 (m, 2H, $\text{CH}_2\text{-CH}_2\text{-N}$), 2.42 (m, 2H, $\text{CH}_2\text{-CH}_2\text{-S}$), 1.90 (m, 2H, $\text{CH}_2\text{-CH}_2\text{-CH}_2\text{-N}$), 1.51 (m, 2H, $\text{CH}_2\text{-CH}_2\text{-CH}_2\text{-S}$), 1.49 (m, 2H), 1.42 (m, 2H), 1.35-1.20 (m, 10H). ^{13}C (CDCl_3 , 75 MHz): δ = 146.2, 128.5, 128.3, 128.0, 126.0, 120.8, 50.1, 34.0, 33.9, 29.6, 29.5, 28.9, 28.8, 28.6, 28.2, 22.2.

Characterization of product 2:

^1H NMR (CDCl_3 , 300 MHz): δ = 7.61 (s, 1H, N-CH=C), 4.65 (s, 2H, C-CH $_2$ -Br), 4.36 (m, 2H, $\text{CH}_2\text{-CH}_2\text{-N}$), 2.46 (m, 2H, $\text{CH}_2\text{-CH}_2\text{-S}$), 1.92 (m, 2H, $\text{CH}_2\text{-CH}_2\text{-CH}_2\text{-N}$), 1.53 (m, 2H, $\text{CH}_2\text{-CH}_2\text{-CH}_2\text{-S}$), 1.49 (m, 2H), 1.41-1.20 (m, 12H). ^{13}C (CDCl_3 , 75 MHz): δ = 143.6, 124.4, 48.1, 34.0, 33.9, 29.6, 29.5, 28.8, 28.7, 28.1, 22.4, 21.2.

Characterization of product 3:

^1H NMR (CDCl_3 , 300 MHz): δ = 6.98 (s, 1H, N-CH=C), 4.35 (m, 2H, $\text{CH}_2\text{-CH}_2\text{-N}$), 4.05 (t, 2H, J = 8Hz, C-O-CH $_2$ -C), 3.96 (t, 2H, J = 8Hz, $\text{CH}_2\text{-CH}_2\text{-OH}$), 3.76-3.74 (m, 2H, O-CH $_2$ -C), 3.65-3.62 (m, 2H, $\text{CH}_2\text{-CH}_2\text{-O}$), 2.47-2.42 (m, 2H, $\text{CH}_2\text{-CH}_2\text{-S}$), 1.94-1.92 (m,

2H, CH₂-CH₂-CH₂-N), 1.57-1.53 (m, 2H, CH₂-CH₂-CH₂-S), 1.47 (m, 2H), 1.41-1.20 (m, 12H). ¹³C (CDCl₃, 75 MHz): δ = 152.8, 116.2, 73.4, 72.8, 64.7, 61.3, 61.2, 50.1, 34.1, 34.0, 29.6, 29.5, 28.9, 28.2, 26.7, 23.9.

Characterization of product 4:

¹H NMR (CDCl₃, 300 MHz): δ = 8.42 (s, 1H, N-CH=C), 4.44 (t, 2H, *J* = 12 Hz, CH₂-CH₂-N), 2.46-2.40 (m, 2H, CH₂-CH₂-S), 1.91-1.88 (m, 2H, CH₂-CH₂-CH₂-N), 1.56-1.53 (m, 2H, CH₂-CH₂-CH₂-S), 1.49 (m, 2H), 1.40-1.17 (m, 12H). ¹³C (CDCl₃, 75 MHz): δ = 164.1, 139.4, 131.7, 51.3, 34.0, 33.9, 29.6, 29.6, 29.5, 28.9, 28.6, 28.2, 22.2.

Characterization of product 5:

¹H NMR (CDCl₃, 300 MHz): δ = 11.42 (br s, 1H, C-NH-Ar) 10.42 (s, 1H, N-CH=C), 7.95-7.92 (m, 2H, Ar), 7.39-7.37 (m, 2H, Ar), 7.16 (m, 1H, Ar), 4.80 (m, 2H, CH₂-CH₂-N), 2.47-2.42 (q, 2H, *J* = 8 Hz, CH₂-CH₂-S), 1.95-1.89 (m, 2H, CH₂-CH₂-CH₂-N), 1.57-1.53 (m, 2H, CH₂-CH₂-CH₂-S), 1.48 (m, 2H), 1.38-1.20 (m, 12H). ¹³C (CDCl₃, 75 MHz): δ = 160.3, 139.4, 139.3, 129.6, 123.8, 122.4, 120.4, 48.2, 34.0, 33.9, 29.6, 29.5, 28.9, 28.7, 28.1, 22.5.

Characterization of product 6:

¹H NMR (CDCl₃, 300 MHz): δ = 11.12 (br s, 1H, C-NH-Ar), 10.31 (s, 1H, N-CH=C), 6.81-6.78 (m, 2H, Ar), 4.83 (m, 2H, CH₂-CH₂-N), 2.49 (s, 6H, Ar-CH₃), 2.48-2.44 (m, 2H, CH₂-CH₂-S), 2.25 (s, 3H, Ar-CH₃), 1.93-1.89 (m, 2H, CH₂-CH₂-CH₂-N), 1.57-1.54 (m, 2H, CH₂-CH₂-CH₂-S), 1.46 (m, 2H), 1.38-1.20 (m, 12H). ¹³C (CDCl₃, 75 MHz): δ = 163.5, 145.1, 140.0, 139.2, 137.3, 128.9, 124.1, 48.0, 33.9, 29.6, 29.5, 28.9, 28.7, 28.2, 22.2, 21.1, 19.5.

Characterization of product 7:

^1H NMR (CDCl_3 , 300 MHz): δ = 10.83 (br s, 1H, C-NH-Ar), 10.42 (s, 1H, N-CH=C), 7.73 (m, 2H, Ar), 7.13 (m, 2H, Ar), 4.82 (t, 2H, J = 8 Hz, $\text{CH}_2\text{-CH}_2\text{-N}$), 2.63 (m, 2H, Ar- $\text{CH}_2\text{-C}$), 2.47-2.43 (m, 2H, $\text{CH}_2\text{-CH}_2\text{-S}$), 1.94-1.90 (m, 2H, $\text{CH}_2\text{-CH}_2\text{-CH}_2\text{-N}$), 1.75-1.69 (m, 2H, Ar- $\text{CH}_2\text{-CH}_2\text{-C}$), 1.64-1.45 (m, 10H), 1.39-1.15 (m, 20H), 0.91 (m, 3H, $\text{CH}_2\text{-CH}_3$). ^{13}C (CDCl_3 , 75 MHz): δ = 162.1, 140.1, 139.0, 138.6, 131.1, 122.4, 119.9, 48.3, 35.4, 34.0, 33.9, 32.1, 31.3, 29.9, 29.8, 29.6, 29.5, 29.4, 29.3, 29.1, 29.0, 28.7, 28.2, 22.9, 22.2, 14.2.

Characterization of product 8:

^1H NMR (CDCl_3 , 300 MHz): δ = 10.71 (br s, 1H, C-NH-Ar), 10.21 (s, 1H, N-CH=C), 8.92 (m, 2H, Ar), 7.42 (m, 1H, Ar), 4.78 (t, 2H, J = 8 Hz, $\text{CH}_2\text{-CH}_2\text{-N}$), 2.47-2.44 (m, 2H, $\text{CH}_2\text{-CH}_2\text{-S}$), 1.93-1.89 (m, 2H, $\text{CH}_2\text{-CH}_2\text{-CH}_2\text{-N}$), 1.57-1.53 (m, 2H, $\text{CH}_2\text{-CH}_2\text{-CH}_2\text{-S}$), 1.44 (m, 2H), 1.38-1.20 (m, 12H). ^{13}C (CDCl_3 , 75 MHz): δ = 159.9, 141.3, 139.8, 134.1, 133.8, 133.3, 132.7, 132.6, 132.5, 131.7, 131.3, 126.6, 121.9, 121.4, 121.3, 120.0, 119.3, 112.6, 48.1, 34.0, 33.9, 30.0, 29.6, 29.5, 28.9, 28.6, 28.2, 22.6.

Characterization of product 9:

^1H NMR (CDCl_3 , 300 MHz): δ = 8.72 (s, 1H, N-CH=C), 4.45 (t, 2H, J = 10 Hz, $\text{CH}_2\text{-CH}_2\text{-N}$), 4.33 (t, 2H, J = 4 Hz, $\text{O=C-O-CH}_2\text{-C}$), 3.74 (m, 2H), 3.70 (m, 4H), 2.46-2.41 (m, 2H, $\text{CH}_2\text{-CH}_2\text{-S}$), 1.93-1.87 (m, 2H, $\text{CH}_2\text{-CH}_2\text{-CH}_2\text{-N}$), 1.61-1.52 (m, 2H, $\text{CH}_2\text{-CH}_2\text{-CH}_2\text{-S}$), 1.46 (m, 2H), 1.42-1.20 (m, 12H). ^{13}C (CDCl_3 , 75 MHz): δ = 159.9, 139.0, 130.3, 72.8, 69.2, 64.3, 61.3, 49.5, 34.0, 33.9, 29.7, 29.6, 29.5, 28.8, 28.7, 28.3, 21.9.

Characterization of the products from table 2

Characterization of product 1:

^1H NMR (CDCl_3 , 300 MHz): δ = 7.78 (m, 2H, $\text{CH-C(CH}_3\text{)-CH}$), 7.68 (m, 2H, CH-C(C)-CH), 7.53-7.52 (m, 2H, CH-C(C)-CH), 7.47-7.43 (m, 2H, CH-CH-CH), 7.34 (m, 1H, CH-CH-CH), 2.34 (s, 3H, C-CH_3). ^{13}C (CDCl_3 , 75 MHz): δ = 141.4, 138.5, 136.6, 129.5, 128.7, 127.1, 21.0.

Characterization of product 2:

^1H NMR (CDCl_3 , 300 MHz): δ = 7.59-7.54 (m, 4H), 7.41-7.37 (m, 2H), 7.31 (m, 1H), 7.01-6.99 (m, 2H), 3.85 (s, 3H). ^{13}C (CDCl_3 , 75 MHz): δ = 259.5, 142.3, 131.1, 129.6, 128.9, 127.4, 127.3, 115.1, 55.5.

Characterization of product 3:

^1H NMR (CDCl_3 , 300 MHz): δ = 7.55-7.49 (m, 1H), 7.31-7.27 (m, 2H), 7.24 (m, 1H), 7.21-7.18 (m, 2H), 7.11 (m, 2H), 2.74 (s, 6H). ^{13}C (CDCl_3 , 75 MHz): δ = 145.6, 140.0, 132.3, 130.2, 127.8, 127.3, 125.0, 22.8.

Characterization of product 4:

^1H NMR (CDCl_3 , 300 MHz): δ = 7.78-7.68 (m, 4H), 7.63-7.60 (m, 2H), 7.50-7.42 (m, 3H). ^{13}C (CDCl_3 , 75 MHz): δ = 145.6, 139.2, 132.5, 129.0, 128.6, 127.6, 118.9, 110.9.

6.5. References.

- [1] A. P. Alivisatos, K. P. Johnsson, X. Peng, T. E. Wilson, C. J. Loweth, M. P. B. Jr., P. G. Schultz, *Nature (London)* **1996**, 382, 609.
- [2] M.-C. Daniel, D. Astruc, *Chem. Rev.* **2004**, 104, 293.
- [3] R. Elghanian, J. J. Storhoff, R. C. Mucic, R. L. Letsinger, C. A. Mirkin, *Science* **1997**, 277, 1078.

- [4] E. D. Goluch, J.-M. Nam, D. G. Georganopoulou, T. N. Chiesl, K. A. Shaikh, K. S. Ryu, A. E. Barron, C. A. Mirkin, C. Liu, *Lab Chip* **2006**, *6*, 1293.
- [5] C. A. Mirkin, R. L. Letsinger, R. C. Mucic, J. Storhoff, *Nature (London)* **1996**, *382*, 607.
- [6] N. L. Rosi, C. A. Mirkin, *Chem. Rev.* **2005**, *105*, 1547.
- [7] L. Pasquato, P. Pengo, P. Scrimin, *J. Mater. Chem.* **2004**, *14*, 3481.
- [8] A. K. Boal, V. M. Rotello, *J. Am. Chem. Soc.* **1999**, *121*, 4914.
- [9] R. Cao, R. Villalonga, A. Fragoso, *IEE Proc-Biotechnolog.* **2005**, *152*, 159.
- [10] G. L. Liu, Y. Yin, S. Kunchakarra, B. Mukherjee, D. Gerion, S. D. Jett, D. G. Bear, J. W. Gray, A. P. Alivisatos, L. P. Lee, F. F. Chen, *Nature Nanotech.* **2006**, *1*, 47.
- [11] I. H. El-Sayed, X. Huang, M. A. El-Sayed, *Nano. Lett.* **2005**, *5*, 829.
- [12] L. Pasquato, F. Rancan, P. Scrimin, F. Mancin, C. Frigeri, *J. Chem. Soc., Chem. Commun.* **2000**, *22*, 2253.
- [13] M. Brust, M. Walker, D. Bethell, D. J. Schiffrin, R. Whyman, *J. Chem. Soc., Chem. Commun.* **1994**, 801.
- [14] A. C. Templeton, W. P. Wuelfing, R. W. Murray, *Acc. Chem. Res.* **2000**, *33*, 27.
- [15] R. C. Price, R. L. Whetten, *J. Phys. Chem. B.* **2006**, *110*, 22166.
- [16] R. C. Price, R. L. Whetten, *J. Am. Chem. Soc.* **2005**, *127*, 13750.
- [17] T. G. Schaaff, R. L. Whetten, *J. Phys. Chem. B.* **1999**, *103*, 9394.
- [18] M. Brust, J. Fink, D. Bethell, D. J. Schiffrin, C. Kiely, *J. Chem. Soc., Chem. Commun.* **1995**, 1655.

- [19] M. J. Hostetler, S. J. Green, J. J. Stokes, R. W. Murray, *J. Am. Chem. Soc.* **1996**, *118*, 4212.
- [20] A. C. Templeton, M. J. Hostetler, C. T. Kraft, R. W. Murray, *J. Am. Chem. Soc.* **1998**, *120*, 1906.
- [21] M. J. Hostetler, A. C. Templeton, R. W. Murray, *Langmuir* **1999**, *15*, 3782.
- [22] R. Huisgen, J. Sauer, H. J. Sturm, J. H. Markgraf, *Chem. Ber.* **1960**, *93*, 2106.
- [23] R. Huisgen, *Angew. Chem., Int. Ed. Engl.* **1968**, *7*, 321.
- [24] Z. P. Demko, K. B. Sharpless, *Angew. Chem., Int. Ed. Engl.* **2002**, *41*, 2113.
- [25] Z. P. Demko, K. B. Sharpless, *Angew. Chem., Int. Ed. Engl.* **2002**, *41*, 2110.
- [26] H. C. Kolb, M. G. Finn, K. B. Sharpless, *Angew. Chem., Int. Ed. Engl.* **2001**, *40*, 2004.
- [27] W. G. Lewis, L. G. Green, F. Grynszpan, Z. Radić, P. R. Carlier, P. Taylor, M. G. Finn, K. B. Sharpless, *Angew. Chem., Int. Ed. Engl.* **2001**, *51*, 1053.
- [28] V. D. Bock, H. Hiemstra, J. H. v. Maarseveen, *Eur. J. Org. Chem.* **2006**, 51.
- [29] D. A. Fleming, C. J. Thode, M. E. Williams, *Chem. Mater.* **2006**, *18*, 2327.
- [30] J. L. Brennan, N. S. Hatzakis, T. R. Tshikhudo, N. Dirvianskyte, V. Razumas, S. Patkar, J. Vind, A. Svendsen, R. J. M. Nolte, A. E. Rowan, M. Brust, *Bioconjugate Chem.* **2006**, *17*, 1373.
- [31] L. Sun, R. M. Crooks, V. Chechik, *J. Chem. Soc., Chem. Commun.* **2001**, 359.
- [32] J.-B. Kim, M. L. Bruening, G. L. Baker, *J. Am. Chem. Soc.* **2000**, *122*, 7616.
- [33] P. Appukkuttan, W. Dehaen, V. V. Fokin, E. Van der Eycken, *Org. Lett.* **2004**, *6*, 4223.
- [34] K. Yoon, P. Goyal, M. Weck, *Org. Lett.* **2007**, *9*, 2051.

- [35] D. T. S. Rijkers, G. W. v. Esse, R. Merkx, A. J. Brouwer, H. J. F. Jacobs, R. J. Pieters, R. M. J. Liskamp, *J. Chem. Soc., Chem. Commun.* **2005**, 4851.
- [36] W. J. Sommer, M. Weck, *Adv. Synth. Catal.* **2005**, 348, 2101.
- [37] H.-U. Blaser, A. Indolese, F. Naud, U. Nettekoven, A. Schnyder, *Adv. Synth. Catal.* **2004**, 346, 1583.
- [38] F. M. Dautzenberg, P. J. Angevine, *Catal. Today* **2004**, 93-95, 3.
- [39] D. S. McGuinness, K. J. Cavell, *Organometallics* **2000**, 19, 741.
- [40] M. Larhed, A. Hallberg, *J. Org. Chem.* **1996**, 61, 9582.
- [41] O. Navarro, H. Kaur, P. Mahjoor, S. P. Nolan, *J. Org. Chem.* **2004**, 69, 3173.
- [42] M. G. Gardiner, W. A. Herrmann, C.-P. Reisinger, J. Schwarz, M. Spiegler, *J. Organomet. Chem.* **1999**, 572, 239.

CHAPTER 7

SUMMARY AND NEXT STEPS

Abstract

This chapter commences with a summary of the work accomplished with the poly(norbornene) supported Pd-pincers and Pd-*N*-Heterocyclic carbene and the gold nanoparticles supported Pd-*N*-Heterocyclic carbene describe in the previous chapters. The different conclusion drawn from each chapter will be discussed. Stemming from these investigations, new proposed directions for this project will be outlined. A new support, poly(styrene), is considered. The advantages of this support will be discussed. The evaluation of this support using techniques that were discussed in this thesis is proposed.

7.1. Summary

In chapter 3, poly(norbornene)-supported Pd-SCS pincer was described. The investigation on the activity of this system resulted in the discovery that the organometallic complex was not responsible for the catalysis. To establish this conclusion, different methods to probe if the organometallic complex was the actual catalyst were developed. The unique combinations of kinetic and poisoning studies confirmed the hypothesis that the active species in the Heck-Mizoroki transformation is a leached Pd species. In the kinetic studies, the presence of induction times indicated that the Pd pincer complex had to go through some transformation to become active. Moreover, the recycling experiments indicated a significant loss of activity after each

consecutive run. Finally, the poisoning tests, consisting on adding PVPy or mercury to trap any leached Pd species from the Pd-SCS complex were conclusive, showing no activity.

In chapter 4, Pd-PCP pincer complex were tethered on poly(norbornene) and silica. The different complexes synthesized were evaluated using the tests that were developed previously in chapter 3. The results indicated that Pd(II)-PCP pincer complexes were also not stable under Heck reaction conditions. Furthermore, the presence of phosphorus atoms in the Pd-PCP complexes allowed the investigation of the decomposition pathway using ^{51}P NMR. Results from this study showed that triethylamine is playing a key role in the decomposition of Pd-pincer complexes. To understand this role, mass spectroscopy experiments were carried out, mimicking a study done previously by Louie and Hartwig. The results suggest that triethylamine binds to the Pd when a binding site is free during the on-off equilibrium of the phosphorus arms. Finally, computational studies were carried out, showing the possibility of having triethylamine binding to the Pd complex. It was calculated that after the binding of one triethylamine, the energy required to bind a second one is negligible. Overall, the investigations carried for supported Pd-pincer complexes resulted in the discard of Pd(II)-pincer complexes to be used as catalyst.

In chapter 5, a new Pd complex was attached to poly(norbornene), Pd and Ru-*N*-Heterocyclic carbene complexes. Three different Pd-NHC were grafted onto the polymer, NHC-Pd(OAc), NHC-Pd(dba) and NHC-Pd(allyl)Cl. The three poly(norbornene)-supported Pd-NHC complexes were tested for any potential leaching using kinetic studies and poisoning tests. Resulting from this study was the unstability of NHC-Pd(dba) for the

Suzuki and Sonogashira transformations. In addition, each complex decomposes during the Heck reaction of iodobenzene with *n*-butyl acrylate in DMF at 120 °C. Eventhough, two of the Pd-NHC complexes seemed to be stable for Suzuki and Sonogashira reactions, the system was not recyclable. The recycling of the system consisted on precipitating the polymer after the reaction. Unfortunately, the polymer was less and less soluble after each consecutive cycle. Furthermore, the yields for each consecutive reaction dropped drastically. This result suggested that the polymer support was reacting during the catalysis, making it unable to be used as a support for catalysis.

In chapter 6, a new methodology was developed to graft a variety of functionalities onto gold nanoparticles. Using the 1,3-cycloaddition of a terminal alkyne with an azide, a new “recipe” using a microwave reactor was developed. Utilizing this new method Pd-NHC complex odified with a terminal alkyne was grafted onto gold nanoparticles. The system showed great promises with good yields for the Suzuki-Miyaura coupling of a variety of aryl chlorides with phenyl boronic acid. However, when the system was recycled, the gold nanoparticles became insoluble. Further investigations suggested that the support was reacting with the base used for the catalysis, changing its morphology. This last results lead to the formulation of new directions where this project should be taken.

Each chapters presented innovative ways to evaluate the catalyst that was supported. Utilizing the kinetic studies as well as poisoning, computational and NMR studies, several conclusions were drawn regarding the stability of the catalysts that were supported. Pincer complexed with Pd(II) decompose under reaction conditions to become Pd reservoirs, distilling a small amount of the active species during the catalysis. Pincer

complexes are not suitable to be supported. The Pd-*N*-heterocyclic carbene complexes proved to be stable for the Sonogashira and Suzuki transformations. Unfortunately, poly(norbornene) did not allow for recycling. After the precipitation of the polymer in order to reuse the catalyst, the polymer became insoluble. The different studies conducted to understand what led to this insolubility were inconclusive. Overall, poly(norbornene) is not a suitable polymer to be used as a support for catalysts. In addition, the use of gold nanoparticles as a support leads to a similar conclusion. After precipitating the particles, they became insoluble. Gold nanoparticles are not a suitable support for catalysts.

An alternative polymer that proved to be stable under various catalytic reactions is poly(styrene). The Weck group investigated this support with the Jacobson catalyst for the hydrolytic kinetic resolution of various epoxides. This polymer is easy to synthesize and should tolerate the Pd-NHC complex. One of the side phenyl of the NHC ligand can be modified to allow the polymerization of this new monomer. The advantages of poly(styrene) are multiple. Besides the stability of the polymer and the non-reactive moiety, the polymerization can be highly controlled, allowing for a variation in the loading of the catalyst. Poly(styrene) can also be cross-linked fairly easily by adding cross-linkers such as divinyl benzene. This advantage can be utilized to study the activity of the catalyst on a soluble support, and on a non-soluble support with the different stages of swellability and solubility in between. In this chapter, I proposed the synthesis of three different poly(styrene) supported Pd-NHC complexes.

7.2. Soluble poly(styrene) as a support

The synthesis of linear poly(styrene) functionalized with NHC-Pd complex can be accomplished via two methods. The Pd complex can be added to the styrene monomer before or after the polymerization. The solubility of the support and the ability to control the loading of the catalysts makes it an interesting system. Two different NHC ligands can be synthesized; one with the tether on the phenyl ring (Figure 7.1), and another one with the tether coming from the imidazole ring (Figure 7.2). With these two complexes in hand, the activity of the supported NHC-Pd can be investigated.

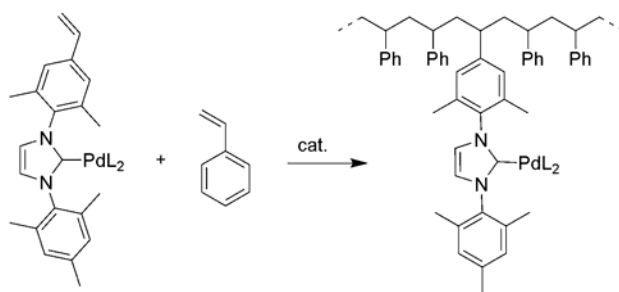


Figure 7.1. Synthesis of poly(styrene) supported Pd-NHC complex tethered to the side

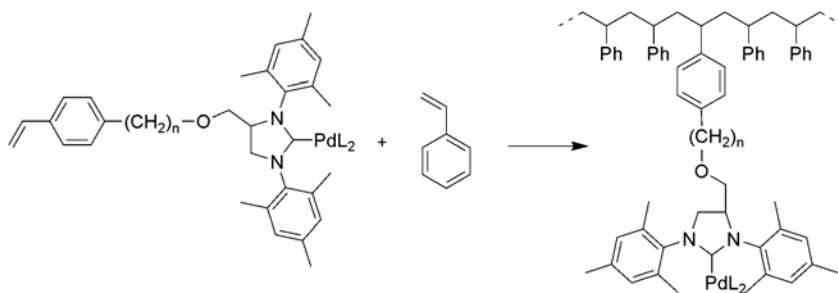


Figure 7.2. Synthesis of poly(styrene) supported Pd-NHC complex tethered to the back.

The influence of the tether can be investigated by comparing the activity of the two different systems. The poly(styrene) supported Pd-NHC tethered from the imidazole ring resembles most of the catalyst currently used. In addition, both systems can be tested for any potential palladium leaching. The battery of tests that were developed such as kinetic studies, recycling experiment and poisoning studies can be utilized. Both systems can be evaluated with the Suzuki-Miyaura and Heck-Mizoroki reactions. The latest transformation is the most demanding with high temperature and longer reaction times. This study can confirmed the hypothesis that the Heck-Mizoroki reaction conditions are too extreme for any palladium complexes to be stable.

7.3. Cross-linked poly(styrene) as a support

Another possibility to introduce the Pd-NHC complex is through the cross-linker. Seebach *et al.* first reported a similar system using the Jacobson ligand with cobalt metal. The NHC ligand can be modified to have the styrene moieties on the side chains and can be cross-linked with styrene monomers. This system would allow an investigation of the

activity of a solid supported NHC-Pd. The amount of cross-linker added would offer an understanding of the swellability behavior of this polymer and the effects on the catalytic activity. In addition, the pores of the resin can be tuned by varying the amount of cross-linker added, expanding the spectra of tests that can be performed to analyze the catalytically active species. Finally, the comparison between the lightly cross-linked with the highly cross-linked polymer should give an understanding on the affect of solubility on the activity of the supported catalyst.

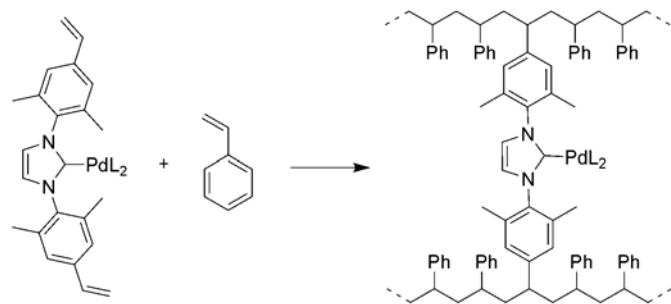


Figure 7.3. Synthesis of cross-linked supported Pd *N*-Heterocyclic carbene complexes

7.4. Conclusion

Three different supported NHC-Pd complexes are proposed. Poly(styrene) offers opportunities to have a better understanding of the affect of the support on the catalysis. Using the different tests described in this thesis, the activity and the stability of the catalyst can be investigated. In addition, the physical properties of the polymer can be modified using a variety of cross-linkers. It can also help understand the factors that can

be responsible for the decomposition of the catalyst. Understanding these factors can help for the synthesis of better catalysts.

APPENDIX A

X-ray Absorption Spectroscopy of Immobilized SCS Pd Pincer Compounds

Experimental Methods

X-ray absorption spectroscopy was conducted on beamlines X10C and X18B at the National Synchrotron Light Source, Brookhaven National Lab, Upton, NY. The Pd K edge spectra of catalysts and reference compounds were recorded at room temperature except those collected during the Heck reaction performed at 393 K. Spectra of samples in solvent or reaction medium were recorded in the fluorescence mode whereas other spectra were recorded in the transmission mode. For transmission measurements, ion-chambers were filled with Ar to have an absorbance of 10% in the first chamber and 80% in the second. A Pd foil (Goodfellow) was placed between the second and third ion chambers for energy calibration. At least four spectra were averaged for each sample studied in the transmission mode. For the samples examined during the Heck reaction, an in-situ cell was constructed with Teflon as body material and Kapton as the window. The reaction slurry was continuously pumped from a heated, stirred reactor vessel to the in-situ cell. To improve the signal-to-noise ratio during the measurement, at least ten scans were averaged. Two data analysis methods were used in this work, specifically, fitting of a linear combination of the edge spectra and fitting of standard multi-shell EXAFS data. The data analysis was performed with the WinXAS 2.1 program. The pre-edge background was removed with a linear function and the post-edge background was subtracted with a cubic spline method. According to the Nyquist theorem,¹ the number of free parameters for EXAFS curve-fitting are determined by the available data range in k

space and R space : $N_{pts} = 2\Delta k \cdot \Delta R / \pi + 2$. Typically, 16 parameters can be determined from the data.

Results and Discussion

Reference Compounds

The X-ray absorption near edge structure (XANES) associated with the Pd K edge of different reference materials is shown in Supplemental Figure 1. The zero valent Pd foil revealed a distinctly different edge shape compared to the other reference compounds having Pd in a higher oxidation state. The PdS and PdCl₂ samples have very similar XANES spectra, and the quick decay of oscillations above the peak at ~ 24360 eV in Pd(NH₃)₄Cl₂ was due to the presence of light N atoms as the nearest neighbor backscatterers. The Fourier transforms of the k^3 weighted EXAFS data are shown in Supplemental Figure 2. The large peak in each transform results from the first shell backscatterer atoms. The position of the peak is related to the first shell interatomic distance, not corrected for phase shift, whereas the intensity of the peak is related to the number of nearest neighbor backscatterers, the atomic number of the backscatterer and the disorder in the sample.

We used the program FEFF 8.20 to calculate theoretical reference files containing the appropriate backscattering amplitudes and phase shifts for various absorber-backscatterer pairs.² We then used the EXAFS data from the reference spectra to calibrate the reference files calculated by FEFF. The known structural parameters for each standard compound listed in Table 1 were used in the calibration process. Curve-fitting of reference data with k^3 - weighting was performed in R-space to produce a set of parameters for the calibration

of theoretical FEFF reference files. Table 2 summarizes these parameters derived from curve fitting that were subsequently input to the revised theoretical FEFF reference files.³ Since a reference compound having a Pd-C first shell was not available, we used the Pd-N reference file as a substitute.

Influence of immobilization

Supplemental Figure 3 shows the XANES of immobilized SCS pincer compounds on SBA and polymer support. Although the spectra are similar, with an obvious white line present at the absorption threshold, a subtle difference in the XANES can still be observed. The k^2 weighted Fourier transform of the EXAFS (Supplemental Figure 4) revealed that both samples have light backscatterers around Pd (at ~ 1.9 Å) associated with the pincer complex, but that a new peak was present at ~ 2.5 Å in the SBA-immobilized compound. It is reasonable to assume that this long distance may be due to the presence of some Pd in the first coordination shell, presumably from a small amount of Pd metal. Assuming the spectrum can be decomposed into contributions from the SCS pincer complex and metallic Pd, we performed a fitting analysis utilizing a linear combination of the edge spectra for SBA immobilized SCS pincer Pd. This method has been used previously to study the local structure around an absorbing atom.^{4,5} The XANES fitting analysis was performed in a region up to 150 eV above the edge. The fitting parameters in Table 3 indicated that 6.5% of the Pd in SBA immobilized SCS pincer complex was metallic in nature whereas 93.3% of the Pd was present in the SCS pincer complex. The estimated coordination number of the Pd-Pd shell was only about 0.8.

Curve-fitting of the EXAFS data with FEFF reference files utilizing k^2 weighting in R space was performed on the spectra of SBA and polymer-immobilized SCS pincer complex with a fixed S_0^2 value of 0.9. Since the number of free parameters in the fitting routine is so high (16), many are correlated, and the Nyquist theorem dictates only 16 can be independently fit, the coordination numbers and interatomic distances were fixed to a small region near the estimated values. In addition, the Debye-Waller factor was forced to be non-negative. Reasonable values of Debye-Waller factor and ΔE_0 as shown in Table 4 suggest that immobilization of the complex on the SBA support and the polymer did not cause a significant change in the atomic structure around Pd bound in the SCS pincer complex. However, curve-fitting for SBA immobilized SCS pincer Pd provided a coordination number of 1.4 and an interatomic distance of 2.71 Å for Pd-Pd shell as shown in Table 4. The Pd-Pd bond length is 0.04 Å shorter than that in bulk Pd, which suggests that the metallic particles must be nanometer size or less. Both fitting methods suggest that the new peak in Fourier transform of SBA-immobilized SCS pincer Pd can be assigned to the presence of small metallic Pd particles on the support, and most of Pd still remain bound in SCS pincer complex after immobilization on SBA support. It should be noted that if any O atoms were present on the Pd metal surface, they could not be distinguished from nearest neighbor C atoms associated with Pd in the pincer complex.

In-situ X-ray Absorption Spectroscopy during Heck Reaction

The influence of the solvent DMF on the structure of polymer-immobilized SCS pincer Pd was also investigated. As shown in Supplemental Figure 3, no change in XANES was observed between a sample in air and one dissolved in DMF. Likewise, the

Fourier transform of the EXAFS region showed the same backscattering contribution in both samples (not shown). The linear combination of XANES analysis showed only the contribution from SCS pincer complex after stirring in DMF. Apparently, there is little change in the local environment around Pd with solvent addition.

To better understand the reaction mechanism of Heck catalysis, Evans *et al.* performed an *in-situ* X-ray absorption study of the Heck reaction with Pd acetate as catalyst.⁶ We also performed an *in-situ* study during the Heck reaction catalyzed by polymer immobilized SCS Pd in DMF, with iodobenzene and butylacrylate as substrates and triethylamine as base. The Heck reaction was first carried out in flask at 393 K. Then the reacted solution was pumped into an *in-situ* cell from the reactor. A uniform suspension of catalyst in solution was achieved by recirculation between the cell and the reactor. Supplemental Figure 5 shows k^2 -weighted Fourier transform of the EXAFS for a sample in air and a sample during Heck reaction. A new feature was observed at ~ 2.5 Å, which could arise from the backscattering contribution of a Pd-Pd or a Pd-I shell. In order to distinguish between them, we performed a fitting of the edge spectra involving SCS pincer complex on polymer, metallic Pd and PdI₂. The fitting results presented in Table 3 suggest that iodine was present in the first coordination shell of Pd. Although most of the Pd was associated with SCS pincer complex (85.5%), a Pd-I coordination number of ~ 0.6 was derived from the fitting procedure. Interestingly, no evidence for metallic Pd was found in the XANES, as shown in Supplemental Figure 6. To further support this conclusion, a similar study was also performed with the SBA-immobilized SCS pincer complex, which was insoluble in DMF. In this case, the XANES fitting results also showed the presence of Pd-I in addition to a large amount of SCS pincer complex. A

small amount of metallic Pd determined by the XANES fitting results may have been formed in the process of the immobilization, as discussed above. The observation of Pd-I compounds during Heck catalysis is in a good agreement with the results reported by Evans *et al.*.⁶

The coordination number of Pd-I in Table 4 was about 1.2 as determined by EXAFS fitting in R space with k^2 weighting, the experimental data are compared to the fitted results with k^2 -weighting in Supplemental Figure 7. The average Pd-I coordination number was slightly lower than those reported by Evans *et al.* (1.8 or 2.3) who studied Pd acetate as a catalyst for the Heck reaction.⁶ The Pd in our study remained mostly bound in the SCS pincer complex, which may be related to its higher stability during Heck catalysis compared to Pd acetate. In order to achieve a good fitting for the Pd-I contribution, the interatomic distance of Pd-I shell need be lengthened to 2.67 Å, which is somewhat longer than the value in PdI₂. A long Pd-I bond was also observed by Evans *et al.* during their EXAFS study of [Pd₂I₆][NEt₃H]₂ dissolved in CH₃CN.⁶

Summary

The X-ray absorption spectroscopic studies have provided the following information on the Pd(II) SCS-O system in support of our previous results:⁷

- The Pd species are altered under reaction conditions, with a fraction of the pincer species supported on poly(norbornene) or silica decomposing to form new species.
- Heating the immobilized species in DMF did not result in any notable change in the Pd species as determined by spectroscopy. Previously, it was shown that

base and one of the reactants was required for generation of soluble catalytic species. Additionally, in this work, it has been shown that the addition of base is the key step that causes complex decomposition.

Furthermore, additional information obtained during this study:

- Pd(II) SCS-O pincer species supported on silica have a small amount of Pd(0) that is formed during synthesis, most likely during the immobilization step. Pd(II) SCS-pincer species supported on poly(norbornene) look similar to the small molecule complex as determined by EXAFS.'
- Palladium(II) iodo species are hypothesized to be the primary species formed under reaction conditions based on EXAFS and XANES analysis.⁸ This is consistent with our works, which have found that Pd-iodo species are the primary resting state for Pd in the Heck reaction. This signal may also be enhanced in the EXAFS spectra by halide exchange under reaction conditions resulting from exchange of the HI formed in the reaction with the Pd-Cl bonds in the remaining unreacted pincer complexes (only a fraction decompose) to create Pd-I bonds and liberate HCl.

XYZ Coordinates in Ångstroms for Figures 9 and 10

Figure 9b:

C	0.2017977411	-1.1573849355	-1.4332789682
C	-0.5108596459	0.0717572842	-1.6060191868
C	-1.8711902409	0.0419084322	-2.0079445296
C	-2.5368629910	-1.1786151565	-2.2135787896
C	-1.8545718818	-2.3887247739	-2.0006727131
C	-0.4942304515	-2.3972864156	-1.5981262983
H	-2.4050750587	0.9890765083	-2.1501325646
H	-3.5855319571	-1.1867717953	-2.5298596558
H	-2.3752538562	-3.3439882114	-2.1375613669
C	0.1488155890	-3.7394000215	-1.2939136427
H	-0.1270260903	-4.0789570547	-0.2753199423
H	-0.1658811647	-4.5269871989	-2.0015389573
C	0.1137063438	1.4245553454	-1.3110678386
H	-0.1731082167	1.7707393682	-0.2978809801
H	-0.2054435557	2.2008909764	-2.0292646288
P	2.0475396975	-3.5400266442	-1.2908361936
P	2.0142650949	1.2498866032	-1.2927167913
C	3.7617815144	-6.8698692220	1.5610891966
C	4.3542771977	-5.5912442005	1.5218517926
C	3.8327373335	-4.5925957457	0.6719407424
C	2.7159474733	-4.8785091170	-0.1468726573

C	2.1232122924	-6.1641513845	-0.1110009029
C	2.6459362193	-7.1548234007	0.7451378577
H	4.1679195606	-7.6427168983	2.2227801443
H	5.2212980357	-5.3681741229	2.1529693912
H	4.2884821455	-3.5953457689	0.6353582242
H	1.2649622628	-6.4022152389	-0.7493592029
H	2.1849763194	-8.1481174710	0.7709807609
C	3.3856239081	-4.8565713726	-5.6188188363
C	2.3141583400	-3.9547285746	-5.4440028037
C	1.9200384239	-3.5655066616	-4.1483953485
C	2.5876163585	-4.0904365479	-3.0154865848
C	3.6657429156	-4.9868351338	-3.1928372452
C	4.0620587596	-5.3668908562	-4.4923341105
H	3.6938221995	-5.1538726127	-6.6268610649
H	1.7870925289	-3.5526653620	-6.3157747473
H	1.0970802468	-2.8528092994	-4.0236227082
H	4.1940378650	-5.3940116874	-2.3251574533
H	4.8974426089	-6.0637518928	-4.6201830186
C	3.6657467527	4.6084181088	1.5623767612
C	4.2685775435	3.3342794521	1.5389507751
C	3.7661478030	2.3264566638	0.6883268769
C	2.6576236826	2.5985013507	-0.1462291970
C	2.0550869717	3.8798652812	-0.1268778798

C	2.5587271399	4.8797597644	0.7298872636
H	4.0570791684	5.3884760068	2.2244504602
H	5.1291152995	3.1220067221	2.1825157455
H	4.2314457990	1.3333796176	0.6622275998
H	1.2035497227	4.1070972337	-0.7779224333
H	2.0897718809	5.8695766626	0.7431340372
C	3.3806219345	2.5591754869	-5.6132365605
C	2.3022646994	1.6647234086	-5.4436175446
C	1.8972723203	1.2816345503	-4.1496602255
C	2.5627575407	1.8016010455	-3.0136222554
C	3.6484797140	2.6898974220	-3.1855068511
C	4.0542189316	3.0658611402	-4.4832589141
H	3.6964475379	2.8536598317	-6.6196954759
H	1.7769586560	1.2643818772	-6.3174060575
H	1.0666337455	0.5779819354	-4.0277250258
H	4.1757649517	3.0932342731	-2.3154537501
H	4.8949582305	3.7569433036	-4.6071778783
Pd	2.1828812231	-1.1428082415	-0.9734934968
Cl	4.6257788325	-1.1234243379	-0.2505141229

Figure 9c:

C	0.1377908571	-0.9689989180	-1.7439967400
C	-0.4623285828	0.2251630874	-2.2165288019

C	-1.7272918808	0.1356338258	-2.8528403605
C	-2.3548000874	-1.1124872933	-3.0066562143
C	-1.7220915269	-2.2900526594	-2.5573263499
C	-0.4534299416	-2.2449756149	-1.9298120603
H	-2.2083763347	1.0481327370	-3.2234121793
H	-3.3365187080	-1.1748388907	-3.4872084467
H	-2.2167201149	-3.2550417239	-2.7087176685
C	0.3044513693	-3.5025599762	-1.4965911032
H	1.1270112771	-3.7316881178	-2.2029676889
H	0.7764680463	-3.3626740857	-0.5012717969
C	0.2276831362	1.5588624886	-2.0390644484
H	-0.2810691184	2.1835192063	-1.2799270766
H	0.2802900360	2.1427652660	-2.9753694088
P	-0.7873846702	-5.0869007193	-1.2227906909
P	1.9944435556	1.1887203859	-1.3902187363
C	-1.8067350580	-6.8999576490	-5.4773978526
C	-2.3224809018	-7.4533337883	-4.2859352990
C	-1.9833291389	-6.8877750397	-3.0417209412
C	-1.1169727144	-5.7670021223	-2.9694893914
C	-0.5959384216	-5.2251598657	-4.1664586907
C	-0.9457939308	-5.7862396392	-5.4143078141
H	-2.0792781415	-7.3311713830	-6.4465064379
H	-2.9948811804	-8.3172856469	-4.3255146976

H	-2.4035916528	-7.3137019715	-2.1221273352
H	0.0767805130	-4.3612707277	-4.1415652531
H	-0.5447506883	-5.3513045786	-6.3363075708
C	2.4902213889	-8.0680087572	0.4550162368
C	1.6216430541	-7.3753534074	1.3240078219
C	0.6546344442	-6.4919049700	0.8004873873
C	0.5551193501	-6.2871726887	-0.5970865936
C	1.4291569958	-6.9855825616	-1.4629825236
C	2.3914011930	-7.8731933512	-0.9389329535
H	3.2357743969	-8.7604423213	0.8604572392
H	1.6900254557	-7.5273590020	2.4069219298
H	-0.0307760156	-5.9727301352	1.4813397280
H	1.3493237100	-6.8502458645	-2.5469721896
H	3.0611672424	-8.4130695098	-1.6178811619
C	3.1546922241	4.5540706229	1.6775621181
C	3.7532202356	3.2797061551	1.7569872545
C	3.3893299597	2.2658573960	0.8483205860
C	2.4225552410	2.5324971616	-0.1490925879
C	1.8131809625	3.8085572683	-0.2262296561
C	2.1856137023	4.8163474616	0.6876941055
H	3.4400108522	5.3379635411	2.3868957441
H	4.5005274689	3.0703156596	2.5291914997
H	3.8386991206	1.2679564108	0.9234255257

H	1.0661802913	4.0352816876	-0.9939192665
H	1.7169478855	5.8036265135	0.6216968337
C	4.9285738450	1.7578826355	-5.0164673450
C	4.3642378745	0.4898597275	-4.7631539568
C	3.4982123981	0.3113587056	-3.6654436916
C	3.1993196001	1.4071740790	-2.8276042970
C	3.7623749978	2.6804697644	-3.0726920563
C	4.6272739620	2.8493335778	-4.1742751456
H	5.6073480243	1.8929990816	-5.8651134818
H	4.6057033488	-0.3599015312	-5.4100843279
H	3.0722126615	-0.6758603771	-3.4511031304
H	3.5385606674	3.5306913865	-2.4214527986
H	5.0693344399	3.8321184887	-4.3685291142
Pd	1.7671594418	-1.0385931362	-0.6392539700
Cl	3.7670029662	-1.3163225884	0.8864932841

Figure 9d:

C	0.3833021356	-0.9220123766	-0.2358184110
C	0.0072401933	0.3670955018	0.2333837565
C	-1.3211970749	0.5808702905	0.6764408645
C	-2.2626404458	-0.4616445110	0.5879090904
C	-1.9052418769	-1.6902720911	0.0000014241
C	-0.5801976880	-1.9439589209	-0.4415502142

H	-1.6136019958	1.5651064637	1.0612192064
H	-3.2903514242	-0.3029378695	0.9325060145
H	-2.6678041947	-2.4636923256	-0.1425330176
C	-0.2123485192	-3.1972088868	-1.2398031806
H	-0.2286627419	-2.9312358682	-2.3152544855
H	0.8171948522	-3.5242564913	-1.0134655581
C	1.0039441315	1.5059546004	0.1003580965
H	1.7475019753	1.5430240228	0.9188464776
H	0.5245341195	2.4980911058	0.0278779030
P	-1.4503339252	-4.6914761431	-1.0863957524
P	2.0222679966	1.0571206334	-1.4793355734
C	-0.7621466221	-7.2893551648	-4.9856443207
C	-1.7256961728	-7.6341953245	-4.0131732314
C	-1.8669472599	-6.8497912534	-2.8528754266
C	-1.0406595336	-5.7154287614	-2.6341790435
C	-0.0704006642	-5.3849440252	-3.6089693355
C	0.0619501406	-6.1653525853	-4.7796999820
H	-0.6612116994	-7.8890448051	-5.8967422815
H	-2.3751916607	-8.5034121386	-4.1645502422
H	-2.6367987380	-7.1115604455	-2.1160945901
H	0.5933978974	-4.5238876387	-3.4745787202
H	0.8130672907	-5.8900431767	-5.5286223081
C	0.2594913760	-7.3249585645	2.4685269584

C	-0.6308420067	-6.2573970664	2.7089842603
C	-1.1122653735	-5.4827353754	1.6330855656
C	-0.6970786283	-5.7567959067	0.3055966971
C	0.1950890664	-6.8298402512	0.0727813670
C	0.6679228307	-7.6110922481	1.1489643786
H	0.6244202462	-7.9354628478	3.3018925337
H	-0.9610327694	-6.0344892702	3.7298643125
H	-1.8274318728	-4.6741336728	1.8256333164
H	0.5151344098	-7.0619986530	-0.9480490647
H	1.3533876067	-8.4438827724	0.9543867463
C	5.6245651587	4.0942694428	-1.6379561693
C	5.7305877095	2.8931397127	-0.9072332253
C	4.6541547137	1.9828828022	-0.8768376005
C	3.4610190467	2.2779521065	-1.5756269599
C	3.3521372178	3.4865205819	-2.3035980332
C	4.4345904182	4.3892086600	-2.3353354493
H	6.4676012163	4.7926848350	-1.6713993338
H	6.6578025229	2.6539296098	-0.3758877432
H	4.7604318094	1.0206218566	-0.3657281740
H	2.4341456279	3.7218553877	-2.8504402407
H	4.3472107915	5.3194600274	-2.9069331414
C	-0.5882052723	2.1159118751	-5.2536808430
C	-1.1520106764	2.2469775378	-3.9689324924

C	-0.3890469318	1.9432625820	-2.8223664274
C	0.9473456673	1.5052515037	-2.9579222573
C	1.5090098587	1.3670254678	-4.2514821310
C	0.7441671411	1.6734300870	-5.3930156933
H	-1.1834253140	2.3524361766	-6.1417621298
H	-2.1866970298	2.5870688874	-3.8536575810
H	-0.8467594027	2.0442989769	-1.8347104310
H	2.5420396470	1.0211392416	-4.3706879058
H	1.1879606269	1.5653222083	-6.3883070445
Pd	2.3135035377	-1.2055791930	-0.5855761538
Cl	4.8419994745	-1.4716150077	-1.2015266858
N	2.6051711405	-2.6440585787	1.1832949323
C	3.6522099908	-1.9203728352	1.9848127100
H	4.5242828686	-1.7325809721	1.3427737321
H	3.2391845936	-0.9628578559	2.3409223435
H	3.9498700767	-2.5349433482	2.8621995618
C	3.1660911218	-3.9426530479	0.6809028525
H	4.0042396788	-3.7237060161	0.0026130677
H	3.5203404772	-4.5655843302	1.5299193078
H	2.3840562932	-4.4996630335	0.1420974754
C	1.4170927603	-2.8950579239	2.0564476800
H	1.7154437779	-3.5008663634	2.9384894234
H	1.0035583879	-1.9337986964	2.3971704086

H	0.6450646941	-3.4415785453	1.4985701130
---	--------------	---------------	--------------

Figure 9e:

C	-0.6584098148	-1.0120719894	-1.3910233240
C	-0.8882638310	0.3664149890	-1.1587298153
C	-2.2095937152	0.7545369493	-0.8106196279
C	-3.2401260846	-0.1954200577	-0.7080269563
C	-2.9743556117	-1.5525599513	-0.9525133457
C	-1.6656593708	-2.0047890499	-1.2905068746
H	-2.4215507548	1.8137001137	-0.6292614002
H	-4.2538896654	0.1248512535	-0.4458410577
H	-3.7831441308	-2.2892580179	-0.9028067361
C	-1.4662801069	-3.4761982341	-1.5994763980
H	-2.3761459172	-3.8831960492	-2.0771540291
H	-0.6226082428	-3.6277402363	-2.2984818106
C	0.2081128410	1.4168382528	-1.2976257415
H	0.0975766775	1.9925057079	-2.2379122897
H	1.2044338044	0.9386763846	-1.3411072779
P	-0.9636253241	-4.6817927729	-0.1101161930
P	0.2873323555	2.6566688988	0.2078104040
C	-4.5906397810	-5.0388081945	2.9169070345
C	-4.0895194871	-6.1936378726	2.2835524975
C	-3.0589349680	-6.0887554581	1.3265399184

C	-2.5091130079	-4.8266671204	0.9929149357
C	-3.0088391033	-3.6728553370	1.6477645469
C	-4.0477196507	-3.7787449752	2.5939573330
H	-5.3878395438	-5.1209290830	3.6629472902
H	-4.4973784555	-7.1794007195	2.5332506904
H	-2.6785261532	-6.9946540993	0.8466446409
H	-2.5823802145	-2.6877477948	1.4339038520
H	-4.4225397532	-2.8759170847	3.0884908032
C	-0.9379475769	-8.7540067350	-2.5412762249
C	0.2020787004	-8.3286789265	-1.8253326370
C	0.1642991639	-7.1149143996	-1.1011353556
C	-1.0116396043	-6.3173621186	-1.0851302248
C	-2.1528986943	-6.7536878853	-1.8046332033
C	-2.1162013937	-7.9657501890	-2.5280601866
H	-0.9110509019	-9.6948314144	-3.1054149431
H	1.1185762816	-8.9369085927	-1.8331479346
H	1.0509441210	-6.7920554303	-0.5410895869
H	-3.0780452184	-6.1587153832	-1.7914372977
H	-3.0050388409	-8.2947052343	-3.0804154052
C	-2.2117556692	6.4888497856	-1.0413762004
C	-1.5075821743	6.4208969094	0.1833487873
C	-0.7647971587	5.2681677106	0.5073900783
C	-0.7034339602	4.1697757375	-0.3926838236

C	-1.4109198836	4.2451748348	-1.6156431317
C	-2.1632271459	5.3992781976	-1.9365012868
H	-2.7972838031	7.3816752966	-1.2906056899
H	-1.5437801707	7.2612244601	0.8880342022
H	-0.2330116415	5.2217611013	1.4675106666
H	-1.3909139896	3.4132562561	-2.3308511192
H	-2.7078666447	5.4410234694	-2.8881254936
C	4.7580881659	4.2061679792	-0.1244144898
C	4.3766266203	3.2780388657	0.8660187677
C	3.0374274553	2.8369847840	0.9407413410
C	2.0712787479	3.3105819833	0.0193643880
C	2.4605285059	4.2483895426	-0.9644287776
C	3.7975743066	4.6934789985	-1.0361713968
H	5.7957403284	4.5551716688	-0.1807503316
H	5.1144410672	2.9070301446	1.5856566372
H	2.7381310644	2.1416420042	1.7343362352
H	1.7195026821	4.6390865503	-1.6698256710
H	4.0883667149	5.4213028295	-1.8021842013
Pd	1.0589469942	-1.4644147440	-2.1208730467
Cl	3.3246423468	-1.9409657604	-3.3132769568
N	1.9899801633	-1.7412125529	-0.1045009554
C	3.1503919807	-0.7834675724	-0.0613986831
H	3.7535182262	-0.9173327410	-0.9706829586

H	2.7809451193	0.2516739025	-0.0046673458
H	3.7640473749	-0.9921299819	0.8380152390
C	2.5194383994	-3.1541609635	-0.1274448842
H	3.1320155120	-3.2900059957	-1.0308580934
H	3.1388127604	-3.3249337610	0.7767308435
H	1.6727968369	-3.8559173276	-0.1208240745
C	1.1205633486	-1.5499797141	1.1039290578
H	1.7259709135	-1.7050963914	2.0217580633
H	0.7018869595	-0.5323159767	1.1135696446
H	0.3077557590	-2.2871793889	1.0815458608

Figure 9f:

C	0.0905360263	-1.0055609575	-1.6998211445
C	-0.4197644953	0.3123982371	-1.5519618439
C	-1.7919566936	0.5339508057	-1.8421641926
C	-2.6195320653	-0.5173669256	-2.2731042252
C	-2.0886841222	-1.8104504743	-2.4323512318
C	-0.7238842605	-2.0798654253	-2.1530227969
H	-2.1992935727	1.5455582853	-1.7360078043
H	-3.6762076100	-0.3297334959	-2.4928667848
H	-2.7310089115	-2.6249565687	-2.7867340071
C	-0.1845901199	-3.5048580715	-2.2529667344
H	0.9194633136	-3.5055826238	-2.2884502820

H	-0.4836408757	-4.0902204219	-1.3626742634
C	0.4592672302	1.4838736123	-1.1451827297
H	0.4080349827	2.3047204737	-1.8845759828
H	1.5109115247	1.1530126261	-1.0795382124
P	-0.8582128895	-4.5509536354	-3.7695183402
P	0.0893382619	2.2228022042	0.6290757702
C	2.8885378777	-4.9463167567	-6.6405884282
C	1.6810567819	-4.3731537495	-7.0884792817
C	0.5811595714	-4.2669580798	-6.2101350949
C	0.6837217714	-4.7235747813	-4.8742263791
C	1.9013570686	-5.2962181045	-4.4327126803
C	2.9967786694	-5.4118518065	-5.3123769353
H	3.7412656292	-5.0349348864	-7.3226388911
H	1.5911776627	-4.0126510158	-8.1192875881
H	-0.3605576662	-3.8321361087	-6.5648522110
H	1.9899284352	-5.6655828550	-3.4058351272
H	3.9314287584	-5.8643224476	-4.9631957790
C	-1.3913653135	-8.8502313692	-1.8187801955
C	-1.9201289432	-7.7012752278	-1.1937857162
C	-1.7159744267	-6.4277020383	-1.7626013554
C	-0.9672264787	-6.2785912888	-2.9581239726
C	-0.4507861265	-7.4390915494	-3.5836563016
C	-0.6614329606	-8.7145330364	-3.0175619693

H	-1.5516298829	-9.8404671011	-1.3785077718
H	-2.4959271959	-7.7930447626	-0.2653154895
H	-2.1631999005	-5.5540929929	-1.2724999984
H	0.1204356171	-7.3532491968	-4.5138261073
H	-0.2501309047	-9.6007760506	-3.5144339706
C	-3.5299971869	5.2253162613	0.0814756732
C	-3.3699582647	4.4722302998	1.2631123259
C	-2.2884382272	3.5741603598	1.3834986818
C	-1.3539033354	3.4274843428	0.3294483711
C	-1.5174173226	4.1943036986	-0.8497401964
C	-2.6045864982	5.0838665249	-0.9755770882
H	-4.3714245387	5.9203096710	-0.0155315149
H	-4.0841140310	4.5791134714	2.0883090003
H	-2.1710847354	2.9814316478	2.2993974767
H	-0.7977444907	4.1117866868	-1.6735317489
H	-2.7246946060	5.6696363317	-1.8945056620
C	3.7980223803	5.1595338047	1.1188993486
C	3.9864416398	3.7749964834	0.9269369673
C	2.8744075633	2.9256034276	0.7569869552
C	1.5558279465	3.4460607241	0.7612848653
C	1.3787190798	4.8367129599	0.9529845774
C	2.4909248255	5.6856282498	1.1358030269
H	4.6608245646	5.8191428510	1.2584490463

H	4.9981662780	3.3577746715	0.9120239034
H	3.0417845847	1.8501125491	0.6308554330
H	0.3715905717	5.2632260979	0.9614500317
H	2.3330013606	6.7590023854	1.2873684959
Pd	1.9459176804	-1.4028306370	-1.2389688252
Cl	4.4083955856	-2.1807308783	-0.7060149781
N	1.3347685505	-2.0617122459	0.8288820038
C	2.1928988402	-1.2532249388	1.7634569302
H	3.2448065635	-1.3785900312	1.4716024489
H	1.9007650779	-0.1933476860	1.6928796670
H	2.0410956358	-1.5970325600	2.8092576713
C	1.6991996514	-3.5144806641	0.9554011271
H	2.7533687584	-3.6385111440	0.6692276982
H	1.5434267015	-3.8547059224	2.0007626737
H	1.0620921905	-4.1115562050	0.2875529894
C	-0.1056528466	-1.8748300303	1.2154879761
H	-0.2619422063	-2.2278902003	2.2565711484
H	-0.3676730900	-0.8085295396	1.1477802731
H	-0.7533836184	-2.4489761358	0.5387007633
N	2.6186716811	-0.7142020942	-3.2625993430
C	3.6265531249	0.3723808466	-2.9845313479
H	4.3581920586	-0.0052237132	-2.2562729178
H	4.1458494568	0.6587218199	-3.9237461158

H	3.1077868122	1.2559064071	-2.5826267925
C	1.5915783543	-0.1948791731	-4.2254597120
H	1.0711771313	0.6700734860	-3.7923248787
H	2.0895059195	0.1154753087	-5.1681477290
H	0.8575546851	-0.9841108149	-4.4427324882
C	3.3154469763	-1.8889710931	-3.8918220541
H	3.8105045801	-1.5698286620	-4.8332990087
H	4.0632242928	-2.2754755275	-3.1867498239
H	2.5771597877	-2.6721340755	-4.1165475357

Figure 10b:

C	-3.8606025642	4.0655574811	3.1879171373
C	-3.0675179066	3.9954922288	2.0160572903
C	-3.2824915498	2.9937682740	1.0374039603
C	-4.2961814558	2.0339121061	1.2655711625
C	-5.0813187487	2.0826598048	2.4269844142
C	-4.8642081211	3.0871709020	3.3816416776
Pd	-1.5981291090	5.2644286651	1.7747363266
H	-4.4562803749	1.2430882165	0.5225617329
H	-5.8530452470	1.3239074580	2.5969405201
H	-5.4685413311	3.1200634533	4.2963150886
C	-3.6669576656	5.1428569405	4.2213093528
H	-4.1079667904	6.1094835718	3.9273454980

H	-4.0296280813	4.8546283569	5.2200211821
C	-2.4662762618	2.9250423651	-0.2260608732
H	-2.7709934850	3.6676435636	-0.9813824066
H	-2.4494893788	1.9199623605	-0.6751308188
S	-0.6683683269	3.3949997181	0.2937456792
S	-1.7613055159	5.4347115920	4.3244112819
C	-1.0264832529	9.3977369979	6.6438034210
C	-1.1542509488	9.4328458129	5.2430936890
C	-1.4106552995	8.2512538595	4.5228530765
C	-1.5409704039	7.0428549357	5.2266956393
C	-1.4032874382	6.9896243994	6.6268610337
C	-1.1496610003	8.1778756377	7.3342609514
H	-0.81711117630	10.3197867267	7.1982891737
H	-1.0432053545	10.3800913512	4.7031375707
H	-1.4629697150	8.2592974231	3.4296510339
H	-1.4750984941	6.0329987570	7.1568146545
H	-1.0375358363	8.1445083936	8.4241542000
C	1.7901634296	4.1172294803	-3.5884506907

Figure 10c:

C	-2.2087376257	9.0060827825	4.5171749623
C	-1.9683975861	8.0581899428	3.4866687611
C	-2.6503498636	8.1028170096	2.2524869930

C	-3.5934353791	9.1488935525	2.0838418150
C	-3.8382943644	10.1065350348	3.0709190444
C	-3.1400721217	10.0400750076	4.2825500760
Pd	-0.5617807627	6.7786516812	3.8124519870
H	-4.1205913527	9.2023803617	1.1235890151
H	-4.5637055767	10.9081778351	2.8923284597
H	-3.3045330909	10.7908390967	5.0655669567
C	-1.5372232029	8.9408420281	5.8562423632
H	-1.4992523025	9.9136254424	6.3708249405
H	-1.9954764201	8.1897256571	6.5211858249
C	-2.5068357361	7.0736440637	1.1476870487
H	-3.3761551716	6.3955855143	1.1301016944
H	-1.6079937075	6.4596409629	1.2684046321
S	-2.4231789327	7.8301868239	-0.6158066414
S	0.2678491647	8.3515782360	5.5738731883
C	1.1382478996	5.8709895182	9.4145168833
C	-0.0401882920	5.6194095056	8.6877008957
C	-0.3154405015	6.3462307025	7.5173684769
C	0.5911696832	7.3334864399	7.0952434250
C	1.7727388502	7.5961553963	7.8093976728
C	2.0428546611	6.8523375927	8.9728721367
H	1.3499709809	5.2996732574	10.3258587867
H	-0.7456526003	4.8509034142	9.0238526452

H	-1.2186821580	6.1294512243	6.9353655827
H	2.4655187925	8.3751822034	7.4726460825
H	2.9601412754	7.0516017103	9.5389973678
C	-5.8128465998	5.8061181569	-3.0910797165
C	-4.5015781639	5.8935035899	-3.5912449239
C	-3.4814751454	6.4676388015	-2.8120236777
C	-3.7798198651	6.9658394996	-1.5293919023
C	-5.0939756630	6.8963945073	-1.0285822642
C	-6.1032514462	6.3040467754	-1.8075921551
H	-6.6058063746	5.3540361466	-3.6982612423
H	-4.2626623919	5.5043039643	-4.5885401773
H	-2.4552629235	6.5162544180	-3.1940994563
H	-5.3403664682	7.3058045078	-0.0418553767
H	-7.1253792712	6.2509463545	-1.4130499149
Cl	-1.4155396936	4.6250678966	2.9485765001

Figure 10d:

C	-2.7288883663	7.5999481450	4.8107769736
C	-2.1371416982	7.1585849399	3.6017553457
C	-2.2380595906	7.9196914079	2.4166794951
C	-3.0007813044	9.1073810764	2.4582459124
C	-3.6196004326	9.5428535037	3.6380175792
C	-3.4699536295	8.8018190743	4.8167784281

Pd	-1.0191089219	5.5540362786	3.6848582278
H	-3.0910772300	9.7013126628	1.5406158372
H	-4.2004373994	10.4728803843	3.6403194807
H	-3.9171537253	9.1526700110	5.7560523826
C	-2.5384723179	6.8340688864	6.0867296384
H	-2.6874887029	7.4400190956	6.9949687829
H	-3.1644768012	5.9260127195	6.1572504862
C	-1.5551278114	7.4498948772	1.1380329672
H	-2.0041018972	6.5094770209	0.7780449167
H	-0.4857353681	7.2372554989	1.3188310940
S	-1.4866232608	8.6590212919	-0.3133280210
S	-0.7572538191	6.0932923590	6.1466116228
C	2.0704725236	9.6337290008	7.1756528456
C	1.6526050089	9.4575596729	5.8444051200
C	0.7791566305	8.4078250966	5.5114742944
C	0.3264020704	7.5475542319	6.5253300466
C	0.7415604034	7.7085235568	7.8595123619
C	1.6157307071	8.7614792555	8.1804717881
H	2.7588433172	10.4487559749	7.4288530340
H	2.0117877917	10.1330766955	5.0587999253
H	0.4544017266	8.2541020555	4.4769428289
H	0.3887752653	7.0204029450	8.6358883802
H	1.9442723849	8.8939732778	9.2181780678

C	-5.5435671288	8.5290855790	-2.5919002536
C	-4.4138731620	9.1790737409	-3.1221312070
C	-3.2032563518	9.1912696207	-2.4123508636
C	-3.1196157740	8.5459038115	-1.1604637928
C	-4.2419011057	7.8922426853	-0.6229072065
C	-5.4504591334	7.8901140786	-1.3447802578
H	-6.4884611336	8.5217426449	-3.1477170767
H	-4.4698381656	9.6792746951	-4.0968650306
H	-2.3248424254	9.6944042996	-2.8355637412
H	-4.1887827491	7.3922437501	0.3494046539
H	-6.3254715596	7.3829594870	-0.9205743743
Cl	-2.4233333632	4.3941410859	1.9702254651
N	0.4314200326	3.7074019517	3.7605467086
C	1.5775272358	3.9275276542	4.6699890038
H	1.2159839330	4.0313183170	5.7062687212
H	2.1109990013	4.8495090659	4.3815492018
H	2.2943861954	3.0771192967	4.6301607680
C	0.9342728909	3.5194153335	2.3805393518
H	0.0797428836	3.3726885170	1.7014932129
H	1.6154540102	2.6416528322	2.3159963569
H	1.4906526471	4.4205812675	2.0681012564
C	-0.3303063134	2.5126671911	4.1878292557
H	-0.6951770944	2.6590847593	5.2192025871

H	0.3000709646	1.5961276628	4.1603725621
H	-1.1949976578	2.3831297594	3.5175221037

Figure 10e:

C	-1.3037735766	9.1540532907	2.1401083953
C	-2.0346001994	7.9724604322	2.3803185366
C	-3.4374090523	7.8911892261	2.2453970568
C	-4.1023999702	9.0260863691	1.7214475666
C	-3.4012257414	10.1944689565	1.3932299839
C	-2.0206100961	10.2611594133	1.6214203361
Pd	-1.0999686483	6.3985859409	2.9256272998
H	-5.1909890743	8.9797383441	1.5834340248
H	-3.9352689536	11.0616263101	0.9871968875
H	-1.4686505518	11.1866051845	1.4119873400
C	0.1602022694	9.3345736078	2.4696912901
H	0.3237101121	10.3032551329	2.9710436117
H	0.5382662920	8.5196868769	3.1036473622
C	-4.2510468768	6.7059179698	2.6921716519
H	-3.7082871687	5.7549956293	2.5967695244
H	-5.2121069136	6.6400450000	2.1573407802
S	-4.7059189530	6.8384283085	4.5767781281
S	1.2088513642	9.4078962460	0.8628152275
C	5.0367931546	11.8594990607	1.8808282002

C	4.5224062051	11.8058495083	0.5737404873
C	3.3519661629	11.0797418194	0.2998954298
C	2.6979570862	10.3861928110	1.3383168834
C	3.2124135937	10.4253430855	2.6466247164
C	4.3763916599	11.1720571353	2.9116930538
H	5.9464744102	12.4337009834	2.0930334268
H	5.0256144644	12.3418093322	-0.2388072145
H	2.9424687403	11.0605457524	-0.7160685920
H	2.7291494569	9.8738051228	3.4588386489
H	4.7701981050	11.2044554079	3.9335510459
C	-9.2845840362	6.1606736217	5.0606886835
C	-8.3586201704	5.3575504801	5.7465644063
C	-6.9800494234	5.5329230993	5.5358006559
C	-6.5253735605	6.5332136218	4.6539004648
C	-7.4488009652	7.3482293686	3.9732182662
C	-8.8260416863	7.1489944289	4.1684130798
H	-10.3594646885	6.0231773871	5.2253925105
H	-8.7051436652	4.5855737472	6.4455193613
H	-6.2570751782	4.9005403119	6.0624825769
H	-7.0992612843	8.1495139427	3.3113206720
H	-9.5421535610	7.7868206716	3.6385798852
N	-0.9454409221	5.3876352876	0.9695506078
C	-2.0972958992	4.4879011714	0.7058213089

H	-2.2747245665	3.8423858490	1.5818140727
H	-1.8915098357	3.8434192317	-0.1753600883
H	-2.9964446651	5.0893954520	0.4994653973
C	0.2694688134	4.5736229533	1.2460740633
H	1.1357848405	5.2387143728	1.3860598548
H	0.4824692901	3.8788399518	0.4064049374
H	0.1168136978	3.9727364765	2.1601052065
C	-0.7148389703	6.2591598987	-0.2103875843
H	0.1594399340	6.9026406775	-0.0275247347
H	-1.6028030889	6.8896756078	-0.3759603562
H	-0.5285244066	5.6449578158	-1.1186519449
Cl	-0.9533809750	7.2443293723	5.1969766779

Figure 10f:

C	9.0071685921	3.6139669067	3.6853289169
C	8.3293833954	4.8072617420	3.9712222362
C	6.9571230818	4.9579142224	3.6611977479
C	6.2778167357	3.8663940503	3.0705021469
C	6.9554250284	2.6712827225	2.7317068171
C	8.3274760565	2.5602471368	3.0586103566
H	10.0706681450	3.5133189739	3.9322356563
H	8.8630012581	5.6464058506	4.4364724607
H	8.8595557472	1.6335185015	2.8066599242

Pd	4.4013620451	4.0426971606	2.6221381423
Cl	1.8417555661	4.2955026169	1.9944199788
N	3.8145677873	3.2314439144	4.6194205452
C	2.9627183851	4.2809827060	5.2527507298
H	2.5071482436	3.8849923457	6.1858710780
H	3.5936248448	5.1500591164	5.5026665815
H	2.1731320833	4.5720982248	4.5446829569
C	2.9839692429	2.0249342054	4.3305971269
H	3.6324833959	1.2381201799	3.9103368769
H	2.5240354158	1.6491505417	5.2698417355
H	2.1968978081	2.2984876142	3.6125731600
C	4.8775352845	2.8465673199	5.5887734259
H	5.4922541301	3.7240653188	5.8393702474
H	4.4078485495	2.4580169214	6.5177712129
H	5.5159320066	2.0621054293	5.1553359115
N	4.9708210536	4.8230341036	0.5972497597
C	4.3430989130	6.1733135795	0.4893158626
H	4.4563523141	6.5635626986	-0.5444057686
H	3.2766379732	6.0886460469	0.7456638609
H	4.8424254723	6.8650376771	1.1869507280
C	4.3242835217	3.9040699976	-0.3859462498
H	4.8100633049	2.9163949981	-0.3344272655
H	3.2576886112	3.8084740261	-0.1345674858

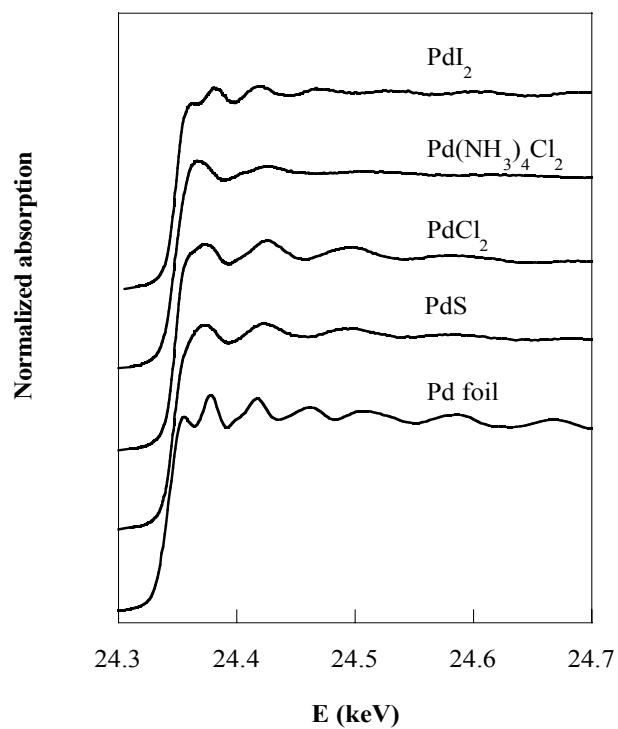
H	4.4390164113	4.3059112675	-1.4152600509
C	6.4122645432	4.9478806581	0.2431621211
H	6.9128078414	5.6337780192	0.9429459893
H	6.8987321172	3.9626878381	0.2976988998
H	6.5103408358	5.3444466376	-0.7888329330
C	6.2855537613	1.5493403259	1.9718163918
H	5.2469047470	1.8010818277	1.7077210884
H	6.8517988128	1.2641989682	1.0697100455
S	6.2100362841	-0.0588755734	3.0521144139
C	4.7559210535	-3.4042947894	0.1541622690
C	6.1285178440	-3.2394627055	0.4111557077
C	6.5705843890	-2.2040953868	1.2543506073
C	5.6309312026	-1.3377202862	1.8439813346
C	4.2555397190	-1.4999703474	1.5918915153
C	3.8214439897	-2.5330469960	0.7424537541
H	4.4130153264	-4.2149252508	-0.4998250509
H	6.8595721876	-3.9204145996	-0.0406133300
H	7.6384591705	-2.0762300228	1.4643644320
H	3.5257756261	-0.8345812968	2.0662048645
H	2.7493100846	-2.6621250306	0.5508613502
C	6.2912153861	6.2909574981	3.9168694088
H	6.8686435576	7.1306830864	3.4965214778
H	5.2584774814	6.3063095461	3.5356195767

S	6.2072314891	6.6336297950	5.8251050838
C	4.5747254675	10.9768251113	6.2637304378
C	3.8055510177	10.0103324201	5.5907540281
C	4.2935848173	8.7024399856	5.4265164719
C	5.5659853732	8.3657758601	5.9262821993
C	6.3453746360	9.3326360284	6.5898474543
C	5.8421116962	10.6342900249	6.7661438122
H	4.1829565777	11.9919417435	6.3989190177
H	2.8123227359	10.2689729771	5.2046258853
H	3.6794815685	7.9442038528	4.9286455087
H	7.3364349551	9.0649229058	6.9735934521
H	6.4487194185	11.3813366185	7.2921567516

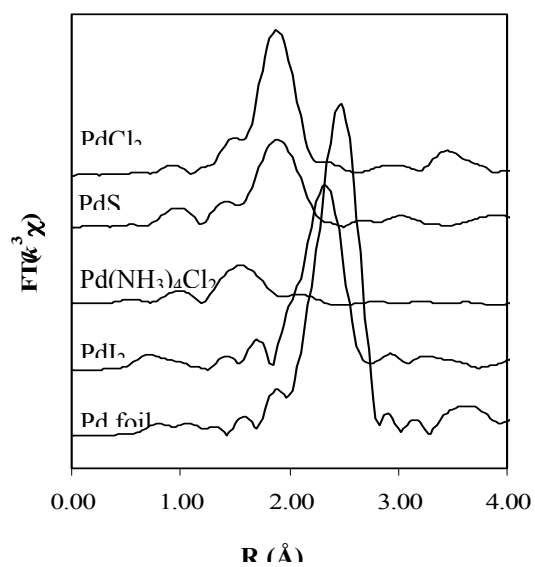
References.

1. E. A. Stern, *Phys. Rev. B.* **1993**, *48*, 9825.
2. A. L. Ankudinov, B. Ravel, J. J. Rehr, S. D. Conradson, *Phys. Rev. B.* **1998**, *58*, 7565.
3. D. C. Koningsberger, B. L. Mojet, G. E. van Dorssen, D. E. Ramaker, *Top. Catal.* **2000**, *10*, 143-155.
4. J. W. Sobczak, E. Sobczak, A. Drelinkiewicz, M. Hasik, E. Wenda, *J. All. and Comp.* **2004**, *362*, 162-166.
5. T. Shido, A. Yamaguchi, Y. Inada, K. Asakura, M. Nomura, Y. Iwasawa, *Top. Catal.* **2002**, *18*, 53.
6. J. Evans, L. O'Neill, V. L. Kambhampati, G. Rayner, S. Turin, A. Genge, A. J. Dent and T. Neisius, *J. Chem. Soc., Dalton Trans.* **2002**, 2207-2212.
7. a) K. Yu, W. Sommer, M. Weck, C. W. Jones, *J. Catal.* **2004**, *226*, 101.; b) K. Yu, W. Sommer, M. Weck, C. W. Jones, *Adv. Synth. Catal.* **2004**, *in press*.
8. M. T. Reetz, J. G. de Vries *Chemical Commun.* **2004**, 1559-1563

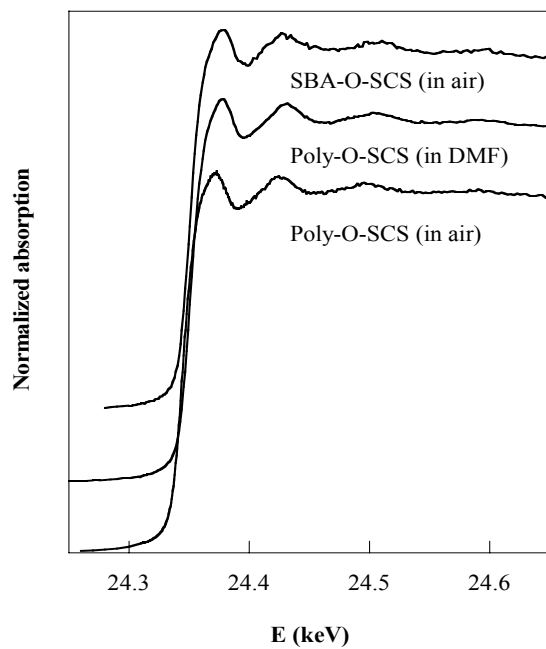
Comment [MW1]: Wrong abbreviation



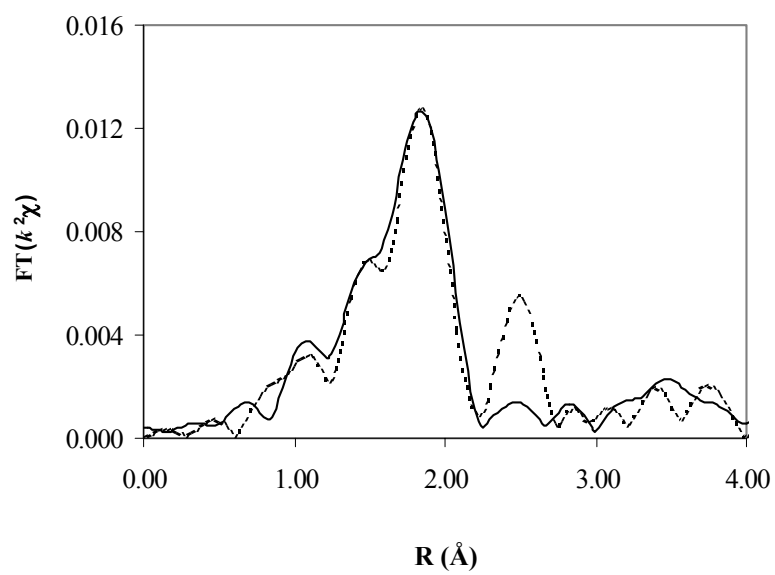
CHAPTER I Supplemental Figure 1. **Pd K edge spectra of standard compounds**



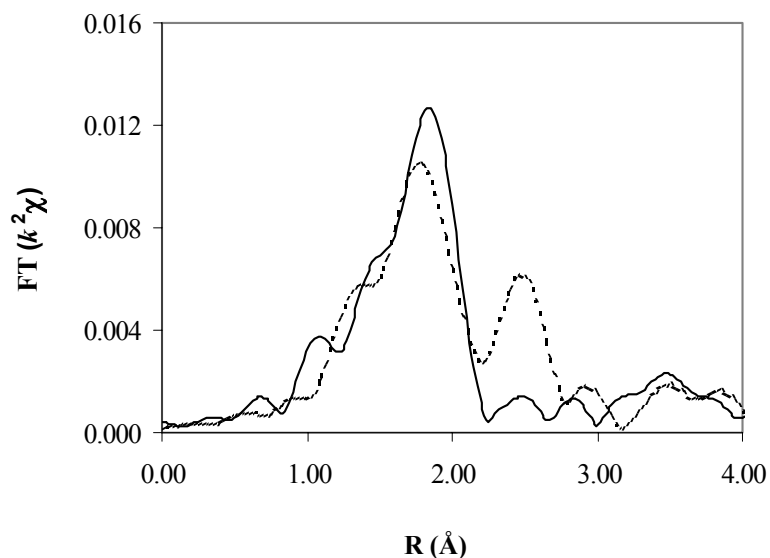
CHAPTER IISupplemental Figure 2. k^3 -weighted Fourier transform of EXAFS for standard compounds



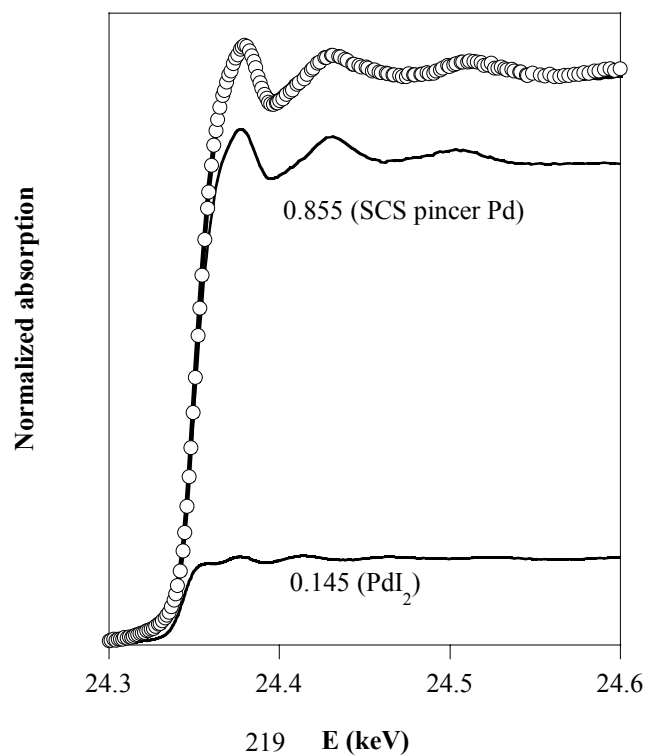
CHAPTER IIISupplemental Figure 3. Pd K edge spectra of SCS pincer compounds



Supplemental Figure 4. k^2 -weighted Fourier transform of EXAFS for immobilized SCS pincer Pd

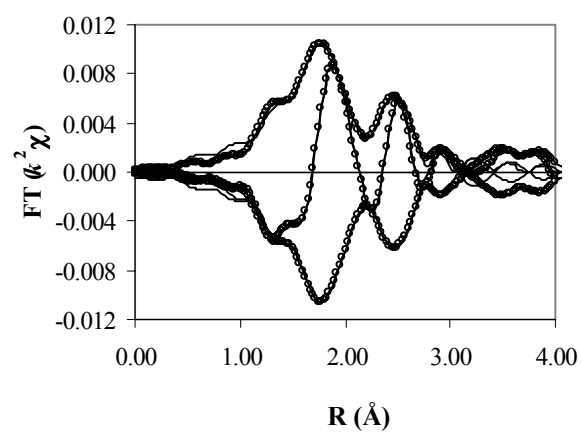
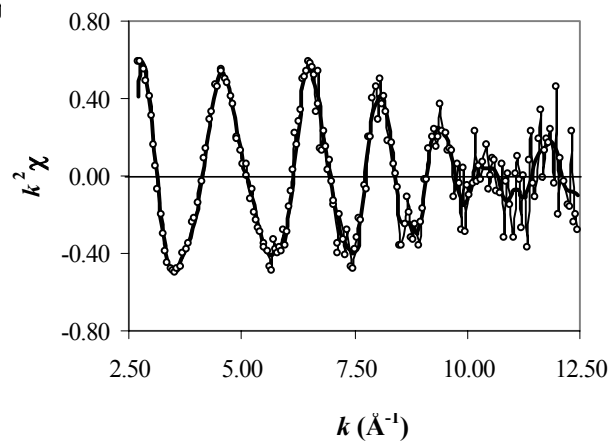


Supplemental Figure 5. k^2 -weighted Fourier transform of EXAFS for polymer immobilized SCS pincer Pd compound (— : in air at RT; ... : during Heck reaction at 120°C)



219 E (keV)

Supplemental Figure 6. Pd K edge spectrum of polymer immobilized SCS pincer compound during Heck reaction (circles), linear combination XANES (thick solid line) and single component



Supplemental Figure 7. Pd K edge k^2 -weighted EXAFS and Fourier transform (magnitude and imaginary part) for polymer immobilized SCS pincer Pd during Heck reaction (— experimental; — fitted)

Table 1. Structural parameters assigned to standard compounds.

Standard	Atom pair	CN	R(Å)
Pd foil	Pd-Pd	12	2.75
PdI ₂	Pd-I	4	2.61
PdCl ₂	Pd-Cl	4	2.31
PdS	Pd-S	4	2.33
Pd(NH ₃) ₄ Cl ₂	Pd-N	4	2.05

Table 2. Parameters used for calibration of theoretical FEFF references derived from fits to standard compounds.

Atom pair	σ^2 (Å ²)	S_0^2	Vr (eV)	Vi (eV)	Δk (Å ⁻¹)	ΔR (Å)
Pd-Pd	0.00550	1.00	-5.5	3.0	3.0-15.0	1.5-3.2
Pd-I	0.00385	0.92	2.5	3.0	3.0-15.0	1.5-3.0
Pd-Cl	0.00303	0.90	2.7	3.0	2.5-14.0	1.5-2.8
Pd-S	0.00337	0.87	1.5	3.0	2.5-12.7	1.5-3.0
Pd-N	0.00008	0.90	0.8	3.0	2.5-12.8	1.0-2.5

Table 3. Fitting results from linear combination of XANES ($\Delta E = 24.20\text{-}24.50$ keV).

Pincer Compound	Measurement condition	SCS Pincer Pd (%)	Metallic Pd (%)	PdI ₂ (%)	Residual factor (%)
Poly-O-SCS	In DMF at RT	100	0	---	0.31
SBA-O-SCS	In air at RT	93.3	6.5 (0.8)	---	0.36
Poly-O-SCS	During Heck reaction at 393 K	85.5	0	14.5 (0.6)	0.41
SBA-O-SCS	During Heck reaction at 393 K	81.7	2.4 (0.3)	15.7 (0.6)	0.44

* The value in parentheses is the estimated coordination number for Pd-Pd or Pd-I.

Table 4. Pd K edge EXAFS curve-fitting results for polymer and SBA immobilized SCS

pincer compounds.

Catalyst	Measurement condition	Scatterer	CN	R (Å)	$\sigma^2(10^{-3}\text{Å})$	ΔE_0 (eV)
SBA-O-SCS	In air at RT	S	2.1	2.29	1.4	-0.45
		Cl	1.0	2.37	5.0	4.53
		C	1.1	1.99	4.0	0.56
		Pd	1.4	2.71	5.4	-4.73
Poly-O-SCS	In air at RT	S	2.3	2.29	2.1	-3.17
		Cl	1.1	2.40	1.0	6.27
		C	1.2	1.99	3.7	1.73
Poly-O-SCS	During Heck reaction at 393 K	S	2.0	2.28	1.9	2.84
		Cl	1.1	2.39	4.0	6.99
		C	1.1	1.98	1.0	2.32
		I	1.2	2.67	3.6	-1.92

R-space fit, k^2 weighting, $\Delta k = 2.5\text{-}12.0$ Å⁻¹, $\Delta R = 0.8 - 3.2$ Å

